NAS CR-134870

Final Report

LIGHTWEIGHT THERMALLY EFFICIENT COMPOSITE FEEDLINES FOR THE SPACE TUG CRYOGENIC PROPULSION SYSTEM

by

D. E. Spond

MARTIN MARIETTA CORPORATION

Prepared for

IONAL AERONAUTICS AND SPACE ADMINISTRATION

NASA Lewis Research Center

Contract NAS3-17796

Joseph Notardonato, Project Manager

1 Report No	2 Government Accession No	3. Recipient's Catalog No
NASA CR-134870		

4 Title and Subtitle	5 Report Date
Final Report, Lightweight Thermally Efficient Composite Feedlines for the Space Tug Cryogenic Propulsion System	August 1975
	6. Performing Organization Code 04236

7. Author(s)	8 Performing Organization Report No
D. E. Spond	
	10 Work Unit No

9. Performing Organization Name and Address	11 Contract or Grant No
Martin Marietta Corporation P.O. Box 179 Denver, Colorado 80201	NAS 3-17796
	13 Type of Report and Period Covered Final Report August 1973 to May 1975

12 Sponsoring Agency Name and Address	14 Sponsoring Agency Code
National Aeronautics and Space Administration Lewis Research Center Cleveland, Ohio 44135	

15 Supplementary Notes

16 Abstract

Six liquid hydrogen feedline design concepts are developed for the cryogenic Space Tug. The feedlines include composite and all-metal vacuum jacketed and nonvacuum jacketed concepts, and incorporate the latest technological developments in the areas of thermally efficient vacuum jacket end closures and standoffs, radiation shields in the vacuum annulus, thermal coatings, and lightweight dissimilar metal flanged joints. The feedline design concepts are evaluated on the basis of thermal performance, weight, cost, reliability, and reusability. Design concepts were proved in a subscale test program. Detail design was completed on the most promising composite feedline concept and an all-metal feedline. Three full scale curved composite feedlines and one all-metal feedline assembly were fabricated and subjected to a test program representative of flight hardware qualification. The test results show that composite feedline technology is fully developed. Composite feedlines are ready for space vehicle application and offer significant reduction in weights over the conventional all-metal feedlines presently used.

17 Key Words (Suggested by Author(s))		18 Distribution Statement
Composite	Lightweight	Unclassified - Unlimited
Feedline	Space Tug	
Cryogenic	Storable Propellants	
Overwrap		
Thermal Efficiency		

19 Security Classif (of this report)	20 Security Classif (of this page)	21 No of Pages	22 Price*
Unclassified	Unclassified	128	

* For sale by the National Technical Information Service, Springfield, Virginia 22151

1 Report No	2 Government Accession No	3 Recipient's Catalog No
NASA CR-134870		

4 Title and Subtitle	5 Report Date
Final Report, Lightweight Thermally Efficient Composite Feedlines for the Space Tug Cryogenic Propulsion System	August 1975
	6 Performing Organization Code: 04236

7 Author(s)	8 Performing Organization Report No
D. E. Spond	
	10 Work Unit No
9 Performing Organization Name and Address: Martin Marietta Corporation, P.O. Box 179, Denver, Colorado 80201	11 Contract or Grant No: NAS 3-17796
	13 Type of Report and Period Covered: Final Report, August 1973 to May 1975
12 Sponsoring Agency Name and Address: National Aeronautics and Space Administration, Lewis Research Center, Cleveland, Ohio 44135	14 Sponsoring Agency Code

15 Supplementary Notes

16 Abstract

Six liquid hydrogen feedline design concepts are developed for the cryogenic Space Tug. The feedlines include composite and all-metal vacuum jacketed and nonvacuum jacketed concepts, and incorporate the latest technological developments in the areas of thermally efficient vacuum jacket end closures and standoffs, radiation shields in the vacuum annulus, thermal coatings, and lightweight dissimilar metal flanged joints. The feedline design concepts are evaluated on the basis of thermal performance, weight, cost, reliability, and reusability. Design concepts were proved in a subscale test program. Detail design was completed on the most promising composite feedline concept and an all-metal feedline. Three full scale curved composite feedlines and one all-metal feedline assembly were fabricated and subjected to a test program representative of flight hardware qualification. The test results show that composite feedline technology is fully developed. Composite feedlines are ready for space vehicle application and offer significant reduction in weights over the conventional all-metal feedlines presently used.

17 Key Words (Suggested by Author(s))		18 Distribution Statement
Composite	Lightweight	Unclassified - Unlimited
Feedline	Space Tug	
Cryogenic	Storable Propellants	
Overwrap		
Thermal Efficiency		

19 Security Classif (of this report)	20 Security Classif (of this page)	21 No of Pages	22 Price*
Unclassified	Unclassified	128	

* For sale by the National Technical Information Service, Springfield, Virginia 22151

FOREWORD

The work described herein was conducted by Martin Marietta Corporation, Denver Division, under NASA Contract NAS3-17796, under the management of the NASA Project Manager, Mr. Joseph Notardonato, Propulsion Systems Branch, NASA Lewis Research Center, Cleveland, Ohio.

In addition to the stated authors, the following persons provided major assistance: Messrs Charles A. Hall, Daniel J. Laintz, John M. Phillips, Lyle L. Mason, and Dr. Murlin T. Howerton.

CONTENTS

SYMBOLS

E	Modulus of elasticity, N/cm^2 (psi)
ξ	Strain in X direction (along tube centerline), cm/cm (in./in.)
K	Constant
L	Length, cm (in.)
M	Moment kg-m (ft-lb)
p	Pressure, N/cm^2 (psi)
r	Radius, cm (in.)
S	Stress N/cm^2 ($lb/in.^2$)
S_b	Critical buckling stress, N/cm^2 ($lb/in.^2$)
S_S	Circumferential shear stress, N/cm^2 ($lb/in.^2$)
T	Torque, kg-m (ft-lb)
t	Thickness, cm (in.)
V	Velocity, mps (fps)
ν	Poisson's ratio

DEFINITION OF TERMS

A listing of commonly used terms and their definitions follows. Familiarity with these terms should help the reader to understand the technical aspects of the document.

Inner line	Line carrying the commodity.
Vacuum jacket	Concentric line installed over the inner line providing an evacuated annulus for thermal efficiency.
Composite vacuum jacket	A vacuum jacket concept that incorporates a thin metallic liner and composite material to provide strength and handling damage resistance.
Overwrap	Fiberglass composite applied on exterior surface of the thin metal tubing liner.
Liner	Thin wall metal tube under the overwrap.
Standoff	Support between the vacuum jacket and the inner line.
End closure	Metal membrane that seals the vacuum annulus between the inner line and the vacuum jacket.
End fitting	Metal ring welded to the ends of the liner providing a surface for welding the end closure and a butt weld end for attaching one tube to another.
Dissimilar metal end fitting	Aluminum to stainless steel joint made by co-extrusion, inertia welding or explosive bonding processes.
Braiding	Process for applying composite overwrap.

SUMMARY

This is the final report of a 22-month program that was conducted under Contract NAS3-17796. The objective of the program was to apply composite tubing technology to the development of lightweight, thermally efficient feedlines for the Space Tug or other cryogenic space vehicles. The program consisted of developing and evaluating competitive feedline design concepts, conducting a subscale test program to evaluate high modulus low density composites and dissimilar metal joints, designing and fabricating all-metal and composite full scale feedline assemblies, conducting a test program that is representative of flight hardware qualification testing, and evaluating the composite versus the all-metal feedlines for application on the cryogenic Space Tug.

It was concluded early in the program that the Space Tug feedline routing may require curved as well as straight line sections; and that to truly demonstrate composite tubing useability, curved composite tubing technology must be developed. The program was redirected accordingly. Competitive approaches for both metal liner fabrication and composite overwrap application were investigated. Thin metallic liners for the composite tubing were successfully produced by chemical milling curved tubing with an initial wall thickness of 0.076 cm (0.030 in.) to a final thickness of 0.023 cm (0.009 in.). One curved tubing liner of 0.015 cm (0.006 in.) wall thickness was successfully fabricated; additional development is required for bending very thin wall tubing. New tooling was produced and used successfully to filament wind curved line sections. A second overwrapping technique consisting of a braiding process, developed by McDonnell-Douglas Astronautics, was successfully demonstrated.

One all-metal and four composite full scale feedline assemblies were designed, fabricated, and tested. Each assembly was of an identical routing configuration and consisted of three individual line sections, three gimbal joints, and one tee junction. The feedlines were 10.2 cm (4 in.) diameter and had a developed length of 564 cm (222 in.). The test program subjected the composite and all-metal feedlines to identical test conditions and compared the results. The identical testing of the composite and all-metal feedlines consisted of proof pressure, leakage, steady state heat input, chilldown and flow quality tests. In addition, the composite feedlines were subjected to structural loading, liquid hydrogen cycling, acoustics, and burst tests.

The composite feedlines survived all testing (destructive burst test excluded) without degradation. All of the composite lines withstood a burst pressure of over 310 N/cm^2 (450 psig), which is 15 times the design operating pressure. It is significant also to note that the lines were burst tested after having

previously been subjected to all of the other test environments. The composite feedlines compared favorably to the all-metal design in every test. The weight of the LH_2 composite feedline assemblies produced was 3.6 kg (8 lb) less than the weight of the all-metal LH_2 feedline. The additional cost elements for the composite feedline assemblies consisted of the cost for chem-milling and applying the composite overwrap. This delta cost was approximately $1600 per feedline assembly resulting in a cost per unit weight saved of $441/kg ($200/lb).

All program objectives were met. It is concluded that the work described herein, in addition to the work performed on previous contracts by the Martin Marietta Corporation for the NASA Lewis Research Center, clearly demonstrates that composite tubing technology is fully developed and ready for space flight application.

I. INTRODUCTION

The essential aspect of developing lightweight, thermally efficient propulsion feed systems is system parameter optimization, which includes thermal flux, weight, cost, reliability, and maintainability. It has been demonstrated that composite tubing provides improved thermal performance and reduced weight at a small increase in cost over conventional all-metal tubing. It has also been demonstrated that composite tubing is reliable and highly resistant to damage.

In three recently completed programs*, the Martin Marietta Corporation analyzed, designed, fabricated, and tested a series of composite propulsion feedlines designed to limit the heat transfer through this portion of the propulsion system. These feedlines incorporated a thin metal liner to provide a leak free pressure carrier and compatibility with cryogenic propellants. The thin metal liners were overwrapped with a glass-fiber material using a suitable matrix. Because glass-fiber overwrap is a good thermal insulator and the thin metal liner has a small cross-sectional area, the thermal conductivity was reduced considerably in both radial and longitudinal directions. Program results confirm the desirability of this concept. Some of the advantages, in addition to low radial and axial thermal flux, are lightweight construction, low axial heat-soakback from engines or vaporizers, rapid chill-down, strength, and resistance to handling damage. The minimum wall thickness used for all-metal feedlines in a great majority of propulsion systems is dictated by handling and maintainability; not stresses. For example, an Inconel 718 or stainless steel tube with a 0.013 cm (0.005 in.) wall thickness could carry internal pressure for many propulsion feedlines and tank vents but could not be handled without incurring damage. Composite tubing can be fabricated with the metal liner wall thickness of 0.013 cm (0.005 in.) and overwrapped with glass-fibers having low density and low thermal conductivity. The results are lighter feedlines with reduced thermal flux characteristics, low weight, and high resistance to damage.

The objective of this program was to develop lightweight, thermally efficient composite feedlines for the Space Tug cryogenic propellant feed system and compare composite and all-metal feedline assemblies under a specific set of test conditions. The program was performed by completing the following tasks:

*Contract NAS3-12047, Glass-Fiber Tubing for Cryogenic Service (ref. 1), Contract NAS3-14370, Composite Propulsion Feedlines for Cryogenic Space Vehicles (ref. 2), and Contract NAS3-16762, Vacuum Jacketed Composite Propulsion Feedlines for Cryogenic Launch and Space Vehicles (ref. 3).

Task I	Definition of Technology Requirements
Task II	Subscale Testing and Analysis
Task III	Feedline Detailed Design
Task IV	Fabrication
Task V	Testing
Task VI	Analysis

The initial task of defining technology requirements consisted of (1) defining the design criteria for the LH_2 and LO_2* feedlines, from a review of available cryogenic Space Tug literature; (2) assessing feedline technology developments in the areas of vacuum jacketed lines, dissimilar metal joints, and high modulus/low density composites; (3) developing and evaluating competitive feedline design concepts; and (4) selecting the most promising designs for fabrication and evaluation by test. The results of this task were reported in NASA CR-134631, Topical Report, Lightweight Thermally Efficient Composite Feedlines, Preliminary Design and Evaluation (ref. 4) and are summarized herein.

The remaining tasks consisted of (1) designing, fabricating, and testing eight subscale composite tubing test specimens with dissimilar metal joints and different composite overwrap materials; (2) designing, fabricating, and testing full scale curved composite and all-metal feedline assemblies; and (3) performing analysis to evaluate the composite feedline concept readiness for application to the Space Tug system.

All program objectives were accomplished resulting in a useable concept for reducing propulsion feedline weight on the Space Tug and other space vehicles.

*The evaluation of the Space Tug LO_2 feedline along with the LH_2 feedline was included in the initial program. The LO_2 feedline was deleted to make funds available for developing curved composite technology. The design and fabrication approach for a LO_2 feedline would be the same as that defined herein for the LH_2 feedline.

II. CONCEPT DESIGN AND EVALUATION

Detailed analyses were performed to provide a basis for the development of six Space Tug feedline concepts:

	Design Concept	Line Condition*	Multilayer Insulation
(1)	Vacuum jacketed metal	Wet	None
(2)	Vacuum jacketed composite	Wet	None
(3)	Nonvacuum jacketed metal	Wet	Purged MLI
(4)	Nonvacuum jacketed metal	Dry	MLI
(5)	Nonvacuum jacketed composite	Dry	MLI
(6)	Nonvacuum jacketed composite	Wet	Purged MLI

*A "wet" line condition refers to a line containing a cryogen during the atmospheric as well as space portion of the flight, that is, during ground hold, ascent, and potentially, reentry in the Space Shuttle cargo bay.

The results of these analyses are reported in NASA CR-134631, Topical Report, Lightweight Thermally Efficient Composite Feedlines, Preliminary Design and Evaluation, June 1974 (ref. 4) and are summarized in this chapter. These analyses provided the basis for selecting design concepts, detail design, fabrication and test of the full scale composite and all-metal feedline assemblies, discussed later.

Feedline Design Conditions

A literature search was conducted to obtain the information necessary to determine the Space Tug liquid hydrogen feedline design conditions and physical configuration. This search included a review of the Space Tug Point Design Studies, conducted by McDonnell-Douglas Astronautics Company, and North American Rockwell (refs. 5 and 6), the Baseline Tug Definition Document, Rev. A (ref. 7), Space Tug Systems Study by General Dynamics/Convair (ref. 8), Space Tug Systems Study (Storable) by the Martin Marietta Corporation (ref. 9), preliminary Space Tug design drawings obtained from the NASA George C. Marshall Space Flight Center, and telephone conversations with numerous personnel who participated in these studies.

During the literature search, it became clear that Space Tug design conditions and physical configuration are not yet firmly established and will continue to change for some time. Therefore, data obtained from the literature surveyed were used to develop a set of design parameters and a liquid hydrogen feedline configur-

ation, which demonstrates a capability for producing virtually any configuration requirement.

The conditions that affect the liquid hydrogen feedline design are system operating requirements and environments in the Space Shuttle cargo bay and during the Space Tug mission. The conditions used in the development of the feedline design concepts are defined in Tables II-1, II-2, and II-3.

Assessment of Technology Developments

Known state-of-the-art technology developments were evaluated to assure that optimum components were used in the development of the liquid hydrogen feedline design concepts. The results of this evaluation are summarized in the following paragraphs.

High modulus composites. - Composite materials consisting of S-glass, Kevlar 49 DP-01, graphite, and boron were evaluated by comparing mechanical properties, thermal conductivity, resistance to fatigue failure, weight, and cost. S-glass and graphite were shown to be the two most promising overwrap materials. Later in the program however, it was determined that Kevlar 49 DP-01 was more desirable than graphite because Kevlar was much easier to apply and provided a more desirable surface finish.

Effect of radiation shields in a vacuum jacketed line annulus. - Effective emittance, system heat flux, weight, and cost versus the number of radiation shields in the liquid hydrogen feedline vacuum jacket annulus were evaluated. It was concluded that eight layers of Superfloc high-performance insulation (aluminized Mylar separated by flocked tufts of Dacron fibers) manufactured by General Dynamics/Convair, provides the optimum configuration eliminating approximately 98% of the heat flux due to radiation.

Vacuum jacketed line standoffs and end closures. - Four vacuum jacketed line standoff designs and five end closure designs were evaluated on the basis of heat flux and weight. The designs evaluated and results obtained are summarized in Figures II-1 and II-2.

Dissimilar metal joints. - Dissimilar metal (stainless steel-to-aluminum) joints were evaluated for the purpose of reducing the weight of feedline connections. It was shown that a weight saving of 0.14 kg (0.3 lb) per flange half in a flanged joint connection could be obtained by the use of dissimilar metal joints. Later in the program dissimilar metal joints were produced, using three different methods of construction, and evaluated. This is discussed in Chapter III.

Thermal coatings on composite lines. - It was shown that composite lines exposed to solar radiation in a space environment will reach an equilibrium temperature of 350°K (170°F). This will not cause structural degradation but will reduce thermal performance. It is recommended that exposed surfaces of the feedline be coated with a material having a low solar absorptivity/surface emissivity.

Liquid Hydrogen Feedline Design Concepts

Drawings of the six feedline design concepts are included in Appendix A. All design concepts include curved and straight line sections and are representative of anticipated Space Tug feedline routing and interface characteristics. The feedline assemblies consist of three flanged line sections to facilitate installation and handling. The vacuum jacketed configurations have eight layers of multilayer insulation (MLI) in the vacuum annulus, a thermal coating on the exterior surface of the vacuum jacket and lightweight/thermally efficient end closures and standoffs. The composite lines are overwrapped with S-glass consisting of a layer of machine hoop wrapped 20 end roving, a half layer of longitudinally oriented strips of glass cloth, and a final layer of hoop wrap. A description of the six design concepts is provided in the following paragraphs.

Concept 1, vacuum jacketed metal configuration description. - Concept 1 consists of an all-metal, conventional vacuum jacketed line assembly.

The inner line is 0.058 cm (0.023 in.) thick stainless steel sheet, formed to the configuration shown in Appendix A. Low profile stainless steel flanges are welded to the inner line for interfacing with the liquid hydrogen tank and the prevalve located at the engine interface. Two additional flange joints are provided, which divide the feedline assembly into three line sections. A tee connection is provided for LH_2 fill and drain through the feedline, if required.

Each of the line sections are vacuum jacketed for thermal insulation. The vacuum jacket consists of a 12.7 cm (5.0 in.) outside diameter by 0.06 cm (0.025 in.) thick stainless steel tube supported to the inner line by standoffs and sealed at the ends by end closures. The standoffs and end closures are of the optimum configurations shown in Figures II-1, Concept (a) and II-2, Concept (c) respectively. Eight layers of Superfloc insulation are installed in the vacuum annulus to reduce radiation heat flux. Internal 0.64 cm (0.25 in.) radius convolutes on 22.8 cm (9.0 in.) centers are formed in the vacuum jacket for resistance to external pressure loading.

Each of the line sections contains a flight weight vacuum sensing connection, vacuum acquisition valve, and a burst disc for over-pressure relief.

The feedline assembly contains three vacuum jacketed gimbals welded into the inner line and into the vacuum jacket. The vacuum annulus is continuous through the gimbals.

Concept 2, vacuum jacketed composite configuration. - Concept 2 is of the same physical geometry as Concept 1. The gimbals, prevalve location, vacuum components, MLI insulation, standoffs, and end closure designs are identical to Concept 1.

The vacuum jacket consists of a 0.023 cm (0.009 in.) thick Inconel 718 liner overwrapped with two hoop layers of S-glass roving applied in a $\pm$ 0.09 rad ($\pm$ 5 degrees) helical pattern. Convolutes of 0.64 cm (0.25 in.) radius, formed in the vacuum jacket on 3.8 cm (1.5 in.) centers, are provided for stiffness.

The inner line consists of a 0.02 cm (0.008 in.) thick Inconel 718 tube liner overwrapped with two hoop layers of S-glass roving and longitudinal strips of glass-fiber cloth sandwiched between the hoop layers. The flange locations are identical to Concept 1. The flanges use inertia welded stainless steel-to-aluminum joints to reduce weight.

Concept 3, nonvacuum jacketed metal, wet, purged MLI configuration. - Concept 3, a conventional all-metal feedline insulated with helium-purged MLI, was established by NASA as the baseline for competitive comparison with the other design concepts. The prevalve is located at the engine turbo pump interface. The gimbal system (except nonvacuum jacketed), flange designs and routing are identical to Concept 1. The feedline is 10 cm (4.0 in.) outside diameter and 0.08 cm (0.030 in.) thick stainless steel tubing.

The insulation system consists of 30 layers of double aluminized Superfloc.

Concept 4, nonvacuum jacketed composite, dry, MLI configuration. - Concept 4 is identical to Concept 3 except the prevalve is located at the liquid hydrogen tank interface and the insulation system is not purged.

Concept 5, nonvacuum jacketed composite, dry, MLI configuration. - Concept 5 is identical to Concept 4 except the pressure line is a composite overwrapped design with dissimilar metal flanges. The pressure line is 0.013 cm (0.005 in.) thick Inconel 718 overwrapped with two layers of S-glass roving and longitudinal strips of glass-fiber cloth identical to the overwrap on the Concept 2 inner line.

Concept 6, nonvacuum jacketed composite, wet, purged, MLI configuration. - Concept 6 is identical to Concept 3 except, as in Concept 5, the pressure line is a composite overwrapped design with dissimilar metal flanges.

Structural Evaluation

Analyses were performed to determine the wall thickness of the composite and all-metal feedlines based on operating pressure, surge pressure, and external loads. It was shown that producibility and handling damage resistance considerations override other criteria for determining the LH_2 feedline wall thickness. A minimum wall thickness of 0.013 cm (0.005 in.) Inconel 718 for the metal liners with 0.05 cm (0.02 in.) thick overwrap was recommended for the composite lines. The minimum wall thickness for the all-metal line was determined to be 0.08 cm (0.030 in.) stainless steel.

Concept Design Evaluation

Each of the six design concepts was analyzed with respect to thermal performance, weight, cost, reusability, and maintainability. The results of these analyses, showing the predicted comparison of the feedline concept designs, is summarized in Tables II-4 through II-7. Concept 5 was shown to be the optimum configuration. Concepts 3 and 5 were selected for further evaluation by fabricating full scale feedline assemblies and performing a qualification type test program. This work was completed and the results are reported in Chapters V, VI, and VII.

III. PRELIMINARY TESTING

Principal factors in thermal and weight optimization of composite feedlines include the use of high-modulus, low-density composites and lightweight, thermally efficient end fittings. The objectives of the preliminary testing program were to design, fabricate, and test subscale composite tubing specimens using three low-density composite overwrap materials and three different aluminum-to-stainless steel bimetallic end fitting designs. In all, eight subscale composite tubes were fabricated and evaluated. It was shown that the low density high modulus composites and dissimilar metal end fittings may be readily applied to composite feedlines and that they provide additional weight reduction.

Design

Eight subscale test specimens were designed incorporating different overwrap materials and end fitting configurations as defined in Table III-1. Each of the specimens were 5.82 cm (2.29 in.) diameter and 20.3 cm (8 in.) long with a 0.013 cm (0.005 in.) thick Inconel 718 tubing liner, overwrapped with a composite roving consisting of one hoop layer, a half layer of longitudinal strips, and a final hoop layer. The various specimen designs are depicted in Figure III-1.

Fabrication

The major steps performed in the fabrication of the subscale test specimens were as follows:

(1) Fabrication of tubing liner;

(2) Dye penetrant inspection of tubing liner seam welds;

(3) Fabrication of end fittings: 8 stainless steel, 4 inertia bonded (aluminum-to-stainless steel), 4 coextruded (aluminum-to-stainless steel), and 2 explosively bonded (aluminum-to-stainless steel);

(4) Dye penetrant inspection of the dissimilar metal fittings;

(5) Welding the Inconel 718 tubing liners and end fittings;

(6) Dye penetrant inspection of end fitting-to-tubing liner welds;

(7) Weld tube caps to end of tubes;

(8) Proof pressure test at 31 N/cm^2 (45 psig);

(9) Helium mass spectrometer leak check at 20.7 N/cm^2 (30 psig); and

(10) Composite overwrap the tubing assemblies: 4 with S-glass and 58-68R resin system, 2 with Kevlar 49 and 58-68R resin system, and 2 with graphite and 58-68R resin system.

A typical subscale test specimen before overwrap and before welding on end caps for test purposes is shown in Figure III-2. This particular specimen incorporated aluminum-to-stainless steel end fittings, fabricated by the coextrusion process.

Testing

The test program for the subscale specimens is defined in Figure III-3. The testing consisted of proof pressure and leakage, temperature cycling, thermal shock, pressure cycle, torsional load, bending load, salt fog, storable propellant compatibility, and burst test.

Proof and leak tests. - Proof tests were performed on all specimens at 31 N/cm^2 (45 psig) (1.5 times operating pressure). Leak tests were performed by pressurizing the test specimens with gaseous helium at 20.7 N/cm^2 (30 psig). Leakage was measured using a helium mass spectrometer for a stabilization period of 30 minutes. See Figure III-4 for leak test setup. All specimens had zero leakage (less than 3×10^{-10} scc/sec).

The leak testing was repeated after each of the remaining tests. All test specimens remained leak free throughout the test program.

Temperature cycle test. - The temperature cycle test consisted of subjecting the test specimens to 10 temperature cycles from 294°K to 78°K (70°F to -320°F). The test specimens were connected in series as shown in Figure III-5, filled with liquid nitrogen until the temperature stabilized, drained, and heated with hot gaseous nitrogen at 294°K (70°F). After 10 cycles, the test specimens were leak tested. All specimens had zero leakage.

Thermal shock test. - For this test, the test specimens were maintained at operating pressure and submerged in boiling water. The temperature was allowed to stabilize in the boiling water. Then the specimen was removed and immediately submerged in liquid nitrogen. When the specimen reached liquid nitrogen temperature, it was removed and again submerged in boiling water. This sequence was repeated for a total of 10 cycles for each test specimen and the leak test was repeated. No leaks were found. Each of the specimens was examined with the aid of a 10X magnifying lens. No degradation was detected. The test setup for the thermal shock testing is depicted in Figure III-6.

Pressure cycle test. - The pressure cycle test consisted of subjecting each of the test specimens to (1) pressurization to 21 N/cm^2 (30 psig) with gaseous nitrogen, (2) maintaining this pressure for 10 to 15 seconds, and (3) reducing the pressure to ambient. This pressurization cycle was repeated 200 times at ambient temperature. After completion the specimens were examined under 10X magnification and leak tested. No degradation was detected.

Torsional load test. - The purpose of this test was to determine the strength of the composite tubes when subjected to torsion loading. The test was performed by applying a torsion load at one end of the specimen while the other end of the specimen was held rigid. After yield strengths of the composite specimens were determined, the remaining specimens were subjected to torsional loading at 75% of yield for 100 cycles at operating pressure and 100 cycles unpressurized. The torsional load test setup is depicted in Figure III-7. The torsional strength was determined by testing two specimens to failure. The pressurized specimen failed at a torque loading of 16.3 kg-m (118 ft-lb) and the unpressurized specimen failed at 9.7 kg-m (70 ft-lb). The nature of the failure was buckling in the Inconel tube liner. The remaining specimens were tested at 10.8 kg-m (78 ft-lb) while pressurized and 6.4 kg-m (46 ft-lb) unpressurized (100 load cycles for each pressure condition). After the cycle testing was completed, all of the specimens were examined under 10X magnification and leak tested. No degradation in the overwrap or leakage was found.

Bending load test. - The bending load test consisted of applying a load in a normal direction to one end of the test specimen while the other end was held rigid. The loads were measured by a load cell, as shown in Figure III-8, and the deflection was measured. The yield and ultimate loads were determined by subjecting specimens to loads that resulted in yield and ultimate failure. The yield load was 20.5 kg-m (148 ft-lb) with the tube unpressurized. The ultimate load was 31.4 kg-m (227 ft-lb) with the tube pressurized and 29.7 kg-m (215 ft-lb) with the tube unpressurized. The remaining tubes were cycled 100 times unpressurized and 100 times pressured with a bending load of 15.8 kg-m (114 ft-lb). The specimens, which were subjected to the 200 bending load cycles, were leak tested and no leaks were found. The yield test specimen had a small leak after yielding. The ultimate test specimens had ruptured liners. Both the yield and ultimate test specimens failed by buckling the Inconel liner at the point of maximum moment (fixed end, liner-to-end fitting interface).

Salt fog test. - Three of the test specimens, consisting of one overwrapped with S-glass, one with graphite, and one with Kevlar, were subjected to a salt fog environment in accordance with MIL-STD-810B, Method 509, Procedure I. The S-glass over-

wrapped test specimen also incorporated aluminum-to-stainless steel end fittings fabricated by the inertia welding process. The salt fog test consisted of subjecting the test specimens to an environment of 85% humidity, 308°K (95°F), and salt fog atomized from a 5% salt solution for a period of 48 hours. During the test, the ends of the test specimens were capped and the aluminum-to-stainless steel dissimilar metal joint was covered with a protective coating of R.T.V. 106 silicone rubber adhesive sealant. After the test, the test specimens were examined visually, proof pressure tested, and leak tested. There was no leakage or apparent degradation. Photographs of the test specimens taken immediately after removal from the test chamber are shown in Figure III-9. A section of the R.T.V. coating was removed from the aluminum-to-stainless steel joint (fig. III-10). The coating did an excellent job of protecting the joint from the corrosive atmosphere. The uncoated portion of the aluminum end fitting and the tube cap were severely corroded as expected.

Storable propellant test. - Two of the test specimens were filled with UDMH (storable fuel) and one specimen was filled with N_2O_4 (storable oxidizer) for a period of 32 days. After this exposure the specimens were flushed, cleaned, and inspected visually for degradation. There was none. The configurations subjected to the storable propellants were as follows:

UDMH	One specimen overwrapped with S-glass. End fittings were aluminum-to-stainless steel made by the coextrusion process.
UDMH	One specimen overwrapped with graphite. End Fittings were conventional stainless steel.
N_2O_4	One specimen overwrapped with Kevlar. End fittings were conventional stainless steel.

Each of the test specimens was subjected to an operating pressure leak test with gaseous helium. The leakage rate was zero as measured with a CEC mass spectrometer leak detector.

Burst test. - The three test specimens were then subjected to a hydrostatic burst test. The results were as follows:

Burst Pressure	Specimen Configuration
1117 N/cm^2 (1620 psig)	S-glass overwrap with aluminum-to-stainless steel end fittings.
1241 N/cm^2 (1800 psig)	S-glass overwrap with stainless steel end fittings.
1158 N/cm^2 (1680 psig)	Kevlar overwrap with stainless steel end fittings.

Analysis of Test Results

The fabrication and test results were analyzed to determine the advantages and disadvantages of the different overwrap materials and the different types of end fittings. The basis of evaluation was weight, cost, fabrication ease, structural capability, and appearance. The test results were also compared to the theoretical structural capability of the test specimens.

Overwrap materials. - The evaluation of the three overwrap materials (S-glass, graphite, and Kevlar-49) is summarized in Table III-2. This evaluation indicates that Kevlar-49 is the most desirable overwrap material, and that S-glass or graphite are also acceptable for application on the Space Tug propellant feedlines.

End fittings (dissimilar metal joints). - The four types of end fittings produced were (1) all stainless steel, (2) aluminum-to-stainless steel made by explosive bonding, (3) aluminum-to-stainless steel made by inertia welding, and (4) aluminum-to-stainless steel made by coextrusion. The stainless steel end on all end fittings was welded directly to the Inconel 718 tubing liners by resistance welding. The all stainless steel end fittings were of a conventional design and were the simplest to produce. Of the three dissimilar metal end fittings the explosive bonded type required the most development and the inertia welded type, the least. Excellent quality was achieved on all three types of joints and all joints performed equally well in test. None of the joints was destroyed. Successful completion of the test program demonstrates that dissimilar metal joints offer excellent potential for weight reduction in flanged joints. Inertia welding appears to be the most promising joining process at this stage in development.

Comparison of actual vs theoretical structural capability. - The test results were compared with theoretical values for torque loading, bending, and burst pressure.

(1) Torque loading: A description of the torque tests is included in the discussion of the subscale specimen test program. The allowable stress and torque for a thin walled tube can be calculated from

$$S_S = KE\left(\frac{t}{r}\right)^{1.35}* \qquad (1)$$

and

$$T = S_S \pi 2r^2 t* \qquad (2)$$

*Roark, Third Edition

where: T = Torque, kg-m (ft-lb)
r = Radius, 2.935 cm (1.15 in.)
t = Liner thickness, 0.013 cm (0.005 in.)
S_S = Circumferential shear stress, N/cm^2 (lb/in^2)
K = Constant, 0.61 based on L/r = 5
E = Young's modulus, 20×10^6 N/cm^2 (29×10^6 lb/in^2)

Considering the metal liner only (no overwrap) the values are

$$S_S = 7{,}805 \text{ N/cm}^2 \text{ (11,322 lb/in}^2\text{)}$$

and

$$T = 5.4 \text{ kg-m (39.2 ft-lb)}$$

Torque loading tests performed with the test item pressurized at operating pressure resulted in yielding at a torque of 16.3 kg-m (118 ft-lb). The test item yielded at 9.7 kg-m (70 ft-lb) when not pressurized. Both tests were performed at ambient temperature. It was concluded from this analysis that (1) torque capability of the tube was increased by a factor of 1.8 due to the composite overwrap on the unpressurized test specimen, (2) overwrap on the pressurized test specimen increased torque capability a factor of 3, and (3) special preparation of the end fittings is required to improve load sharing; methods of end fitting preparation for load sharing were developed under a previous contract, ref. 1.

(2) Bending load: A description of the bending tests is included in the discussion of the subscale specimens test program. The bending moment for thin-walled tubes at which elastic buckling occurs is given by

$$M = K\left(\frac{E}{1 - \nu^2}\right) r t^{2*} \qquad (3)$$

where: M = Moment, kg-m (ft-lb)
K = 1.15
ν = Poisson's ratio, 0.3
E = Young's modulus, 20×10^6 N/cm^2 (29×10^6 lb/in^2)
r = Radius, 2.905 cm (1.15 in.)
t = Liner thickness, 0.013 cm (0.005 in.)

Considering the metal liner only (no overwrap) the allowable bending moment is calculated to be 11.9 kg-m (86.6 ft-lb). Bending load tests were performed on pressurized and nonpressurized test specimens until a

*Roark, Third Edition

yield failure occurred. In both cases the failure occurred in the metal liner with no damage to the overwrap. The moments applied at failure were as follows:

M (Metal liner failure) = 31.4 kg-m (227 ft-lb) specimen pressurized to 21 N/cm^2 (30 psig)

= 29.7 kg-m (215 ft-lb) specimen unpressurized

It was concluded from this analysis that (1) the composite overwrap increased the bending load capability by approximately 2.5 times over that of a nonoverwrapped line, (2) pressurizing the composite tube to operating pressure increased bending load capability approximately 5%, and (3) special end fitting preparation results in a significant increase in composite overwrap load sharing as reported in ref. 1.

(3) Burst pressure: The test specimen's burst pressure can be predicted by the relation

$$S = \frac{pr}{t} \text{ (hoop)} \tag{4}$$

and

$$S = \frac{pr}{2t} \text{ (axial)} \tag{5}$$

where: S = Stress, N/cm^2 (lb/in^2)
p = Burst pressure, N/cm^2 (psi)
r = Tube radius, cm (in.)
t = Tube thickness, cm (in.)

The effect of the composite overwrap is to prevent a hoop failure and force a failure in the axial direction. This results in doubling the pressure carrying capability over that of an unwrapped tube. The anticipated burst pressure is calculated as follows:

Assumptions:

Weld efficiency = 90%

Ultimate stress for Inconel 718: S = 143,395 N/cm^2 (208,000 lb/in^2)

Failure will occur axially.

$$p = \frac{143{,}395 \times .9 \times 2 \times 0.013}{2.92} = 1149 \text{ N/cm}^2 \text{ (1666 psig)}$$

Three test specimens were burst tested at ambient temperature. The pressures recorded at burst were 1117, 1241, and 1158 N/cm^2 (1620, 1800, and 1680 psig). The burst pressure results were almost exactly as predicted. Burst tests results on previous programs show that axial load can be transferred to the overwrap by special end fitting preparation, ref. 1.

IV. DESIGN

The design task consisted of producing detail and assembly designs for the composite feedlines, the all-metal feedline, the test fixtures, and a tool for filament winding curved composite tubing. Extensive evaluation of competitive feedline design concepts was performed to provide a sound basis for design as discussed in Chapter II. The feedline configuration developed is representative of a full-scale cryogenic Space Tug design. The selected configuration incorporates both straight and curved line sections, a short radius elbow, a tee junction, gimbals, and flanged joints. The design demonstrates the capability of incorporating virtually any routing or configuration requirement. The design operating and/or physical criteria are defined in Table IV-1. The test fixture design is not discussed herein; however, schematics and/or photographs of the test fixtures are included in Chapter VI, Testing.

Assembly

The composite and all-metal feedline assemblies have an identical routing configuration, as shown in Figure IV-1. The assemblies consist of three individual line segments that are joined together by bolted, flanged connections. A tee junction, located in the middle line section, is representative of a typical fill and drain port. The tee junction was sealed by a blind flange during test. The assembly incorporates three gimbal joints to accommodate for relative motions between the feedline and the surrounding structure. The gimbal joints were a standard product of SSP Products, previously used on the Saturn SIVB stage in the LH_2 vent line. The gimbals are 10.2 cm (4 in.) diameter socket-type joints capable of $\pm$ 0.09 radian ($\pm$ 5°) motion in any direction, and a 36.5 N/cm^2 (53 psig) proof pressure. The feedline assemblies are designed to interface with a prevalve at either end of the line, i.e., prevalve located at the LH_2 tank interface or at the engine turbo pump interface.

Curved Liner Assemblies

The configurations of the individual line segments are detailed in Figure IV-2. The intermittent line curvatures were selected as opposed to a smooth radius curve to take advantage of existing tube bending tooling. The all-metal feedline design uses 0.076 cm (0.030 in.) thick stainless steel tubing, roll formed and welded with a single longitudinal seam and bent to the required curvature. Two competitive designs were produced for the composite feedline metal liners. The first design used 0.013 cm (0.005 in.) thick Inconel 718 tubing roll formed, seam welded,

and bent, and the second design used 0.076 cm (0.030 in.) thick Inconel 718 tubing chem-milled to 0.013 cm (0.005 in.) after bending. The flanges were designed for welding to the tubing liners after bending and chem-milling as depicted in Figure IV-2. The heat treating specification for the Inconel 718 tubing liners was as follows: Heat treat and age harden in a vacuum furnace at 0.07 N/m^2 (5×10^{-4} torr). Wrap the Inconel 718 in 0.003 cm (0.001 in.) thick tantalum foil to prevent discoloration (stainless foil may be substituted for the tantalum). Heat to 1228°K (1750°F) for one hour, then Argon quench to 367°K (200°F). Age at 1033°K (1400°F) for five hours. Heat treating was specified to be done after bending and before chem-milling.

Composite Overwrap

The composite overwrap specifications for filament winding and braiding are defined in Table IV-2. Line segments were overwrapped with each process for a comparative evaluation as discussed in Chapter VI, Testing.

A tool was designed for applying the composite overwrap on the curved line sections. A polar winding concept was used, i.e., the tool provided for the spool of preimpregnated roving to rotate around the fixed tube as the spool traversed the length of the tube from one end to the other and back. The drive mechanism was mounted on a swing arm with the center of rotation equal to the radius of the tube being overwrapped. The center of rotation can be changed to accommodate tubes of different radii. Photographs of this equipment and further discussion of its operation are included in Chapter V, Fabrication.

V. FABRICATION

One all-metal and three composite overwrapped feedline assemblies were fabricated in accordance with the design depicted in Chapter IV. The major fabrication steps consisted of (1) metal liner forming and bending, (2) heat treating, (3) chem-milling, (4) flange machining and welding to the metal liners, (5) leak testing, and (6) applying the composite overwrap. Composite and all-metal line fabrication was identical except that chem-milling and composite overwrap was not required for the all-metal configuration.

Metal Liner Fabrication

The fabrication of the metal tubing liners was subcontracted to the SSP Products, Inc., Burbank, California. Initially, two metal liner design concepts were pursued concurrently. The first design involved bending thin 0.013 cm (0.005 in.) wall tubing to the required curvature and the second design involved bending heavier 0.076 cm (0.030 in.) tubing and then chem-milling to the required thickness. Early attempts in thin-tube bending failed and led to the decision to use the chem-milling approach for the feedline assemblies. Thin bending process development continued throughout the program and a tube of 10.2 cm (4 in.) diameter by 0.015 cm (0.006 in.) wall Inconel 718 of acceptable quality was produced.

Tube Bending

The thick wall tube bending operation was performed on a standard bending machine using standard procedures at the SSP Products, Inc., Burbank, California. The tubes were annealed before bending and heat treated after bending. The major steps involved in the tube bending procedure are listed in the following tabulation. A typical tube bending setup is shown in Fig. V-1.

(1) The fixed end of the tube is clamped in the bending machine as shown;

(2) A ball-socket train consisting of a series of interlocking hemispheres is inserted inside the tube to provide radial support in the bend. The ball sockets are free to swivel, one within the other, and are connected by a cable passing through their centers;

(3) The ball sockets are pulled incrementally through the tube as the wiper die is moved along the tube forcing it to the contour of the inside radius mandrel. The

ball sockets provide support to the tube preventing collapse and smoothing out small wrinkles as they develop.

Numerous attempts were made at bending the thin-wall tubing with a variety of methods used to provide tube support to prevent wrinkling. The initial bending attempt consisted of bending a 5 cm (2 in.) diameter by 0.013 cm (0.005 in.) Inconel tube around a 38 cm (15 in.) radius. This bend was of good quality, see Fig. V-2. A description of the 10 cm (4 in.) diameter tube bending attempts is provided in the following tabulation.

(1) A tight fitting 0.64 cm (0.25 in.) thick aluminum tube was placed inside the thin Inconel tube to provide internal hoop support and prevent wrinkling. It was planned to remove the aluminum tube after bending by etching. The ball-socket train was used inside the aluminum tube. The bending was not successful. Severe wrinkles developed on the inside radius of the thin tube.

(2) Another bending approach consisted of using an aluminum support tube on the outside of the thin tube. This was not successful.

(3) Another approach used an aluminum support tube on both the inside and the outside of the thin tube; i.e., the thin tube was sandwiched between the thicker tubes. The approach was not successful.

(4) The tube was filled with oil and pressurized during bending; the attempt was not successful.

(5) All the bending tooling was reworked to improve precision before the next attempt. Also, the material annealing process was modified to assure a softer starting material. One successful bend of acceptable quality was achieved using the standard bending procedure for thicker wall tubing. Photos of some of the unsuccessful results and the high quality bent tube are provided in Figure V-2. The thin bending development was stopped at this point because of funding limitations.

Chem-milling Tubing Liners

The chem-milling operation was subcontracted to Aerochem, Inc., Orange, California. The basic elements of construction before chem-milling consisted of roll forming 0.076 cm (0.030 in.) thick Inconel 718 in a 10.2 cm (4 in.) diameter by 183 cm (72 in.) tube, fusion welding a single longitudinal seam, annealing, bending the tube on a nominal 128.5 cm (50.6 in.) radius over the required angle, and heat treating.

The initial chem-milling tube configuration is depicted in Figure V-3. After chem-milling the first tubes, an evaluation was performed to determine wall thickness acceptability. Using the eddy current process, the wall thickness was measured over every square inch of tube along the major, minor, and neutral axes and around the tube circumference (see Figure V-4). As shown, the chem-milled wall thickness varied from 0.015 to 0.043 cm (0.006 to 0.017 in.). The plot along the minor axis shows the thinnest areas to be located in the flat sections between the bend segments and the thicker areas to be located at the inside radius of the bends and at the ends. The major axis plot shows the thinner areas to be located at the outside radius of the bends and the thicker areas located between the bends. The neutral axis plot shows the material to be of comparatively uniform thickness, varying only from 0.036 to 0.043 cm (0.014 to 0.017 in.). The chem-milled thickness variations were compared to the variation in the material before chem-milling, which were as follows:

(1) Flats were 0.010 cm (0.004 in.) thinner than the inside radius of the bends along the minor axis.

(2) Flats were 0.008 cm (0.003 in.) thicker than the outside radius of the bends along the major axis.

(3) Allowable raw material variation before tube bending = 0.004 cm (0.0015 in.).

Superimposing these material variations on the chem-milled thickness plots shows that the chem-milling variation between the flats and the bends closely follows that of the parent material. This does not, however, explain the large variation between the flats on the major and minor axes, 0.036 to 0.015 cm (0.014 to 0.006 in.) thick, respectively. It is believed that this variation was caused by the orientation of the tube in the chem-milling solution as shown in Figure V-5.

The overall variation in thickness from 0.015 to 0.043 cm (0.006 to 0.017 in.) was not considered acceptable. The remaining tubes were selectively masked during the chem-milling operation to obtain a more uniform tube wall thickness. This produced excellent results with the material thickness on these tubes controlled to 0.013 to 0.023 cm (0.005 to 0.009 in.). An additional change to the procedure was implemented after the fourth tube was chem-milled. This consisted of providing a two-step weld land along the longitudinal seam weld and at the ends, as shown in Figure V-3. The purpose of this change was to reduce the stress riser caused by the abrupt change in material thickness at the weld land.

Tee Junction in the Metal Tubing Liner

A tee junction was provided in the middle line section of each feedline assembly. Standard fabrication processes were used in producing the tee. As illustrated in Figure V-6, the fabrication technique consisted of cutting an undersized hole in the tube, pulling a spherical forming tool through the hole forming a smooth cylindrical junction with the main line, trimming, and welding to the smooth cylindrical section.

Composite Overwrap

Two completely different processes were used in applying the composite overwrap to the curved metal tubing liners. The first process consisted of filament winding and the second used a braiding process developed by McDonnell Douglas Astronautics. All but two of the curved line sections were overwrapped by filament winding.

Filament winding curved tubes. - The polar winding tool shown in Figure V-7 was designed and fabricated for the purpose of applying the composite overwrap on curved line segments. Figure V-8 shows the tool in operation. The tubes were overwrapped while pressurized with 13.8 N/cm^2 (30 psig) GN_2.

The overwrap consisted of Kevlar 49 DP-01 applied at a rate of 4.7 turns per cm (12 turns per inch) under 1.4 kg (3 lb) wrap tension*. The Kevlar was preimpregnated with 58-68R epoxy. Longitudinal strips of Kevlar roving were placed at equal spaces around the tubes between the hoop layers of overwrap, resulting in a wrap pattern consisting of layers of 1 hoop - 1/2 longitudinal - 1 hoop. The overwrap on the tee sections was applied by hand layup using S-glass Cloth 181, also impregnated with 58-68R epoxy. The overwrapped tubes were cured at 338°K (150°F) for 1.5 hours and 422°K (300°F) for 4 hours. The tubes were pressurized at 21 N/cm^2 (30 psig) GN_2 during cure.

Braided overwrap on curved tubes. - Two curved tubes were overwrapped by a braiding process much like that used to apply braided shielding on flexible hoses and electrical wiring. The curved tube configurations were identical to the tubes overwrapped with filament winding. The overwrap consisted of two layers of S-glass 20 end roving with a 1.2 rad (35°) braid angle. The roving was applied to the tube dry and 58-68R epoxy was brushed on

*The overwrap machine provides adjustment for presetting the tension in the Kevlar roving as it is applied to the tube. The tension in the roving is determined by the internal tube pressure so that the internal pressure and the external force from the overwrap balance.

after the first and after the second layer of wrap. The tubes were pressurized to 21 N/cm^2 (30 psig) and cured to the same procedure as the filament wound tubes. In-process photos of the braiding are provided in Figure V-9.

VI. TESTING

The test program was conducted in two parts. The first part consisted of structural testing of individual curved composite line segments, overwrapped by both filament winding and braiding processes. This testing was conducted early in the program to determine any inherent advantages in either of the two methods of applying the composite overwrap and to assure the integrity of the curved composite line concepts. The tests consisted of (1) proof pressure and leakage, (2) strain versus internal pressure, (3) deflection versus internal pressure, (4) load versus deflection, and (5) thermal cycle. The second part of the testing program subjected full scale feedline assemblies to a series of tests, representative of flight hardware qualification. Performance data for both composite and all-metal designs was obtained. In all, one all-metal and three composite feedline assemblies were tested. The tests consisted of (1) proof pressure and leakage, (2) steady state heat input, (3) chilldown and flow quality, (4) thermal cycling, (5) acoustics, and (6) burst pressure. A matrix showing the tests that were completed on the individual line segments and feedline assemblies is provided in Table VI-1.

Composite Line Segments Proof Pressure and Leakage Tests

Before the start of structural testing the composite line segments were subjected to a proof pressure with GN_2 at 31 N/cm^2 (45 psig), (1.5 x operating pressure). Also before and after completion of each structural test the lines were leak tested with GHe. All lines remained leak free (leakage less than 3×10^{-10} scc/sec GHe) throughout the test program.

Composite Line Segments Strain Versus Internal Pressure Test

The purpose of this test was to determine the stress/strain characteristics of composite overwrapped curved tubing when subjected to internal pressure at ambient and cryogenic temperatures. The test specimens were instrumented with 12 biaxial strain gages located as shown in Figure VI-1. The specimens were then installed in a test fixture that provided rigid support at one end, and no support at the other end, as shown in Figure VI-2. The test specimens were pressurized to proof pressure 31 N/cm^2 (45 psig), first with GN_2 and then with LN_2. The strain gages were continuously recorded during the pressurization and depressurization cycles.

The strain versus pressure data for the filament wound and braided test specimens at ambient temperature are plotted in Figure VI-3, from which the following observations can be made.

(1) Comparing the two overwrap techniques, there is no consistent pattern of higher strain for either the filament wound or braided tubes.

(2) Four axial strain gages indicated compression loading. Three of these gages were located on the neutral axis opposite the weld land, which was not chem-milled.

(3) The highest recorded strain (ξ) was 450 cm/cm (in./in.), indicating a hoop tension loading. The resulting stress (S) in the liner is calculated by

$$E = \frac{S}{\xi} \tag{6}$$

$S = 0.00045 \times 20 \times 10^6 = 9000$ N/cm^2 (13,000 lb/in^2).

The allowable stress for hoop loading should be about 103,000 N/cm^2 (150,000 lb/in^2), thus indicating a safety factor of about 11. The highest recorded axial compressive strain was 170 cm/cm (in./in.) resulting in a compressive stress of 3400 N/cm^2 (4930 lb/in^2). Tests have shown that the actual buckling strength of thin wall tubing is given by

$$*S_b = 0.3\ E\ (\frac{t}{r}) \tag{7}$$

$$S_b = \frac{0.3 \times 20 \times 10^6\ (0.015)}{5.08} = 17{,}700\ \text{N/cm}^2\ (25{,}700\ \text{lb/in}^2)$$

indicating a safety factor of approximately 5 at proof pressure.

(4) Most of the strain gages indicated a strain in the hoop direction approximately double the strain in the axial direction. This is an indication that the overwrap is sustaining little load at these strain gage locations. There were some locations, however, where the axial and hoop strains were about equal, and other locations where the axial strains were greater than the hoop. Larger strains in the axial direction can be explained by the overwrap thickness variation. The overwrap on the filament wound tubes is thicker at the inside bend radii (strain gage locations 5 and 12). In addition, there is variation in the overwrap thickness near the flanges on both tubes (strain gage locations 1, 3, 5, 7, 9, and 11).

*Ref. Rourk, Formulas for Stress and Strain, Third Edition, Table XVI, Case M.

At these locations, the overwrap is sustaining most of the hoop loading and little axial loading.

Composite Line Segments Deflection Versus Internal Pressure Test

The purpose of this test was to determine the deflection characteristics of composite overwrapped curved tubing when subjected to internal pressure at ambient and cryogenic temperature.

This test was run concurrently with the strain versus internal pressure test. The unrestrained end flange deflection was measured during pressurization at 3.4 N/cm^2 (5 psi) increments from 0 to 21 N/cm^2 (0 to 30 psig) using dial indicators. The free end deflection versus internal pressure data for the filament wound and braided composite tubes at ambient and LN_2 temperature is plotted in Figure VI-4. The following observations are made from the tests data:

(1) At ambient temperature, the braided tube free end deflection was approximately 46% of the filament wound tube deflection.

(2) At LN_2 temperature, the braided tube free end deflection was approximately 31% of the filament wound tube deflection.

(3) When pressurized to 21 N/cm^2 (30 psig) at LN_2 temperature, the filament wound tube free end deflection increased by 15% over the deflection at ambient temperature.

(4) When pressurized to 21 N/cm^2 (30 psig) at LN_2 temperature, the braided tube free end deflection decreased by 19% compared to the deflection at ambient temperature.

The differences in deflection characteristics between the filament wound and braided composite tubes result from the following hardware differences:

(1) A variation in metal liner wall thickness between the test specimens exists due to the chem-milling process. The wall thickness of both test specimens varied between 0.015 cm (0.006 in.) and 0.025 cm (0.010 in.). The location of the thin/thick areas, however, is random, i.e., not in the same location for each tube.

(2) The different overwrap materials and overwrapping processes were responsible for the large differences in deflection characteristics between ambient and LN_2 temperatures. The Kevlar 49 overwrap on the filament wound tubes

provides less restraint when cold, due to the negative coefficient of expansion. The S-glass overwrap on the braided tubes provided more restraint when cold.

(3) The braided composite tube was stiffer than the filament wound tube at both ambient and LN_2 temperatures and was one pound heavier. The deflection characteristics are functions of overwrap material and thickness, and the overwrap selection should be based on controlling design conditions; i.e., minimum weight, minimum deflection, etc. Both test specimens are considered acceptable for Space Tug application.

Composite Line Segments Load Versus Deflection Test

The purpose of the load versus deflection test was to determine the structural characteristics of the composite overwrapped curved tubing when subjected to external bending loads. The testing was performed on composite overwrapped curved line sections, one each overwrapped by filament winding and by the braiding process. For this test one end of the composite tube was supported rigidly while loads were applied at the other end in 0.45 kg (1 lb) increments. The loads were applied in each of three axes and controlled through a load cell. The three-axes deflection was monitored during application and removal of the load. The test was performed with the tube pressurized to 21 N/cm^2 (30 psig) and unpressurized. The test setup is depicted in Figures VI-5 and VI-6.

The load versus deflection data for the unpressurized and pressurized conditions for both the filament wound and braided composite tubes is plotted in Figure VI-7. A comparison of the load versus deflection at 4.5 kg (10 lb) loading is tabulated in Table VI-2. The following observations are made from the load versus deflection curves and tabulated data:

(1) The stiffness of the filament wound tube is increased by approximately 50% in the Y and Z directions when pressurized to 21 N/cm^2 (30 psig). Pressurization provides a small increase in stiffness in the X direction.

(2) The stiffness of the braided tube is increased by approximately 40% in the Y and Z directions when pressurized to 21 N/cm^2 (30 psig). Pressurization provides a small increase in stiffness in the X direction.

(3) At zero pressure the braided tube was approximately 30% stiffer than the filament wound tube in all axes except the axial compression axis.

(4) At 21 N/cm^2 (30 psig) the braided tube was stiffer in all axes by an average of 14%.

(5) It may be concluded from observations (3) and (4) that pressurization of the braided tube had less effect on stiffness than it did on the filament wound tube.

(6) The deflection curves show some motion in the Z axis when the tubes were loaded vertically. This was anticipated because of the weld land along the neutral axis on one side of the tube.

Feedline Assemblies Proof Pressure and Leakage Tests

At the start of the testing program each of the four feedline assemblies was subjected to a proof-pressure test that consisted of pressurizing to 31 N/cm^2 (45 psig) with gaseous nitrogen and maintaining the pressure for five minutes. After depressurizing, each line was visually examined for signs of damage or degradation; none was noted. After proof pressure and each of the following tests, the feedline assemblies were leak checked with a helium mass spectrometer while pressurized with helium at 21 N/cm^2 (30 psig) and at ambient temperature. No leakage was detected during any of the leak tests.

Feedline Assemblies Steady State Heat Input Test

The S/N 1 composite and S/N 4 all-metal feedline assemblies were subjected to this test. The objectives of the test were (1) to measure the heat leakage to the feedlines in a simulated space environment, and (2) to provide heat leak data for comparison of the composite and all-metal feedlines under identical conditions. The test configuration is shown in Figure VI-8. Engine soakback was simulated by an electric heater. The feedline assemblies and the support structure were instrumented with thermocouples located as shown in Figure VI-8. An antigeysering device, consisting of a 6.98 cm (2.75 in.) diameter flexible stainless steel tube, was installed concentrically in the feedline assembly to assure that zero quality liquid hydrogen was maintained in the feedline during the test. The feedline was wrapped with two layers of multilayer insulation (MLI) to control the surface emissivity.

The vacuum chamber pressure was 3.9×10^{-2} N/m^2 (3×10^{-4} torr) during the test. The test was performed by filling the cryogen supply tank and the feedlines with liquid hydrogen, and measuring the boiloff with a flowmeter. The boiloff hydrogen gas was heated to ambient temperature upstream of the flowmeter by a heat exchanger.

A tare run to determine the heat losses which can be attributed to the supply tank and the support structure was performed before installing the feedlines. The boiloff rate was determined by subtracting the tare run boiloff from the total boiloff obtained during the tests. The boiloff data with the tare subtracted out for the composite and all-metal feedlines is plotted in Figure VI-9a. The average boiloff rate was determined at the time when the temperature of the support structure and the feedline were at a near steady state condition, or at time = 150 minutes to 180 minutes. See Figure VI-9b. The average boiloff rates over this period were nearly identical for the composite and the all-metal feedlines. The results are as expected for the configuration tested. A test configuration consisting of a dry feedline penetrating a cryogenic storage vessel would have shown a greater difference in boiloff rates due to the lower axial thermal conductivity of the composite feedline. The configuration tested (feedline full of liquid hydrogen to the engine interface) did not take advantage of the low axial thermal conductivity of the composite feedline.

Feedline Assemblies Chilldown and Flow Quality Tests

The objective of the chilldown and flow quality test is to determine the time required to cool down the composite and all-metal feedlines and obtain zero quality cryogen at the engine interface.

The feedline assemblies were installed in the thermal vacuum chamber and instrumented with pressure and temperature transducers, as shown schematically in Figure VI-10. The feedline configuration was identical to that of the previous test except that the anti-geysering line was removed. The pressure in the vacuum chamber was 1×10^{-2} N/m^2 (8×10^{-5} torr) during the test. The liquid hydrogen was supplied from an insulated tank, pressurized to 30 N/cm^2 (44 psig), through a short insulated line to the feedline. The insulated line contains a flow metering orifice and a flow control valve. The test was performed by opening the flow control valve and flowing liquid hydrogen through the feedline and outlet orifice to the vent. Continuous data recordings of the tank top pressure, pressure at the inlet orifice, and pressure at the outlet orifice were obtained. The feedline chilldown time (time to achieve zero quality flow at the outlet orifice) is the time required for the pressure at the outlet orifice to reach the saturation pressure of liquid hydrogen. Critical test data are plotted in Figure VI-11, which shows the chilldown time to be 0.2 sec for the composite and 0.4 sec for the all-metal feedline assembly. The liquid hydrogen mass flow rate during the test is plotted in Figure VI-12. The higher flow rate experienced by the all-metal feedline was due to the slightly higher tank top pressure maintained during the run. See Figure VI-11.

Feedline Assemblies Strain Cycling Test

Composite feedline assemblies S/N 2 and S/N 3 were subjected to the strain cycling test. The objective of the test was to demonstrate that the composite feedline assemblies could survive 200 pressure/temperature cycles without structural failure. The test consisted of prechilling the feedlines with LN_2, then filling with LH_2 until the temperature stabilized at 21°K (-423°F), pressurizing the lines to 21 N/cm^2 (30 psig), venting to ambient pressure, and purging with hot GN_2 until the line temperature reached ambient. This cycle was repeated 200 times. Photographs of the test setup are provided in Figure VI-13. The test on the two assemblies was performed concurrently. The lines were enclosed by a helium purged polyethylene bag during the test (fig. VI-14). After the cycling was completed the feedline assemblies were leak tested and visually inspected. There were no leaks and no visible evidence of degradation.

Composite Feedline Assembly Acoustic Test

The purpose of the acoustic test was to demonstrate that a composite feedline assembly can withstand the liftoff and boundary layer environments of a typical Space Tug mission.

The acoustic test was performed on composite feedline assembly S/N 3 while filled with LN_2. The test setup is depicted in Figures VI-15 and VI-16, which show the feedline installed in the test support structure. The shroud, shown at top of the photographs, was lowered during the test. The instrumentation consisted of a control microphone, thermocouples, and triaxial accelerometers mounted on the feedline flanges as shown in Figure VI-17.

Typical sound pressure level plots of the liftoff and boundary layer environments are depicted in Figures VI-18 and VI-19. The liftoff environment consisted of an 8-minute exposure of 153 dB and the boundary layer environment was a 150-dB exposure for 29 minutes. Typical plots of the accelerometer data are provided for the liftoff and boundary layer environments in Figures VI-20 and VI-21. The highest loading was 3 grms along the vertical axis by accelerometer 2. See Figure VI-17.

After completion of the acoustic test the feedline assembly was leak tested and visually inspected. There was no leakage and no evidence of structural degradation.

Burst Test

The composite feedline assemblies S/N 2 and S/N 3 were subjected to an ambient temperature pressure test of 83 N/cm^2 (120

psig), which is four times the operating pressure of 21 N/cm^2 (30 psig). The feedlines were inspected and leak tested after the pressure test. There was no leakage or degradation. Then individual line sections of the feedline assembly were pressurized with water and GN_2 until rupture. The results were as follows:

(1) The composite line section containing a gimbal joint ruptured at 283 N/cm^2 (410 psig). The rupture occurred in the gimbal joint, which was rated at 37 N/cm^2 (53 psig) proof pressure. A photograph of the failure is shown in Figure VI-22. The composite line was not damaged by this test, except for the gimbal.

(2) The curved filament wound composite line section experienced buckling failures at 331 and 538 N/cm^2 (480 and 780 psig), i.e., the curved line segment tended to straighten as shown in Figure VI-23. Pressurization was continued until rupture occurred at 696 N/cm^2 (1010 psig). The rupture, as shown in Figure VI-24, started along the edge of the weld land.

(3) The curved braided composite line section ruptured at 651 N/cm^2 (945 psig). The rupture occurred along the edge of the weld land as shown in Figure VI-25. The braided composite line did not experience a buckling failure prior to rupture.

VII. ANALYSIS OF RESULTS

Composite feedline readiness for application to the Space Tug system is evaluated on the basis of system weight and operational characteristics as compared to system design requirements.

System weight. - The feedline system weight is the sum of the weight of the feedline plus the weight of the insulation system, plus the weight of the propellant lost due to thermal boiloff during the space mission.

The composite feedline assemblies produced on this program are representative of a full scale Space Tug LH_2 feedline. The assemblies were made up of three individual line segments with bolted flange joints to facilitate shipping and handling. Each assembly also contained three stainless steel gimbal joints and one flanged tee junction. The weight of each of three composite and one all-metal feedline assemblies produced and tested during this program is listed in the following tabulation. Also shown is a feedline weight of identical one piece construction, i.e., without the flanged joints. The flanged joints may be required on Space Tug to facilitate assembly but are not required for feedline producibility considerations.

	Assembly Weight, kg (lb)	Assembly Weight Without Flanged Joints, kg (lb)*
S/N 1 Composite	13.3 (29.4)	11.5 (25.1)
S/N 2 Composite	13.7 (30.3)	11.7 (25.9)
S/N 3 Composite	13.4 (29.6)	11.5 (25.3)
S/N 4 All-metal	17.0 (37.5)	15.0 (33.2)

*Weight includes flanged joint at the LH_2 tank and prevalve interface. The feedline weight could be reduced by an additional 0.7 kg (1.6 lb) by the use of aluminum/stainless steel bimetallic joints at these interfaces.

The insulation system for the Space Tug LH_2 feedline will be determined on the basis of a wet or dry design and may be the same for either the composite or all-metal feedline. A wet design is one in which the prevalve is located at the engine and a dry design has the prevalve located at the LH_2 tank interface.

The propellant boiloff losses during the space mission include the loss due to feedline chilldown, conduction, and radiation. It is concluded from the thermal testing performed (chilldown and flow quality tests and steady state heat input tests) that there is no significant difference in the boiloff losses between the composite and all-metal feedlines. This conclusion

however is only valid for the wet feedline configuration tested (feedline full of liquid hydrogen to the engine interface). The composite feedline will contribute less boiloff losses than the all-metal feedline in configurations where the axial conductivity is a significant factor, as is the case with cryogenic tank penetrations.

Operational characteristics. - The feedline design operating and/or physical conditions are:

Operating pressure	20.7 N/cm^2 (30 psia)
Proof pressure	41.4 N/cm^2 (60 psia)
Burst pressure	62.1 N/cm^2 (90 psia)
Diameter	10.2 cm (4.0 in.)
Maximum g-loading	X - Axis + 3g
	Y - Axis + 1g
	Z - Axis + 1g
Shuttle cargo bay	200°K (-100°F) minimum
Internal wall temperatures	376°K (+200°F) maximum
Acoustics	OSAPL 155 dB liftoff
	OSAPL 149 dB boundary layer

The composite feedlines were pressure tested as assemblies at 82.7 N/cm^2 (120 psig) without degradation. The composite line pressure capability is a function of the gimbal joint strength. The gimbals used in the test item failed at 283 N/cm^2 (410 psig). The curved composite lines with braided overwrap achieved a pressure of 652 N/cm^2 (945 psig) before failure. The calculated burst pressure for an all-metal (stainless steel) line of the same configuration is 324 N/cm^2 (470 psig).

The composite feedlines were 10.2 cm (4 in.) diameter in accordance with the design criteria. An average mass flow rate of 3.4 kg/sec (7.5 lb/sec) was recorded during the chilldown and flow quality testing.

The composite used for overwrapping the feedlines will withstand temperatures in excess of 450°K (350°F) without degradation.

Acoustic testing was performed on the composite feedline assembly at the required levels. Accelerometers on the feedline during the acoustic testing recorded g-loads of 3 grms. The lines were not degraded by this test.

The test results as discussed above, clearly show that the composite feedline assemblies exceed all operational and physical design requirements.

VIII. CONCLUSIONS

It has been demonstrated by design, fabrication, and test of full scale composite feedlines, representative of a Space Tug configuration, that composite feedline technology is fully developed and ready for space flight application. Virtually any all-metal configuration can be fabricated with composite tubing, including straight lines, curved lines, elbows, and tee sections. Both filament winding and braiding techniques have been demonstrated and are acceptable for producing flight hardware. Chemical milling has been demonstrated as a low cost and reliable method of producing thin metal liners for use in curved composite feedlines. This program was the fourth contract devoted to the development of composite tubing technology. The work performed on the previous contracts is summarized in the following paragraphs.

NAS3-12047, Low Thermal Flux Glass-Fiber Tubing for Cryogenic Service (ref. 1). - During this program a total of 134 composite tubes were fabricated, 12 each of 11 configurations and 2 of the 12th, and tested. Tube fabrication included liner welding, joining of the liners to end fittings, instrumentation installation, overwrapping, curing, and a series of in-process leak checks.

The tubes were subjected to a test program that included burst, thermal cycle, torsion, thermal, and leak check testing. All tubes were eventually destroyed by burst or torsion tests.

Of the 12 original tube configurations, 10 performed very satisfactorily. One design concept affecting 2 tube configurations was abandoned due to an inefficient liner-to-fitting weld. One of these configurations was redesigned to use a solid-state bonding concept and the other configuration was cancelled. The results of the program clearly verified the advantages in using glass-fiber composite lines in cryogenic propellant service. Some of the advantages include low thermal flux, lightweight construction, low heat soak-back from engines, rapid chilldown, strength and handling ease.

NAS3-14370, Composite Lines for Space Shuttle Vehicles (ref. 2). - The objective of this program was to develop lightweight glass-fiber tubing and attachment fittings for use as cryogenic plumbing on space vehicles. Tubing, representative of four different propulsion system requirements, was fabricated in sizes ranging from 5 to 38 cm (2 to 15 in.) diameter and up to 3 m (10 ft) in length.

The smaller tubes were joined together into two separate systems representative of the liquid oxygen (LO_2) Orbital Maneuvering Systems (OMS) and the liquid hydrogen (LH_2) OMS for the Phase B Space Shuttle configuration.

The larger tubes were each 38 cm (15 in.) in diameter and 3 m (10 ft) long. The stronger tube had an internal working pressure level of 258 N/cm^2 (375 psi) including g loading and was representative of the main engine LO_2 feedline for the Phase B Shuttle. The other tube, with a considerably thinner metallic liner, consisting of 0.008 cm (0.003 in.) thick Inconel 718, was used to determine minimum practical fabrication gages and to represent the Shuttle main engine LH_2 feedline, where maximum pressures were then anticipated to not exceed 69 N/cm^2 (100 psi).

A total of 11 tubes were fabricated and tested. Tube fabrication included liner welding, joining of the liners to end fittings, instrumentation installation, overwrapping and curing, a series of in-process leak checks, and other quality determinations as in the earlier program.

The main engine tubes were subjected to a series of tests including pressure cycling, temperature cycling, torsion, bending, and burst.

The OMS tubes were subjected to a series of tests including chilldown, steady state flow, steady state heat input in both the insulated and uninsulated configuration, thermal and pressure cycling, radial thermal conductivity, vibration and application of pressure to failure.

The results of this program clearly verified the advantages in using glass-fiber composite lines with cryogenic propellant service. These advantages can be accomplished with only a moderate increase in cost; in many cases for less than $25 per pound of weight reduced.

NAS3-16762, Vacuum Jacketed Composite Lines (ref. 3). - The objective of this program was to apply glass-fiber tubing technology to vacuum jacketed lines. Twelve vacuum jacketed line test specimens were fabricated and tested. The test specimens were 13 cm (5 in.) and 38 cm (15 in.) diameter by 61 cm (24 in.) long. Composite overwrap was applied to both the inner line and the outer vacuum jacket shell. The test program consisted of proof pressure tests, leakage tests, pressure and thermal cycling, external pressure collapse, vacuum decay, and burst pressure. It was found that (1) the composite overwrap on the inner line required long term vacuum bakeout to preclude outgassing, (2) the composite overwrap on the vacuum jacket provided damage resistance allowing the use of a thinner gage metal liner, and (3) the use of composites provided significant weight reduction as compared to the state-of-the-art all-metal vacuum jacketed lines.

Remaining technology development. - All aspects for composite tubing technology have been developed and successfully tested. These include thin metal liner forming, composite overwrapping

by filament winding and braiding techniques, overwrapping curved line sections with elbows and tees, chemical milling thin metal liners for use in curved line sections, and the fabrication of complete feedline assemblies including gimbal joints and flanges. The feasibility of aluminum-to-stainless steel bimetallic flange joints has also been demonstrated providing additional weight savings potential.

The feasibility of forming thin curved metal [0.015 cm (0.006 in.) thick] tubing liners was also demonstrated. Additional development, however, is required to produce metal liners for curved feedline assemblies using very thin materials. The development program may include new tooling concepts for thin tube bending, establishing minimum wall thickness as a function of tube diameter and bend radius, and evaluating other processes such as cryogenic forming and vacuum deposition. The use of the thin formed curved liners provides some additional weight saving [1.9 kg (4 lb) for the LH_2 feedline assembly] over the chem-milling process used to produce the test hardware on this program. The producibility cost for thin forming, however, probably would be higher than for the chem-milling approach.

Conclusions summary. - The following conclusions are made based on the work done on this program and the previous composite tubing technology programs.

(1) Weight: Composite tubing is lighter weight than all-metal tubing with the same design requirements. Feedline system weight can be reduced by 20% to 60% depending upon the line diameter, operating pressure and external loading.

(2) Damage resistance: Composite tubing has demonstrated a high resistance to damage. Thin gage composite tubing is much less susceptible to damage than all-metal tubing. Additional work is required to quantify this important characteristic.

(3) Corrosion resistance and propellant compatibility: Composite tubing has demonstrated an excellent resistance to corrosion when exposed to a high humidity-salt atmosphere, nitrogen tetroxide, unsymmetrical dimethylhydrazine and cryogenic propellants.

(4) Thermal efficiency: Composite lines compare favorably with all-metal lines in thermal efficiency. Composite line cryogenic tank penetrations are more efficient than all-metal lines because the cross-sectional area of the metal tube is reduced and the conductivity of the composite material is less than metal.

(5) Structural integrity: Composite tubing has demonstrated the ability to withstand all environments typical of a space vehicle mission. The reliability of composite tubing is enhanced in most systems because the loads are not sufficiently high to load the composites. In these systems the primary purpose of the composite is to provide damage resistance and increase design margin.

(6) Producibility: Composite tubing producibility techniques have been developed and demonstrated for virtually any line configuration including straight lines, curved lines, elbows, tees and vacuum jacketed lines.

(7) Use with dissimilar metal joints: Composite tubing with Inconel 718 or stainless steel tubing liners can be joined with aluminum end fittings (flanges, etc.) thus further decreasing system weight. Test specimens with this configuration have been produced and tested, showing that the concept is a viable candidate for minimum weight systems.

(8) Cost: The cost of composite tubing is higher than all-metal tubing due to the additional processes required in thin metal forming and overwrap application. Composite tubing, however, has been shown to be very cost effective in space vehicles where launch weight is expensive.

TABLE II-1. - DESIGN CRITERIA

Cryogenic Feedline Design Conditions	
Condition	LH_2 Line
Operating pressure	20.7 N/cm^2 (30 psia)
Proof pressure	41.4 N/cm^2 (60 psia)
Burst pressure	62.1 N/cm^2 (90 psia)
Diameter	10.2 cm (4.0 in.)
Flow rate	2.7 kg/sec (6.0 lb/sec)

Shuttle Payload Load Factors			
Condition	Axis		
	X(g)	Y(g)	Z(g)
Launch	1.4 ± 1.6	± 1.0	± 1.0
High-Q booster thrust	1.9 ± 0.3	± 1.0	0.8 ± 0.2
End boost (booster thrust)[a]	3.0 ± 0.3	± 0.6	± 0.6
End burn (orbiter thrust)	3.0 ± 0.3	± 0.5	± 0.5
Orbiter entry	- 0.5	± 1.0	- 3.0 ± 1.0
Orbiter flyback	- 0.5	± 1.0	+ 1.0 - 2.5
Landing	- 1.3	± 0.5	- 2.7 ± 0.5

Shuttle Cargo Bay Internal Wall Temperature Environments		
Condition	Temperature °K (°F)	
	Minimum	Maximum
Prelaunch	200 (-100)	322 (120)
Launch	200 (-100)	367 (200)
On orbit (door closed)	200 (-100)	367 (200)
Entry and postlanding	200 (-100)	367 (200)

[a]Excludes booster-orbiter separation loads.

TABLE II-2 ORBITER PAYLOAD COMPARTMENT INTERNAL ACOUSTIC DESIGN CRITERIA SOUND PRESSURE LEVEL

1/3 Octave center band frequency (H_z)	Liftoff	Boundary layer
5	124	124.5
6.3	127	125.0
8	128	126.0
10	129	126.5
12.5	131	127.0
16	132	128.0
20	134	128.5
25	135	129.0
31.5	137	130.0
40	138	130.5
50	139	131.0
63	140	132.0
80	141	132.5
100	143	133.0
125	144	134.0
160	145	134.5
200	145	135.5
250	145	136.0
315	144	136.5
400	143	137.0
500	142	137.5
630	141	138.0
800	140	138.5
1K	139	138.0
1.25K	138	137.0
1.6K	137	136.5
2K	135	135.5
2.5K	134	134.5
3.15K	133	134.0
4K	132	133.0
5K	131	132.0
6.3K	130	131.0
8K	129	130.0
10K	128	129.0
	OASPL 155 dB	OASPL 149 dB

TABLE II-3. - SYNCHRONOUS EQUATORIAL ORBIT - RETRIEVAL MISSION

Event	Seq. no.	Time (hr)		Tug main engine				ACS ΔV mps (fps)
				Full thrust ΔV mps (fps)			Burn time (min) (2)	
		Δ	Total	Ideal	Gravity loss (1)	Total x 1000		
Shuttle liftoff			0					
Shuttle burnout	1		0.14					
Coast to 18.5 x 10^4 m (100 nmi)	1-2a	0.73						
Shuttle 18.5 x 10^4 m x 29.6 x 10^4 m (100x160 nmi) insertion	2a		0.87					
Coast to 29.6 x 10^4 m (160 nmi)	2a-2	0.76						
Circularize at 29.6 x 10^4 m (160 nmi)	2		1.63					
Tug deploy and coast	2-3	13.11						3 (10)
Phasing orbit insertion	3		14.74	1824	16	5.6	4.1	
Coast to TOI	3-4	1.92				(18.4)		
Transfer orbit insertion	4		16.66	6222	33	19.1	9.9	
Coast to 35.8 x 10^6 m (19,323 nmi)	4-5	5.27				(62.5)		15 (50) (3)
Mission orbit insertion	5		21.93	5849	0	17.8	6.1	
Retrieve P/L and coast	5-6	11.15				(58.5)		35 (115) (4)
Transfer orbit insertion	6		33.08	5844	0	11.4	5.1	
Coast to POI	6-7	5.27				(37.3)		15 (50) (3)
Phasing orbit insertion	7		38.35	3720	10	13.2	2.3	
Coast	7-8	3.02				(43.2)		
Circularize for rendezvous	8		41.37	4309	7		2.0	
Shuttle rendezvous and coast	8-9	4.53						
Shuttle deorbit	9		45.90					
Touchdown	10		46.60					

(1) Based on 6795 kg (15 000 lb) thrust engine
(2) Approx burn time 6795 kg (15 000 lb) main engine
(3) Midcourse correction
(4) Rendezvous and dock with P/L

Reference: Space Tug Systems Study NAS8-29676. DATA DUMP General Dynamics/Convair Aerospace Division, 18 September 1973

TABLE II-4. - THERMAL PERFORMANCE OF FEEDLINE CONCEPTS (PER UNIT AREA)

Feedline design concept	Configuration	Feedline heat flux - Watts/M^2 (Btu/hr-ft^2)			
		One-g environment 300°K (80°F)	Space environment		
			256°K (0°F)	322°K (120°F)	367°K (200°F)
1. Vacuum jacketed metal, wet	Without radiation shields	77.0 (24.4)	53.3 (16.9)	91.2 (28.9)	129.7 (41.1)
	With eight radiation shields	42.3 (13.4)	35.3 (11.2)	45.7 (14.5)	53.3 (16.9)
2. Vacuum jacketed composite, wet	Without radiation shields	144.8 (45.9)	89.9 (28.5)	182.7 (57.9)	283.0 (89.7)
	With eight radiation shields	42.3 (13.4)	35.3 (11.2)	45.7 (14.5)	53.3 (16.9)
3. Nonvacuum jacketed metal purged MLI, wet		441.7 (140)	2.62 (0.83)	2.71 (0.86)	2.84 (0.90)
4. Nonvacuum jacketed metal MLI, dry	Stainless steel end fitting	5.4 (1.7)	0.082 (0.026)	0.098 (0.031)	0.114 (0.036)
	Aluminum end fitting	5.7 (1.8)	0.082 (0.026)	0.098 (0.031)	0.114 (0.036)
5. Nonvacuum jacketed composite MLI, dry	Stainless steel fitting	3.0 (0.96)	0.047 (0.015)	0.057 (0.018)	0.065 (0.021)
	Aluminum end fitting	3.2 (1.0)	0.047 (0.015)	0.057 (0.018)	0.065 (0.021)
6. Nonvacuum jacketed composite purged MLI, wet		441.7 (140)	2.62 (0.83)	2.71 (0.86)	2.84 (0.90)

TABLE II-5. - WEIGHT STATEMENT, LH_2 FEEDLINE

Concept 1		Concept 2		Concept 3		Concept 4		Concept 5		Concept 6	
Item	Weight kg (lb)	Item	Weight kg (lb)	Item	Weight kg (lb)	Item	Weight kg (lb)	Item	Weight kg (lb)	Item	Weight kg (lb)
Inner line	8.3 (18 5)	Inner line	4.8 (10.7)	Metal line	7 3 (16.1)	Metal liner	7.3 (16.1)	Metal liner	1.9 (4.1)	Metal liner	1.9 (4 1)
Vacuum jacket	11.4 (25.1)	Wrap, inner line	2.2 (4 8)	2 Layers mylar 0 013 cm (0 005 in.)	0 7 (1 4)	Layer mylar 0.013 cm (0.005 in.)	0.3 (0.7)	Wrap, metal liner	2.3 (4 9)	Wrap, metal liner	2.3 (4.9)
Gimbals	4.7 (10.5)	Vacuum jacket liner	4 2 (9.3)	30 Layers mylar 0.00064 cm (0.00025 in.)	0 6 (1.3)	30 Layers mylar 0.00064 cm (0.00025 in)	0.6 (1.3)	Layer mylar 0 013 cm (0.005 in)	0.3 (0 7)	Two layers mylar 0 013 cm (0.005 in.)	0.7 (1.4)
		Flanges	2.2 (4.8)								
Standoffs	0.5 (1.1)	Wrap, vacuum jacket	2.2 (4.8)	Purge bag	0 1 (0 3)	Velcro	0.1 (0 3)	30 Layers mylar 0 00064 cm (0 00025 in)	0.6 (1.3)	30 Layers mylar 0 00064 cm (0 00025 in)	0.6 (1.3)
End closures	0 7 (1 5)	Gimbals	4.8 (10.5)	Nylon attachments	0.05 (0 1)	Nylon attachments	0.05 (0.1)	Velcro	0.1 (0 3)	Purge bag	0.1 (0 3)
Vacuum valves	0.6 (1.4)	Standoffs	0.5 (1 1)	Velcro	0.1 (0 3)	Gimbals	2.7 (6.0)	Nylon attachments	0 05 (0 1)	Nylon attachments	0 05 (0.1)
Burst discs	0.7 (1.5)	End closures	0.7 (1.5)	Gimbals	2 7 (6 0)	Flanges	2.9 (6 5)	Gimbals	2.7 (6 0)	Velcro	0 1 (0 3)
Vacuum gages	0 3 (0 7)	Vacuum valves	0.6 (1.4)	Insulation end closures	0.1 (0.3)	Purge bag for protection only	0 1 (0 3)	Purge bag	0.1 (0.3)	Gimbals	2 7 (6.0)
Flanges	2.9 (6.5)	Burst discs	0.7 (1.5)	Purge tubing	0.05 (0.1)			Flanges	2 2 (4.8)	End closures	0 1 (0 3)
Eight layers (MLI)	0 2 (0.4)	Vacuum gages	0.3 (0.7)	Flange	2.9 (6.5)					Purge tubing	0.1 (0.1)
Nylon ties	0.05 (0.1)	Eight layers MLI	0.2 (0 4)							Flanges	2.2 (4 8)
		nylon ties	0.05 (0.1)								
Total	30.35 (67.3)	Total	23.4 (51.6)	Total	14.6 (32.4)	Total	14.1 (31.3)	Total	10.3 (22.5)	Total	10 8 (23.6)

Concept 1 - Vacuum jacketed metal (wet)
Concept 2 - Vacuum jacketed composite (wet)
Concept 3 - Nonvacuum jacketed metal (wet-purged MLI)
Concept 4 - Nonvacuum jacketed metal (dry-MLI)
Concept 5 - Nonvacuum jacketed composite (dry-MLI)
Concept 6 - Nonvacuum jacketed composite (wet-purged MLI)

Note. Concepts 1, 2, 3 and 6 (wet concepts) may require a recirculation and a purge system It is estimated that this would add approximately 5.2 kg (11.2 lb) to each of these concepts.

Recirculation System		Purge System	
6.1 m (20 ft) of 1.3 cm (0.5 in.) tubing.	1.0 kg (2.2 lb)	Valve·	0 5 kg (1 0 lb)
Three tubing supports	0.7 kg (1.5 lb)	Regulator	0 9 kg (2.0 lb)
Pump	1.4 kg (3.0 lb)	3 m (10 ft) of 0 6 cm (0 25 in.) tubing	0.2 kg (0.5 lb)
Total	3.1 kg (6.7 lb)	Tubing supports	0.5 kg (1 0 lb)
			2.1 kg (4.5 lb)

TABLE II-6. - REUSABILITY AND MAINTAINABILITY EVALUATION

Feedline design concept	Key considerations	Ranking
1. Vacuum jacketed metal (wet)	More susceptible to asthetic damage (dings, dents, etc) than vacuum jacket composite or MLI. Vacuum maintainability requirements greater than for concepts using MLI.	6
2. Vacuum jacketed composite (wet)	Overwrapped vacuum jacket is more durable and less susceptible to damage than the all-metal vacuum jacket or the MLI (especially true for resisting puncture from sharp objects). Vacuum maintainability requirements greater than for concepts using MLI.	5
3. Nonvacuum jacketed metal (wet - purged MLI)	Installed repairability of MLI system is more feasible than vacuum jacketed configurations. Requires dedicated dry gas purge during reentry.	4
4. Nonvacuum jacketed metal (dry - MLI)	Installed repairability of MLI system may be more feasible than for vacuum jacketed configurations. No maintainability required for purge system.	2
5. Nonvacuum jacketed composite (dry - MLI)	Installed repairability of MLI system is more feasible than vacuum jacketed configurations. No maintainability required for purge system. Metal line less susceptible to damage, due to overwrap, than the all-metal line.	1
6. Nonvacuum jacketed composite (wet - purged MLI)	Installed repairability of MLI system is more feasible than vacuum jacketed configurations. Requires dedicated dry gas purge during reentry.	3

TABLE II-7. - SYSTEM COMPARISON OF FEEDLINE DESIGN CONCEPTS

Design concept	Configuration	System weight, kg (lb)			Cost ($ x 1000) for one feedline assembly	Reliability**	Reusability and maintainability**
		Feedline weight	Boiloff* weight	Total system weight			
1. Vacuum jacketed metal (wet)	With radiation shields	30.5 (67.3)	35.6 (78.6)	66.1 (145.9)	37.9	5	6
2. Vacuum jacketed composite (wet)	With radiation shields	23.4 (51.6)	35.1 (77.3)	58.5 (128.9)	45.4	6	5
3. Nonvacuum jacketed metal (purged MLI - dry)		14.6 (32.2)	3.6 (8.0)	18.2 (40.2)	20.5	4	4
4. Nonvacuum jacketed metal (MLI - dry)	Prevalve open after initial firing	14.1 (31.0)	6.2 (13.8)	20.3 (44.8)	19.9	2	2
5. Nonvacuum jacketed composite (MLI - dry)	Prevalve open after initial firing	10.3 (22.6)	4.1 (9.1)	14.4 (31.7)	24.4	1	1
6. Nonvacuum jacketed composite (purged MLI - wet)		10.8 (23.9)	3.0 (6.7)	13.8 (30.6)	25.0	3	3

* Sum of boiloff during storage in cargo bay and during flight.

** Ranking is in order of preference (1 is best).

TABLE III-1. - SUBSCALE TEST SPECIMEN DESIGN CONFIGURATIONS

Quantity	Drawing number	Liner type	End fitting	Overwrap material
2	EPL 6301139-9	Resistance welded	Stainless steel resistance welded to liner	Kevlar 49 in 58-68R resin system
2	EPL 6301139-19	Resistance welded	Stainless steel resistance welded to liner	Graphite in 58-68R resin system
2	EPL 6301139-49	Fusion welded	Aluminum, explosive bonded to liner	S-Glass in 58-68R resin system
1	EPL 6301139-29	Resistance welded	Aluminum-stainless steel bimetallic fittings resistance welded to liners	S-Glass in 58-68R resin system
1	EPL 6301139-39	Resistance welded	Aluminum-stainless steel bimetallic fittings formed by the coextrusion process, resistance welded to liner	S-Glass in 58-68R resin system

TABLE III-2. - OVERWRAP MATERIAL EVALUATION
(SUBSCALE TEST SPECIMENS, 20.3 cm (8 in.) LONG x 5.8 cm (2.29 in.) DIA)

Evaluation parameter	S-Glass	Graphite	Kevlar-49
Raw material cost $/kg ($/lb)	29 (13)	552 (250)	77 (35)
Fabrication ease	Standard	Most difficult	Slightly more difficult than S-glass
Material density, kg/cm^3 ($lb/in.^3$)	2.3×10^{-3} (0.085)	1.5×10^{-3} (0.055)	1.4×10^{-3} (0.052)
Overwrap weight on test specimen, kg (lb)	0.04 (0.09)	0.02 (0.05)	0.03 (0.074)
Appearance	Good	Fair	Good
Temperature cycle	No degradation	No degradation	No degradation
Thermal shock	No degradation	No degradation	No degradation
Pressure cycle	No degradation	No degradation	No degradation
Torque load, kg-m (ft-lb)	Failure in metal liner pressurized at 21 N/cm^2 (30 psig) T (failure) = 16 (118)	Not tested to failure	Failure in metal liner tube not pressurized T (failure) = 10 (70)
Bending load, kg-m (ft-lb)	Failure in metal liner load (failure) = 31 (227)	Failure in metal liner load (failure) = 30 (215)	Not tested to failure
Resistance to corrosion-salt fog	No degradation	No degradation	No degradation
Resistance to corrosion-storable propellant	No degradation	No degradation	No degradation
Burst pressure N/cm^2 (psig)	Failure in metal liner P (rupture) = 1117 (1620)	Failure in metal liner P (rupture) = 1241 (1800)	Failure in metal liner P (rupture) = 1158 (1680)

TABLE IV-1. - DESIGN CRITERIA

Design parameter	Specification
Operating pressure	20.7 N/cm^2 (30 psia)
Proof pressure	41.4 N/cm^2 (60 psia)
Burst pressure	62.1 N/cm^2 (90 psia)
Diameter	10.2 cm (4.0 in.)
Maximum g-loading	X - Axis ± 3g Y - Axis ± 1g Z - Axis ± 1g
Shuttle cargo bay internal wall temperatures	200°K (-100°F) minimum 367°K (+200°F) maximum
Acoustics	OSAPL 155 dB liftoff OSAPL 149 dB boundary layer

TABLE IV-2. - COMPOSITE OVERWRAP SPECIFICATION

Filament winding	
Parameter	Specification
Material	Kevlar 49, 12-end roving
Resin	58-68R
Wrap pattern	1 layer hoop, ½ layer longitudinal, and 1 layer hoop in that order.
Turns per cm (in.)	6.3 (16)
Pressurization	13.8 N/cm^2 (20 psig) during overwrap
	20.7 N/cm^2 (30 psig) during cure
Cure cycle	½ hour - ambient to 338°K (150°F)
	1½ hours - hold at 338°K (150°F)
	1 hour - 338°K (150°F) to 422°K (300°F)
	4 hours - hold at 422°K (300°F)
	3 hours - 422°K (300°F) to ambient
Braiding	
Parameter	Specification
Material	S-Glass (S/HTS-901 20-end roving)
Resin	58-68R
Wrap pattern	2 layers braided overwrap with 0.61 radians (35°) braid angle
Pressurization	Same as for filament winding
Cure cycle	Same as for filament winding

TABLE VI-1. - TEST DEFINITION MATRIX

Composite Line Segments		
Test	Filament Wound	Braided
Proof pressure	X	X
Leakage	X	X
Strain versus internal pressure	X	X
Deflection versus internal pressure	X	X
Load versus deflection	X	X
Thermal cycle	X	X

Feedline Assemblies				
Test	S/N 1 Composite	S/N 2 Composite	S/N 3 Composite	S/N 4 All-metal
Proof pressure	X	X	X	X
Leakage	X	X	X	X
Steady state heat input		X		X
Chilldown and flow quality		X		X
Thermal cycle		X	X	
Acoustics			X	
Burst pressure		X	X	

TABLE VI-2. - EVALUATION OF LOAD VERSUS DEFLECTION DATA

Loading direction	Filament wound tube			Braided tube		
	(1)	(2)	(3)	(1)	(2)	(3)
Y-Axis down loading	0.749 (0.295)	0.41 (0.155)	47%	0.469 (0.185)	0.350 (0.138)	25%
Y-Axis up loading	0.744 (0.293)	0.36 (0.141)	51%	0.584 (0.230)	0.267 (0.105)	54%
Z-Axis left loading	0.787 (0.310)	0.41 (0.160)	48%	0.660 (0.260)	0.381 (0.150)	42%
Z-Axis right loading	0.965 (0.380)	0.43 (0.165)	59%	0.665 (0.262)	0.409 (0.161)	39%
X-Axis out loading	0.139 (0.055)	0.13 (0.049)	11%	0.091 (0.036)	0.089 (0.035)	—
X-Axis in loading	0.099 (0.039)	0.10 (0.038)	--	0.102 (0.040)	0.089 (0.035)	12%

(1) Tube deflection in cm (in.) when subjected to 4.5 kg (10 lb) loading; no pressure in tube.

(2) Tube deflection in cm (in.) when subjected to 4.5 kg (10 lb) loading; 21 N/cm^2 (30 psig) in tube.

(3) % increase in stiffness when tube was pressurized at 21 N/cm^2 (30 psig).

(4) Stiffness comparison based on amount of total deflection when tubes were subjected to a 4.5 kg (10 lb) bending load.

	Heat flux, Watt (Btu/hr)	Weight, kg (1b)
a. 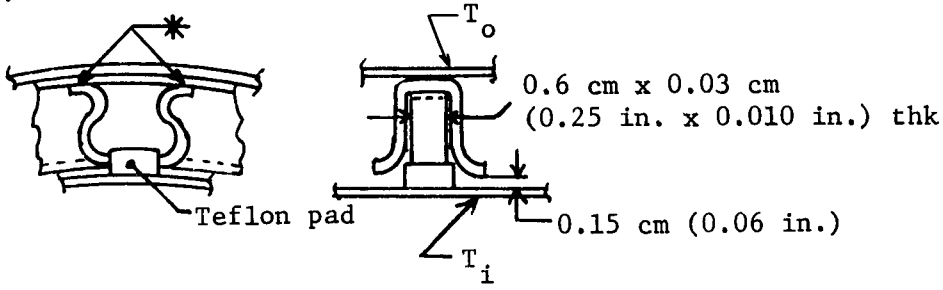	1.5 (5)	0.05 (0.12)
b. 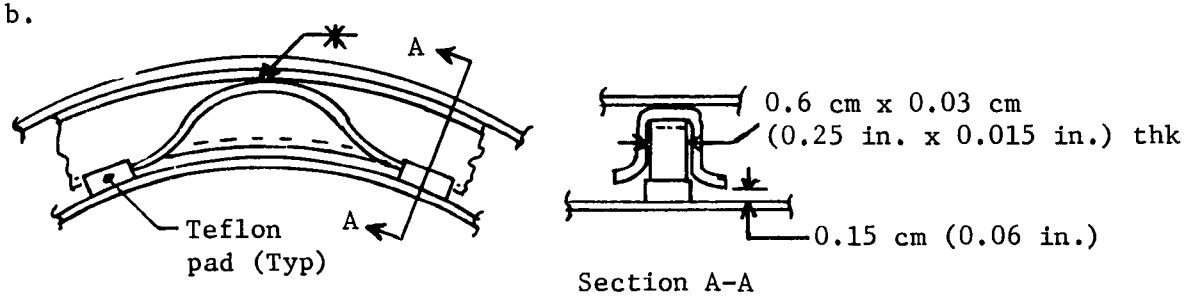	1.5 (5)	0.06 (0.13)
c. 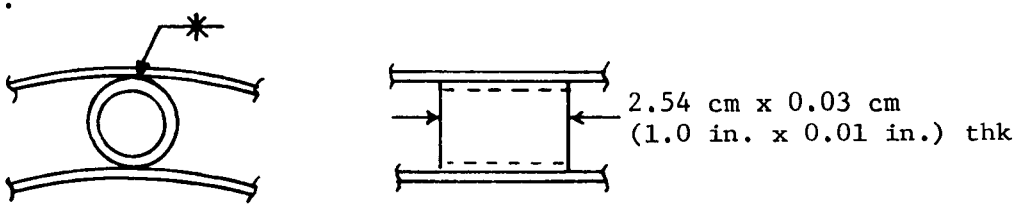	3.0 (10)	0.009 (0.02)
d. 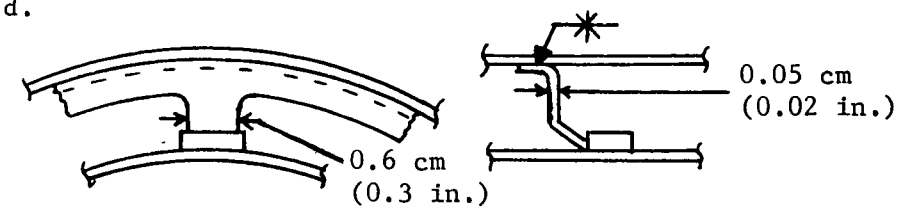	2.3 (8)	0.02 (0.05)

Conditions: T_o = 300 K° (80°F) Annulus = 1.3 cm (0.5 in.) Material: Stainless steel

T_i = 22 K° (-420°F) Line Dia = 10.2 cm (4.0 in.)

*Three standoffs per radial location in each concept

Figure II-1. - Comparison of Candidate Vacuum Jacketed Line Standoff Concepts

	Heat flux, Watt (Btu/hr)	Weight, kg (lb)
a. Half torus 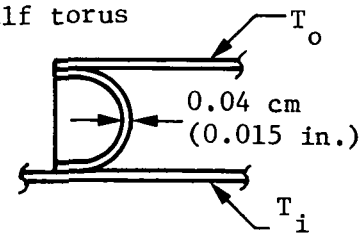	33 (113)	0.02 (0.05)
b. Axial bellows 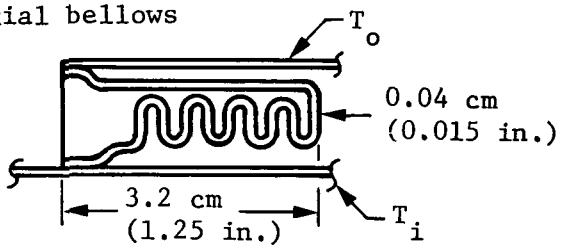	7.3 (25)	0.1 (0.22)
c. Cylindrical cones 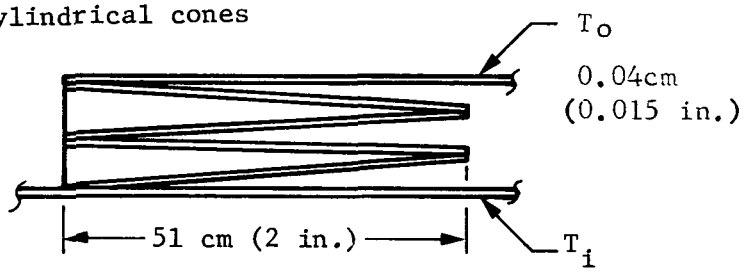	3.2 (11)	0.1 (0.25)
d. Conventional 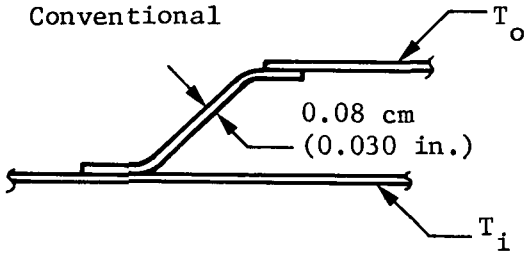	103.8 (354)	0.02 (0.05)
e. Thin metal/glass-fiber 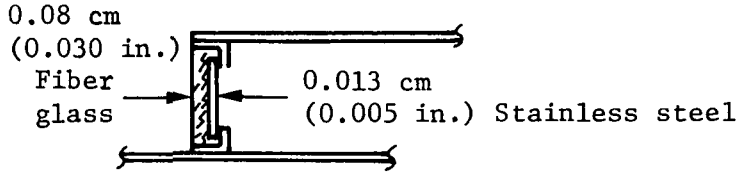	24.3 (83)	0.03 (0.06)

Conditions: T_o = 300 K° (80°F) Line dia = 10.2 cm (4.0 in.)
T_i = 22 K° (-420°F) Material = Stainless steel
Annulus = 1.3 cm (0.50 in.)

Figure II-2.- Comparison of Vacuum Jacketed Line End Closure Concepts

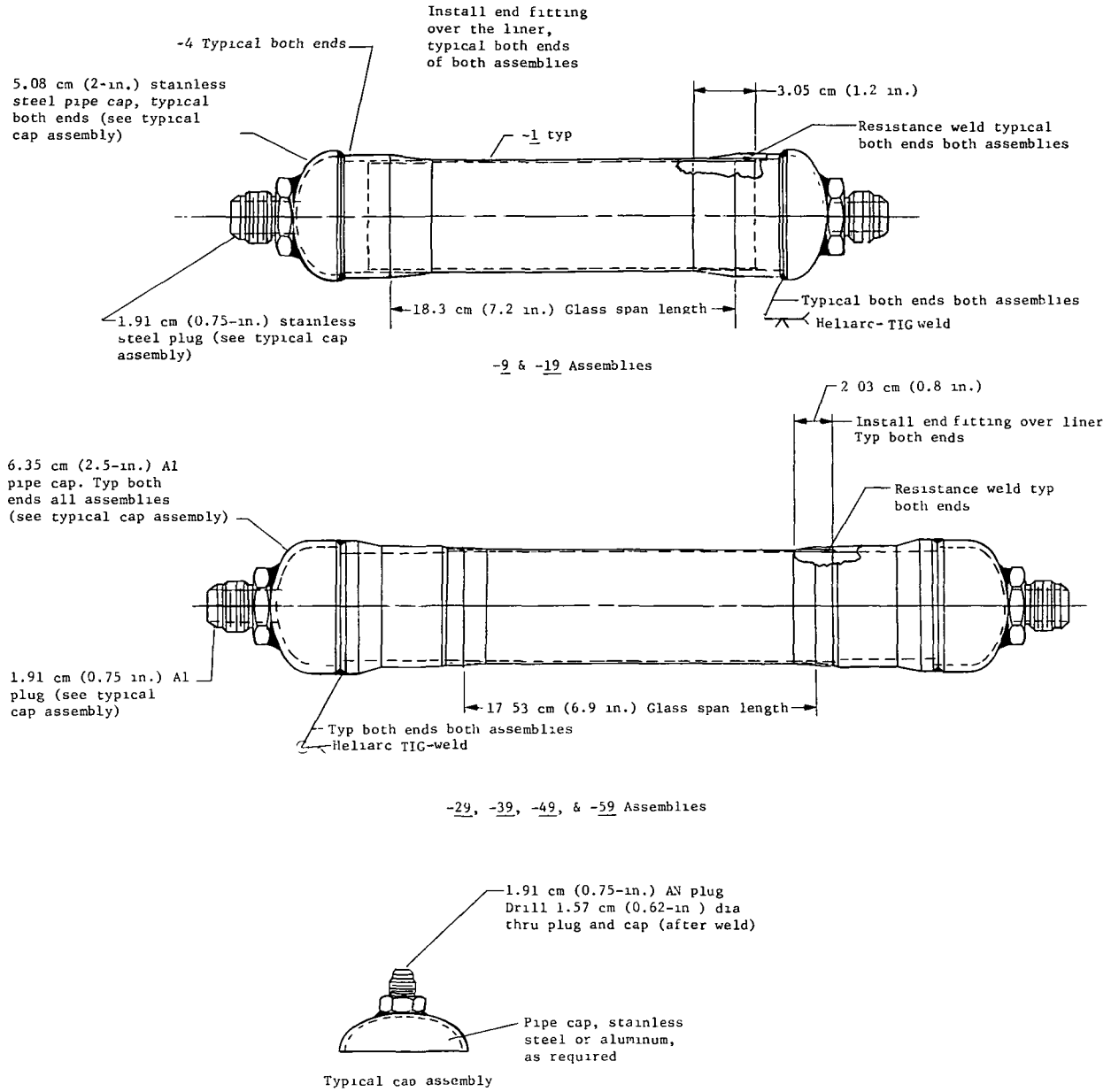

Figure III-1. - Subscale Test Specimen Drawings

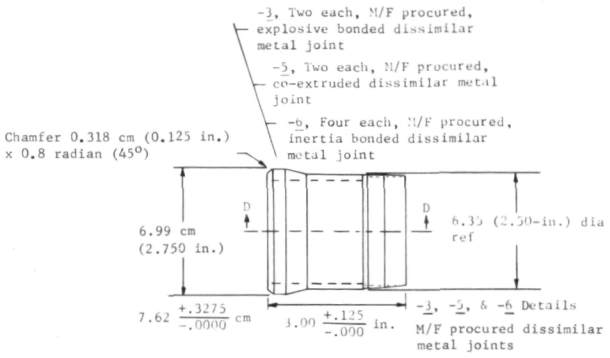

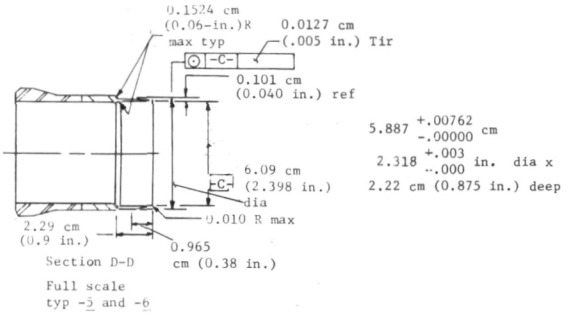

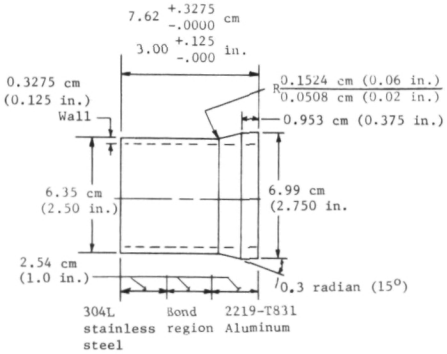

Typical As procured dissimilar metal joints co-extruded (2 each) explosive bonded (2 each) & inertia bonded (4 each)

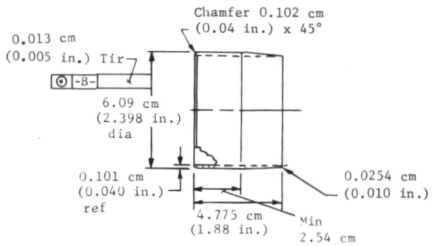

-4 Detail
full scale,
8 required
M/F 304
stainless steel

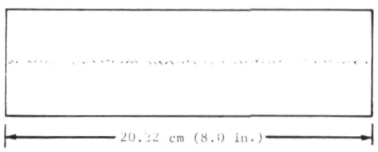

-1 & -2 Details
approx full scale
6 each - 1's reqd
2 each - 2's reqd

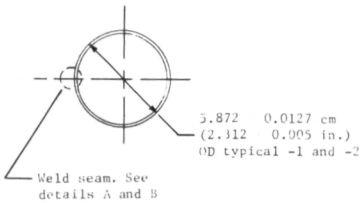

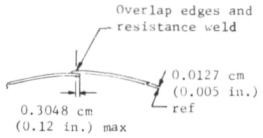

Detail A
No scale
typical -1 details only -

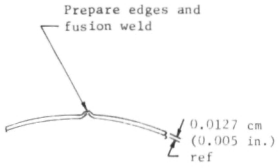

Detail B
no scale,
typical -2 details only

Figure III-1. - Continued

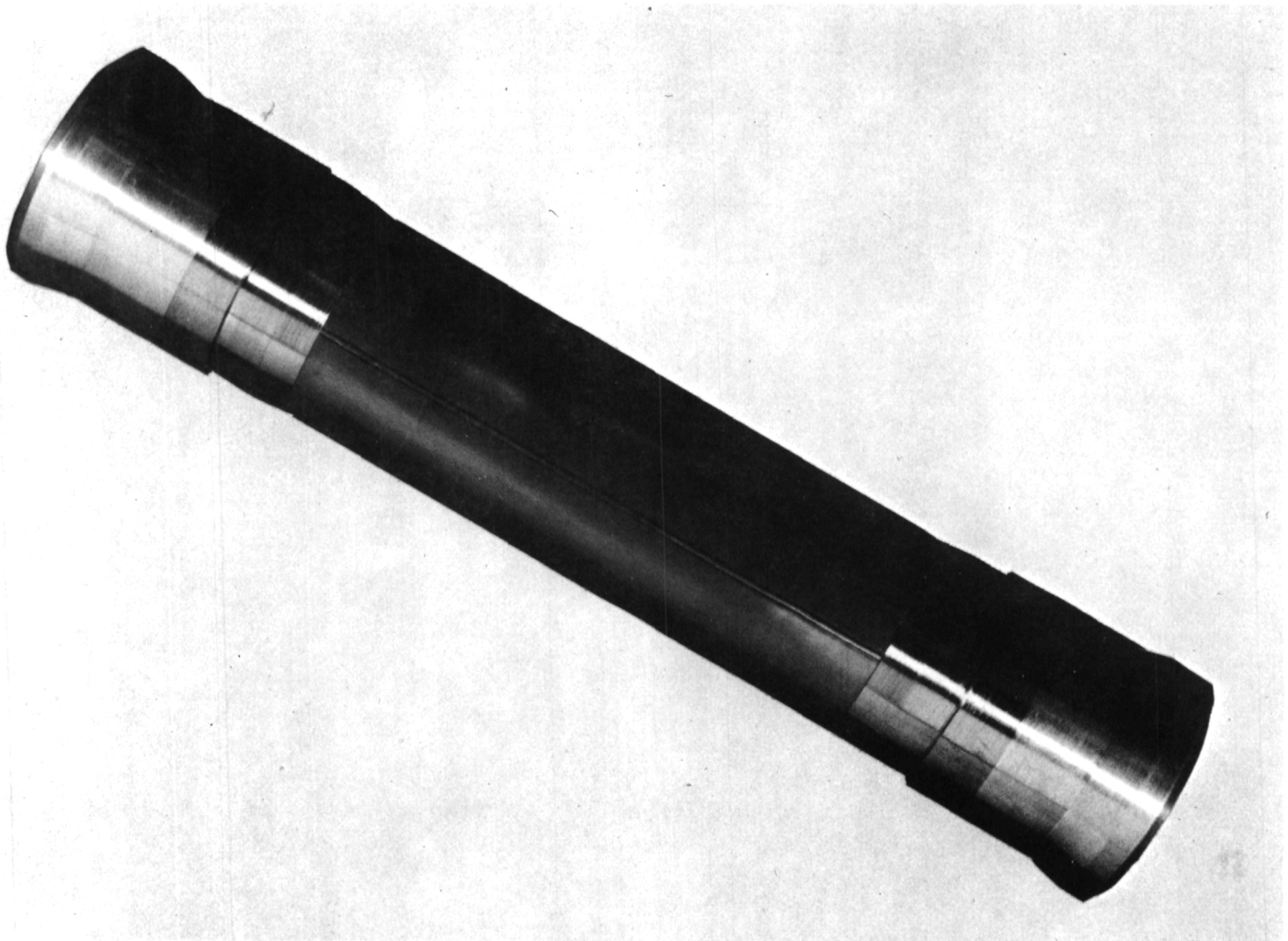

Figure III-2 Subscale Test Specimen with Bimetallic End Fittings Before Overwrap

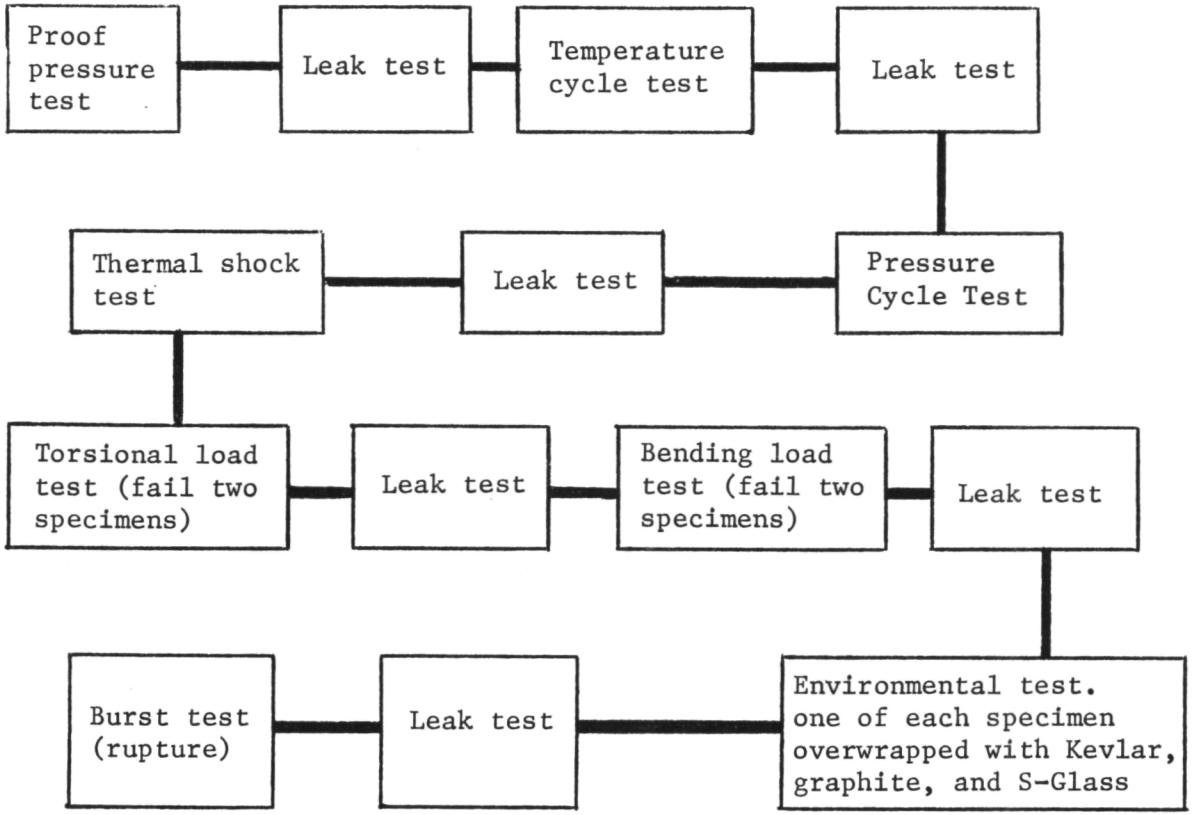

Figure III-3. - Flow Chart, Subscale Test Program

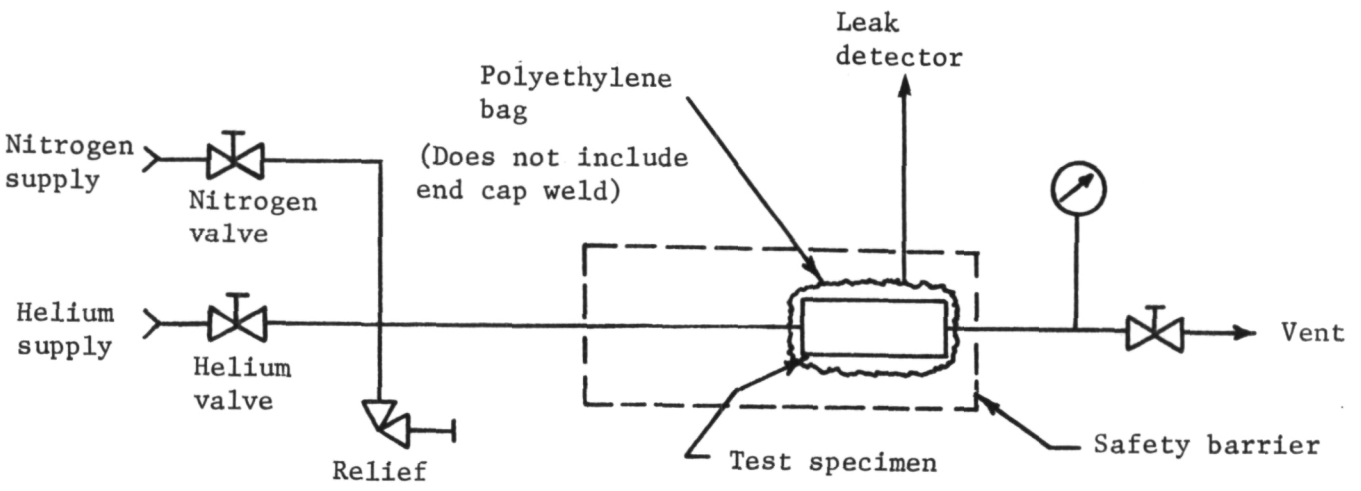

Figure III-4. - Proof Pressure and Leakage Test Schematic

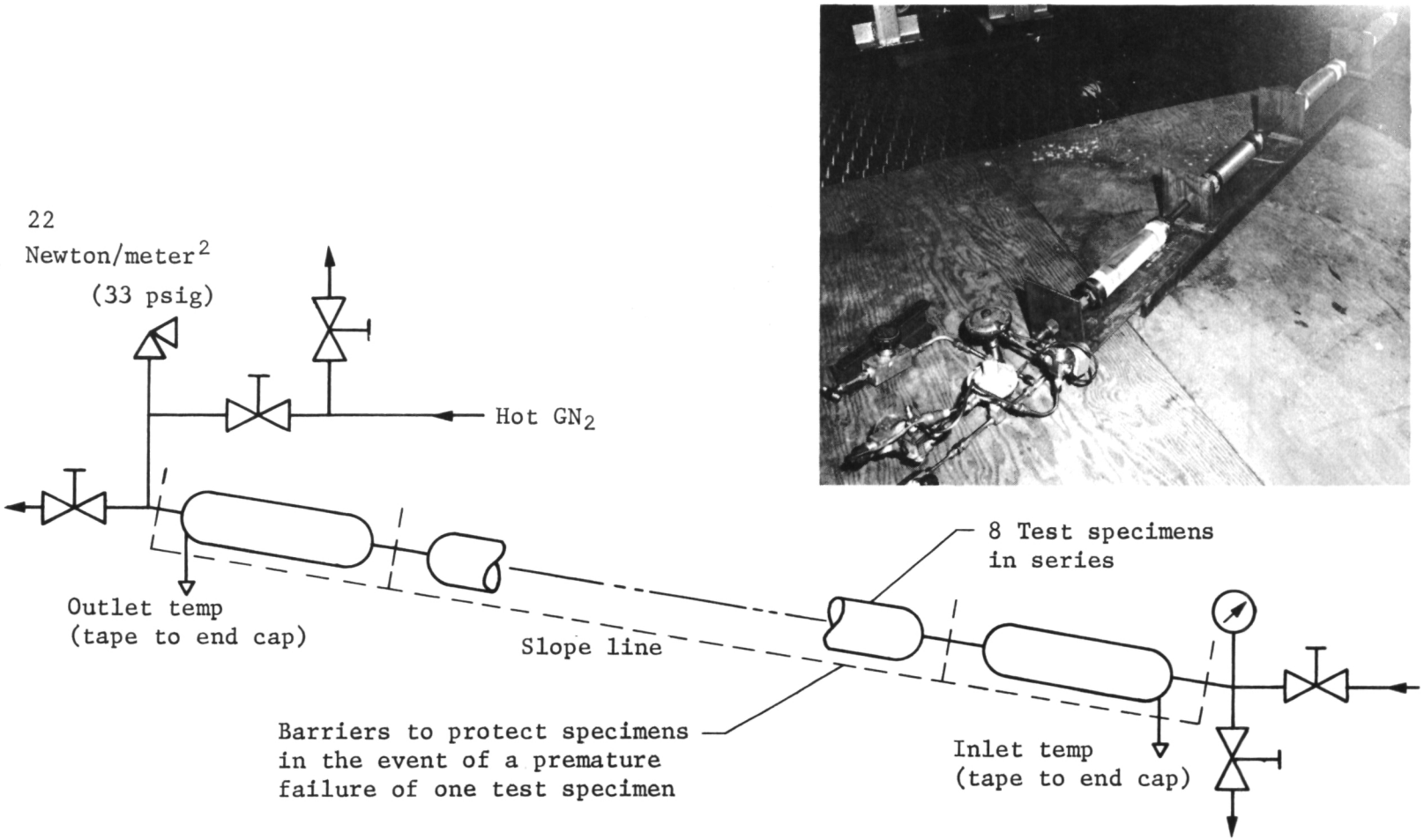

Figure III-5. - Temperature and Pressure Cycle Test Fixture Schematic

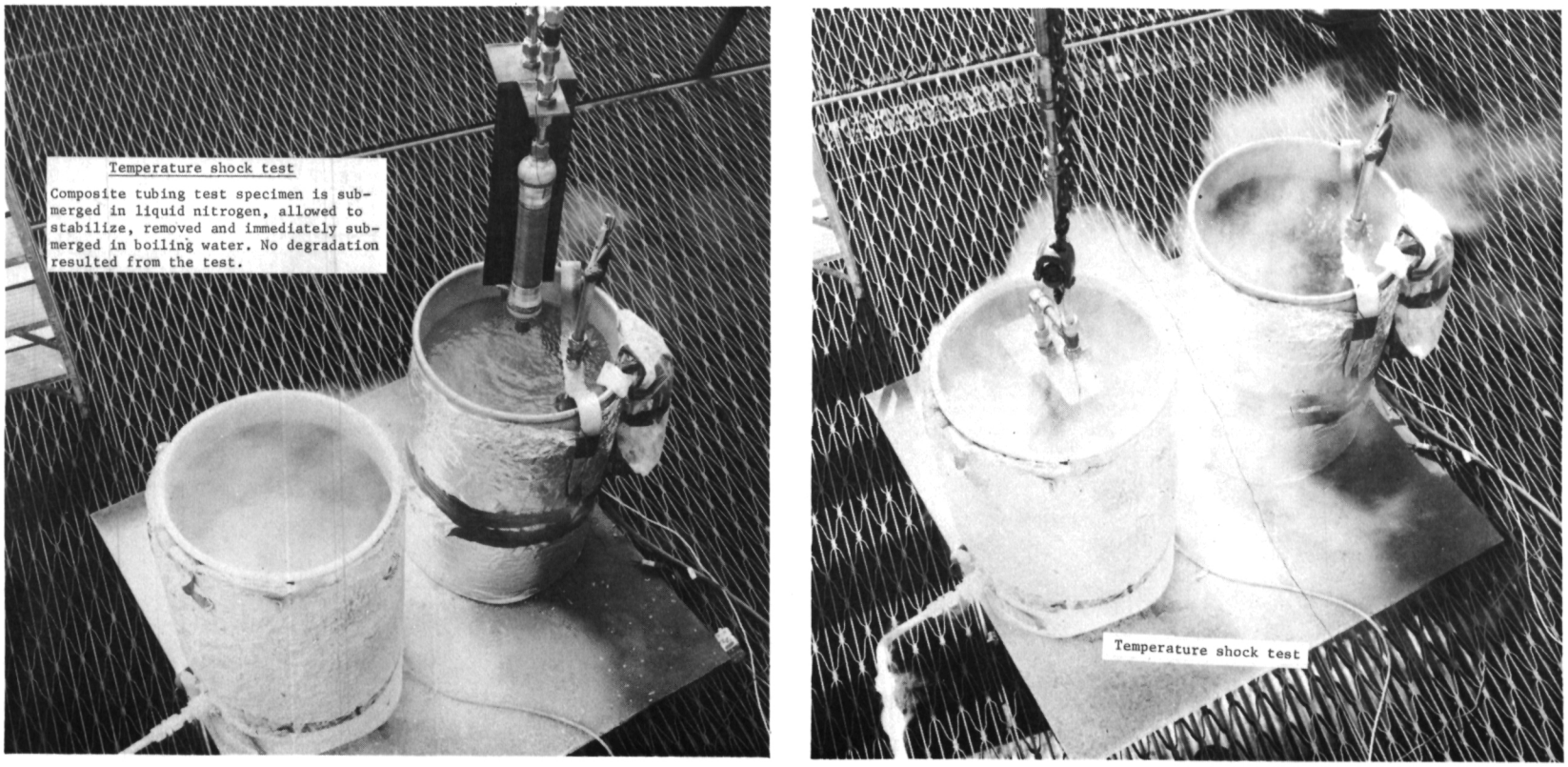

Figure III-6. - Thermal Shock Test, Subscale Test Specimen

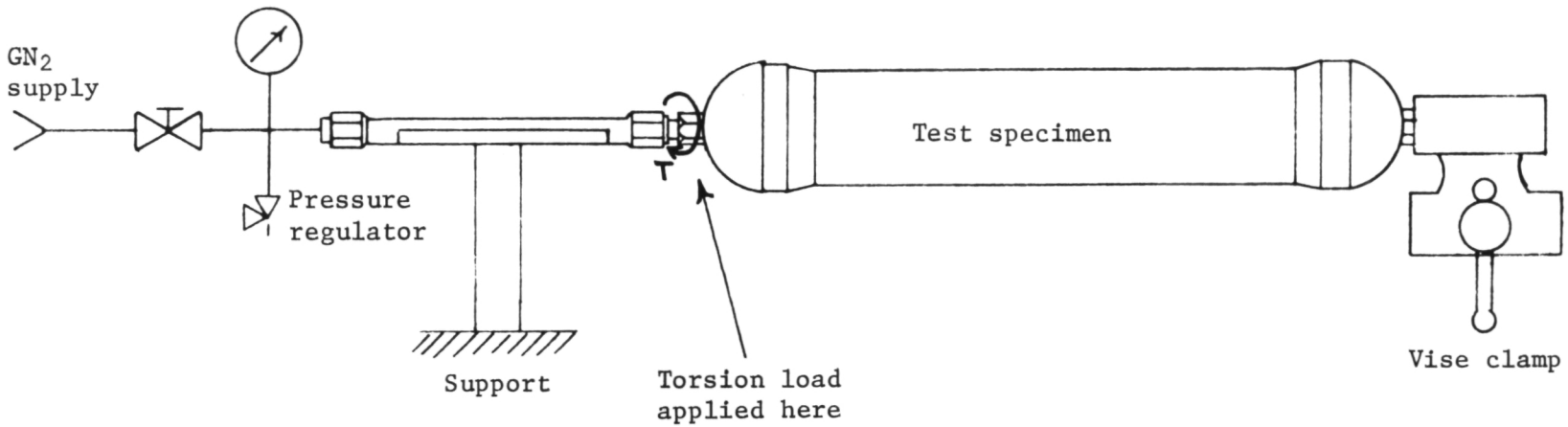

Figure III-7. - Torsion Load Test Setup

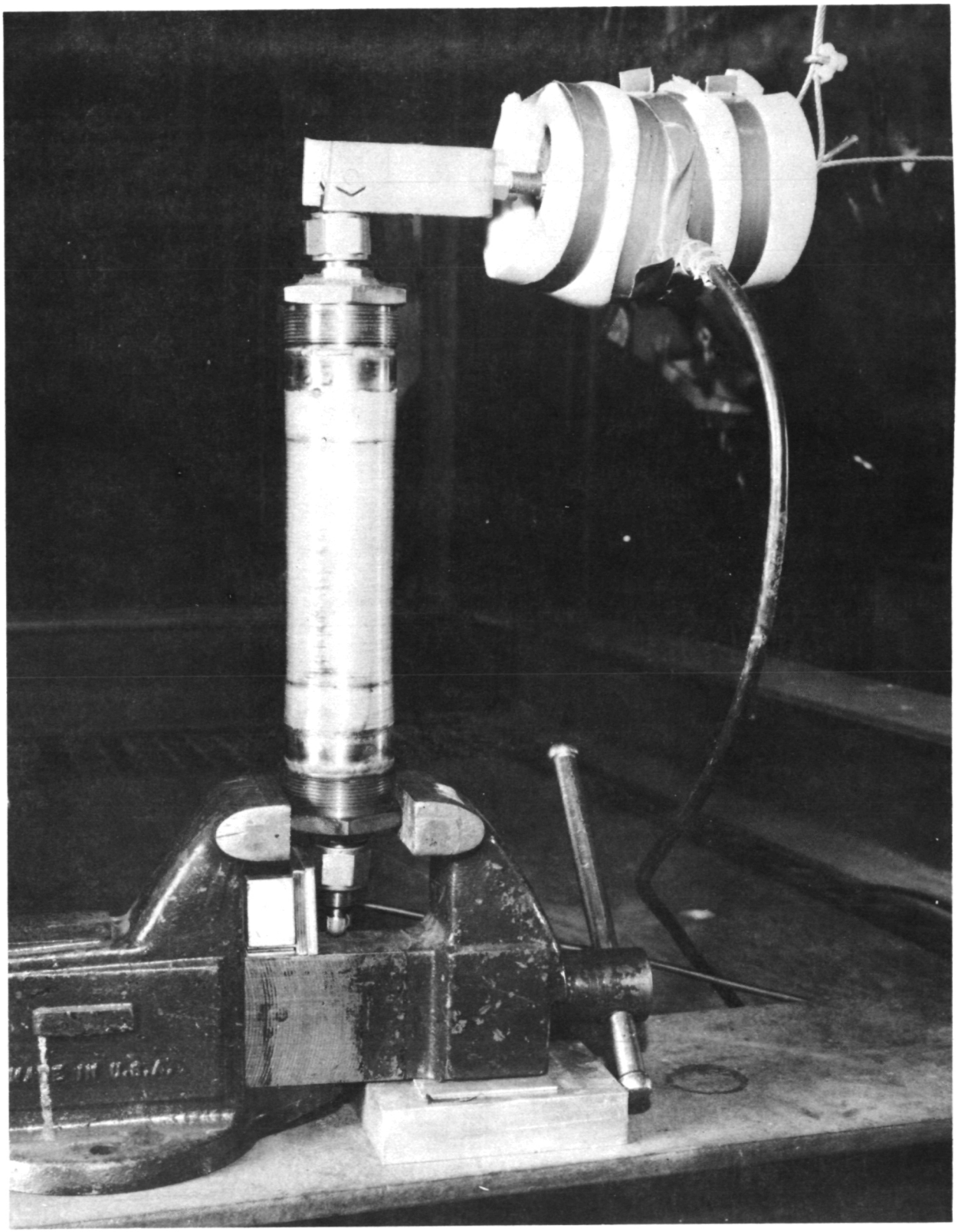

Figure III-8. - Bending Load Test, Subscale Test Specimen

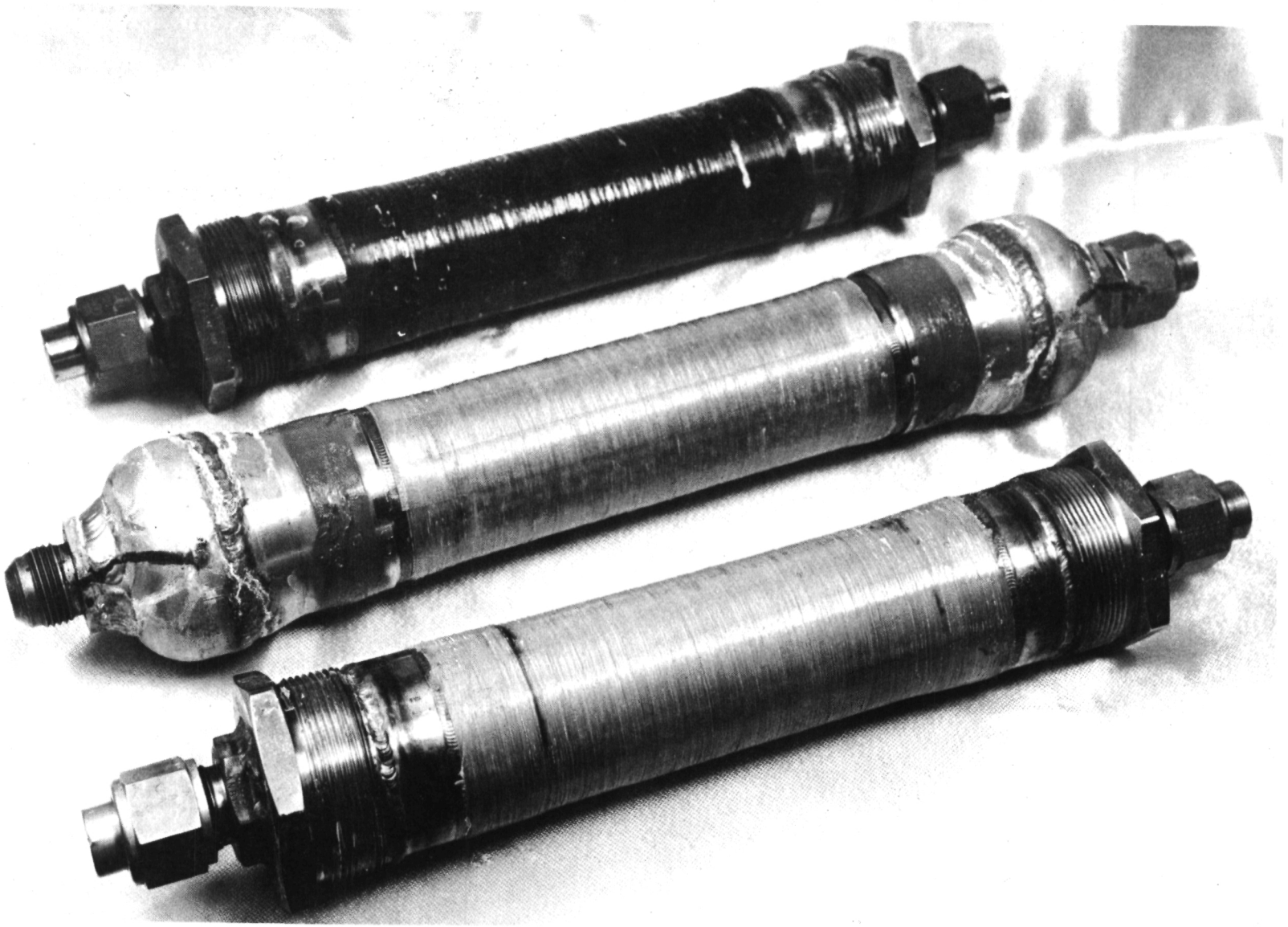

Figure III-9. - Subscale Test Specimen after Salt Fog Environment Test

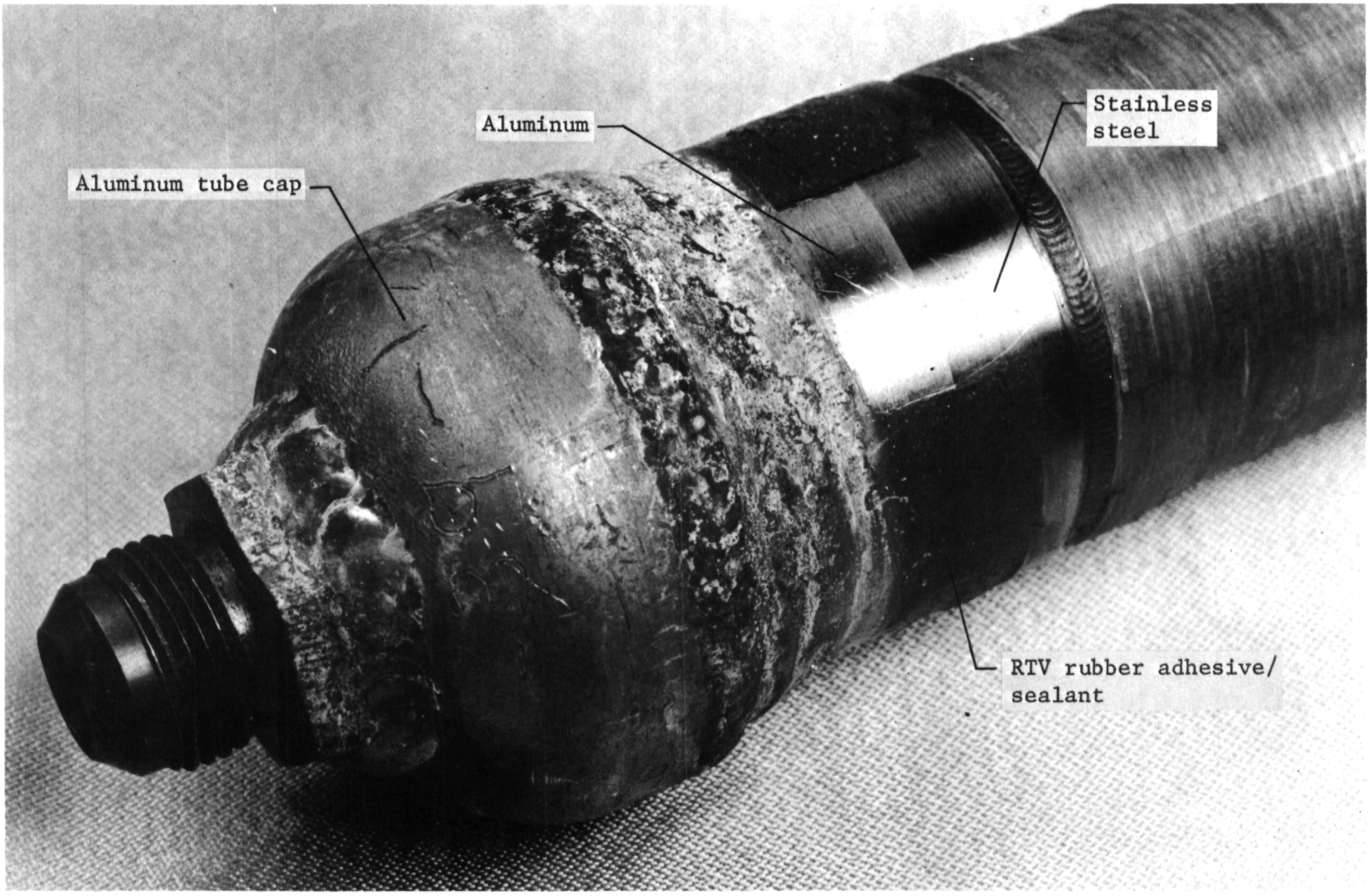

Figure III-10. - Inertia Welded, Dissimilar Metal Joint after Salt Fog Environment Test

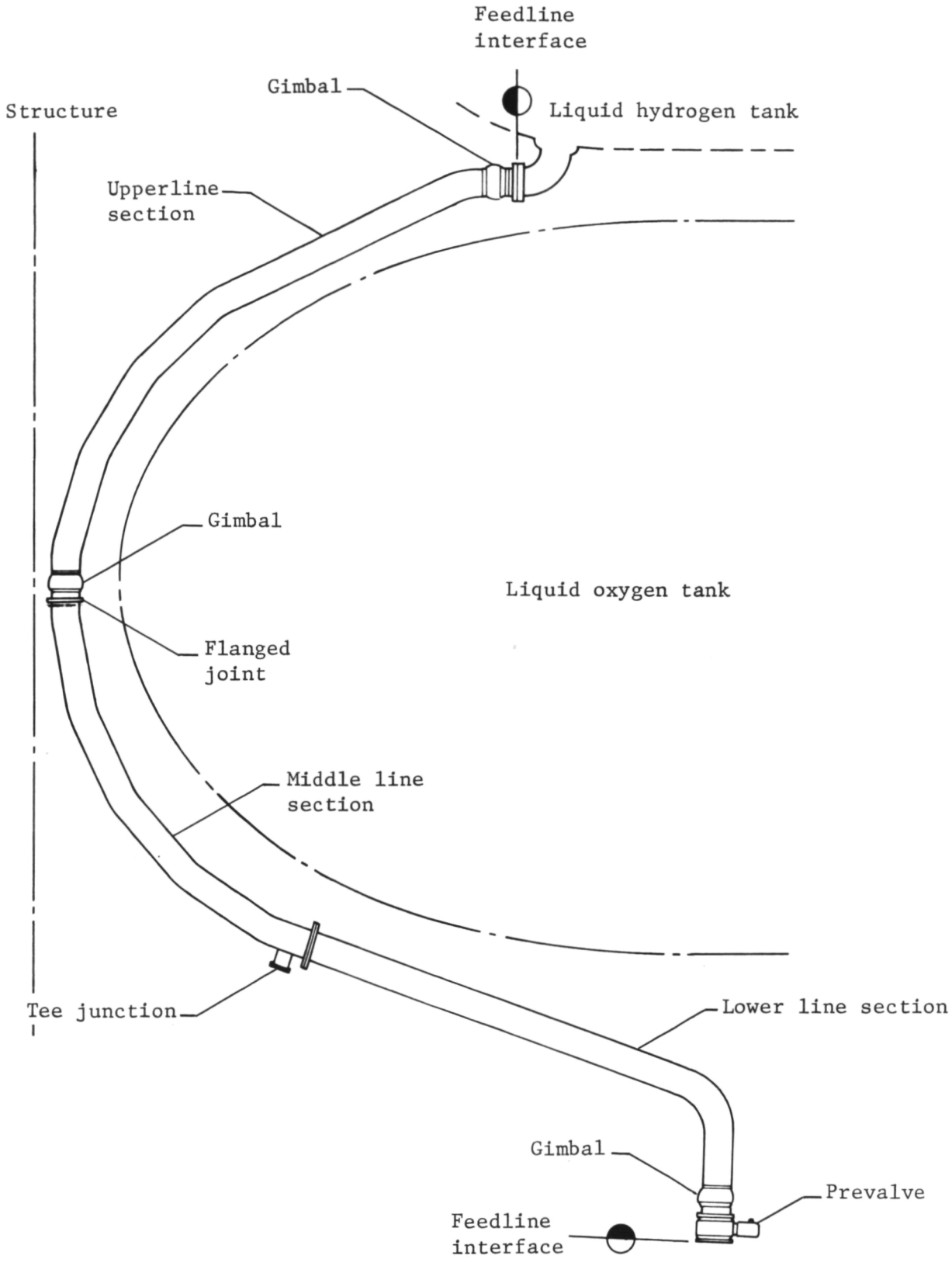

Figure IV-1. - Feedline Assembly

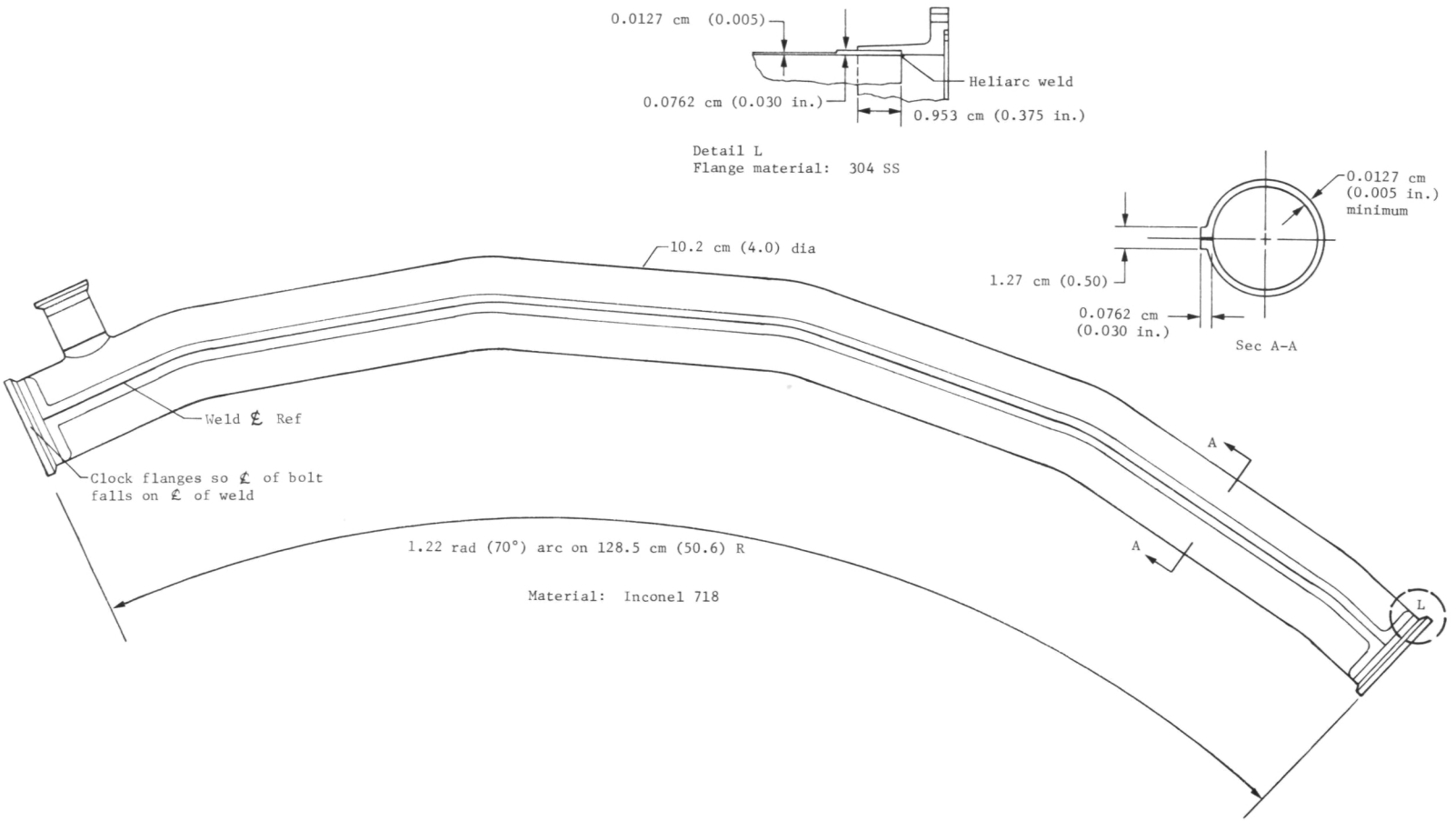

Figure IV-2. - Line Segment Details

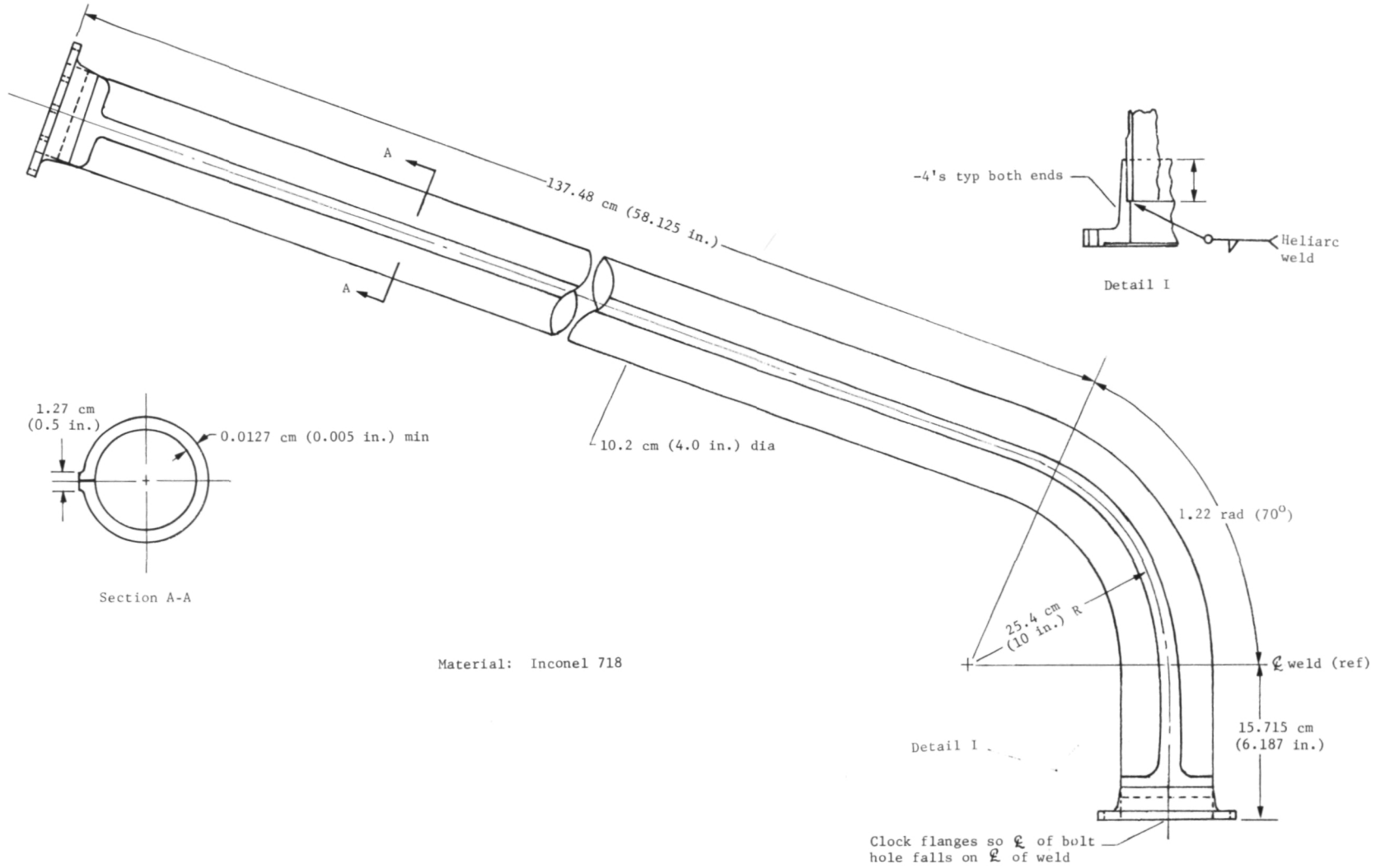

Figure IV-2. - Continued

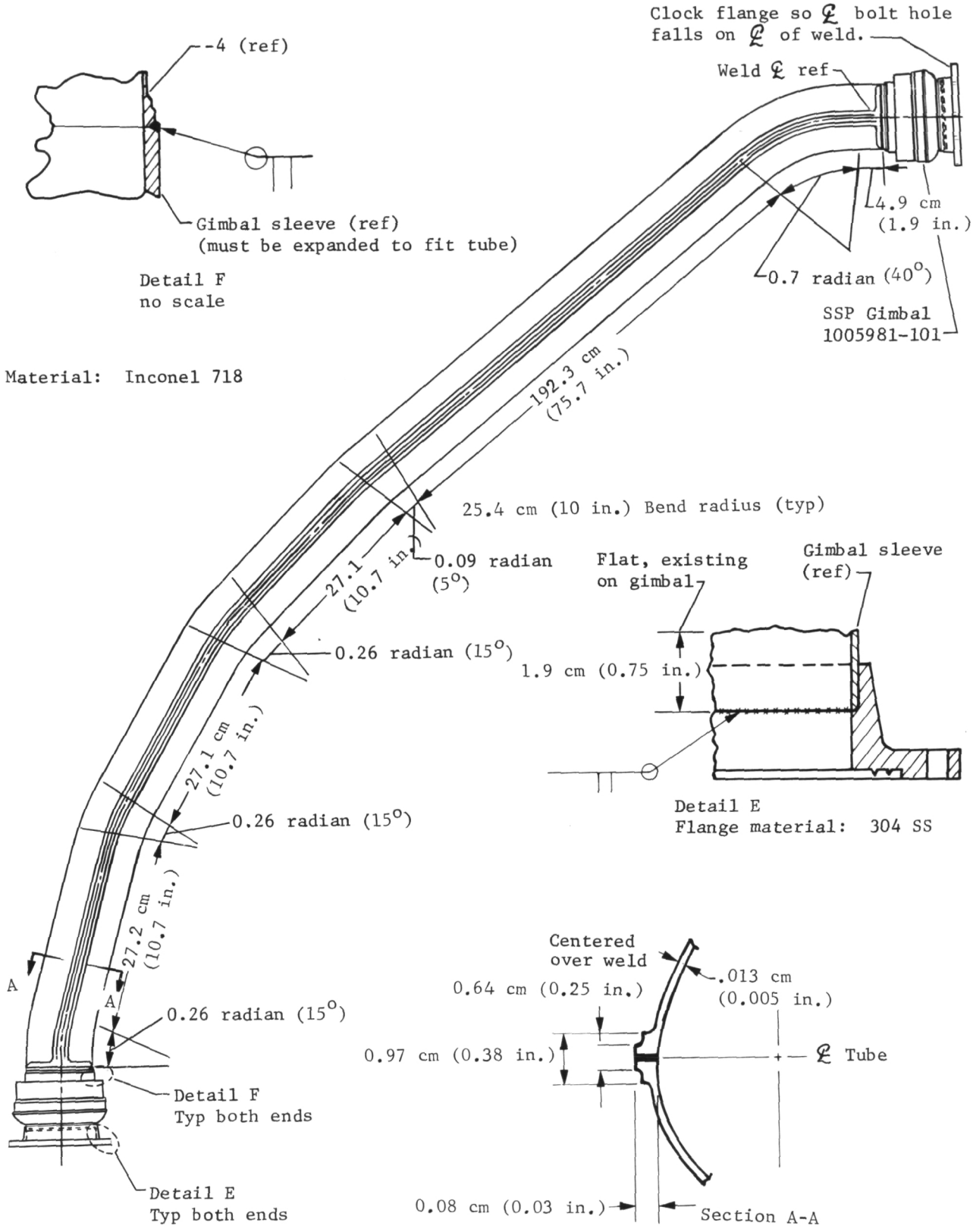

Figure IV-2. - Concluded

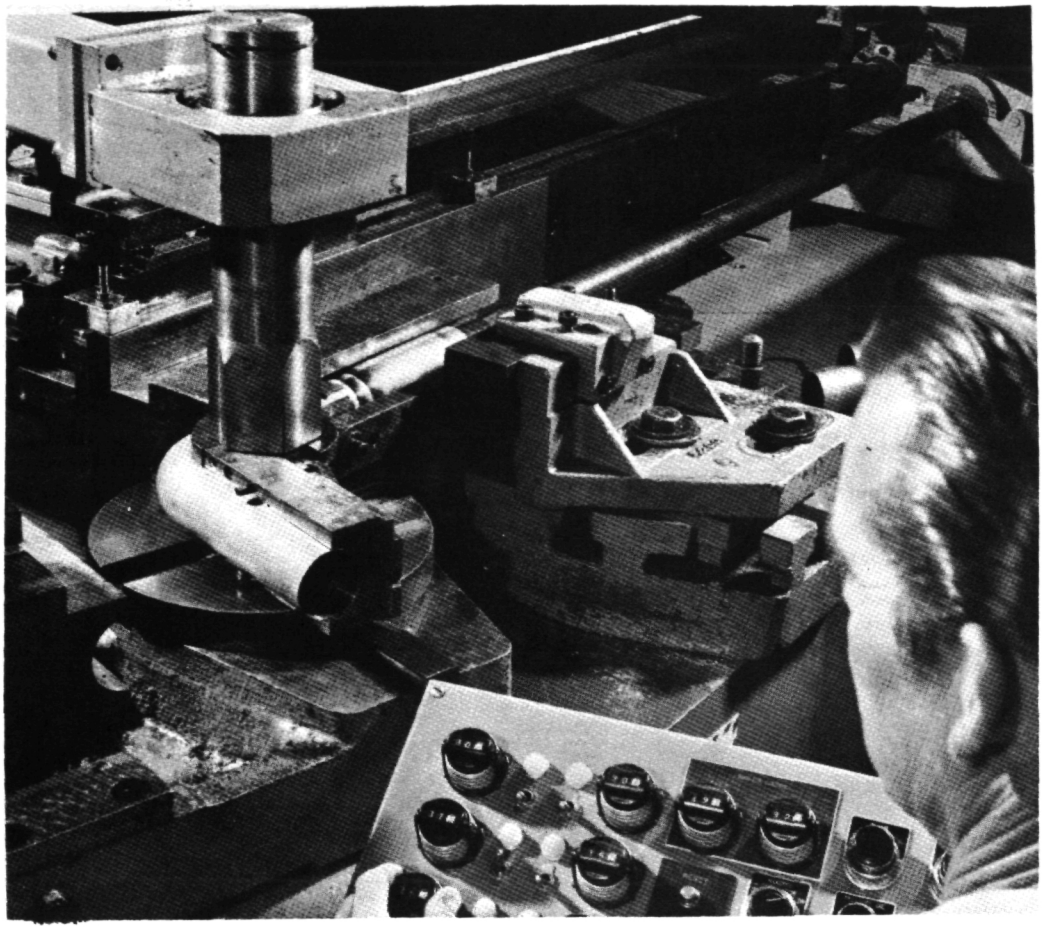

Figure V-I. - Typical Tube Bending Setup

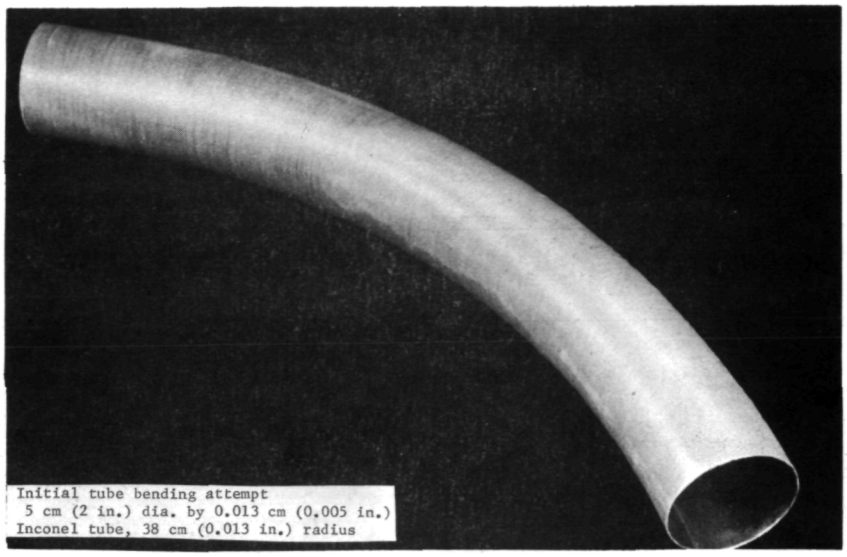

Initial tube bending attempt
5 cm (2 in.) dia. by 0.013 cm (0.005 in.)
Inconel tube, 38 cm (0.013 in.) radius

Aluminum support tube
on outside of thin
Inconel liner to provide
support during bending

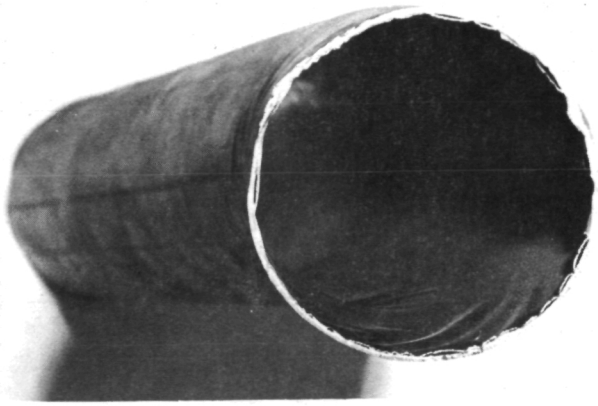

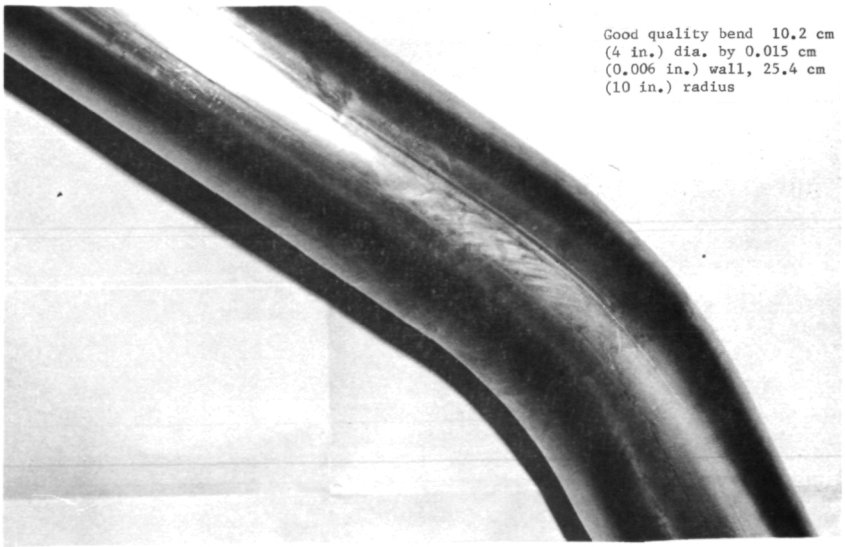

Good quality bend 10.2 cm
(4 in.) dia. by 0.015 cm
(0.006 in.) wall, 25.4 cm
(10 in.) radius

Figure V-2. - Photos of Thin Bending Results

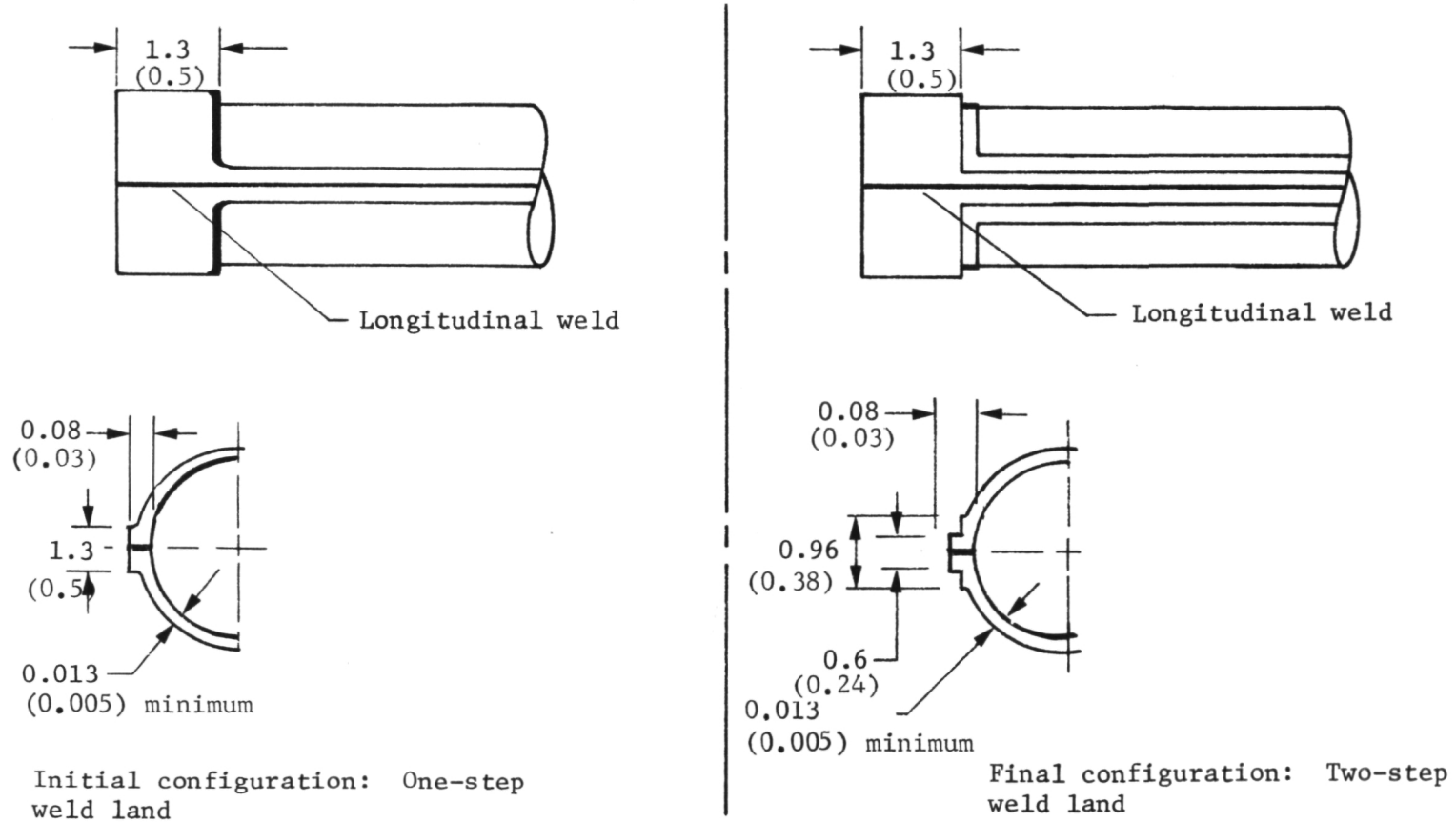

All dimensions in centimeters (in.)

Figure V-3. - Initial and Revised Chem-Milling Configuration

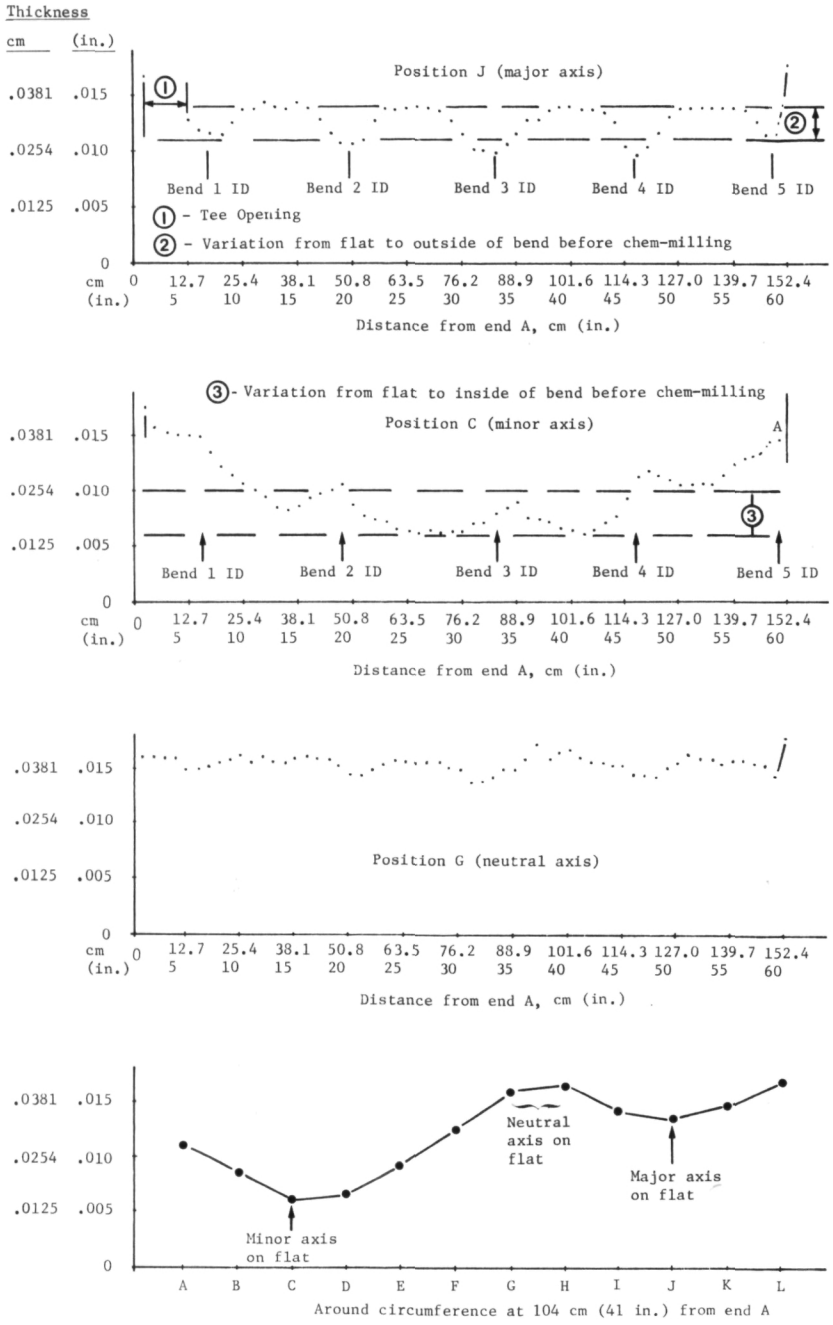

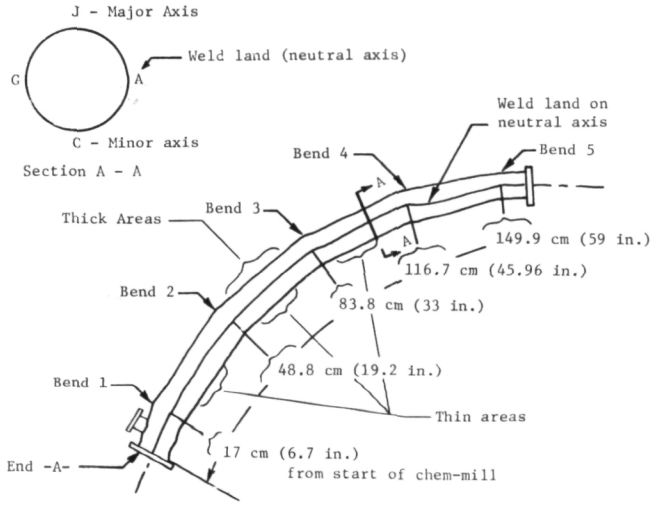

Figure V-4. - Eddy Current Measurement of Chem-Milled Tube Wall Thickness

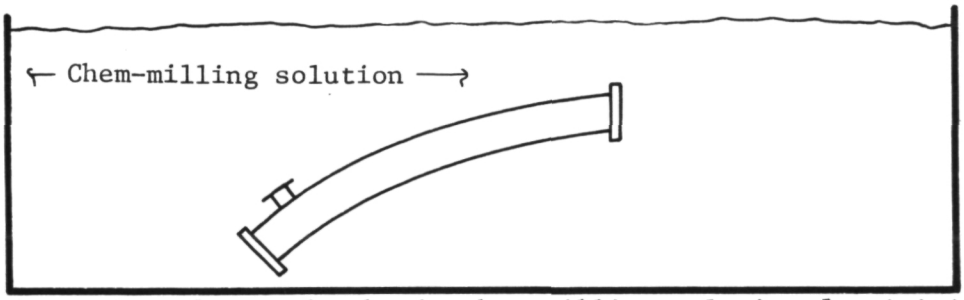

Orientation of curved tube in chem-milling solution for initial chem-milling operation and subsequent operations

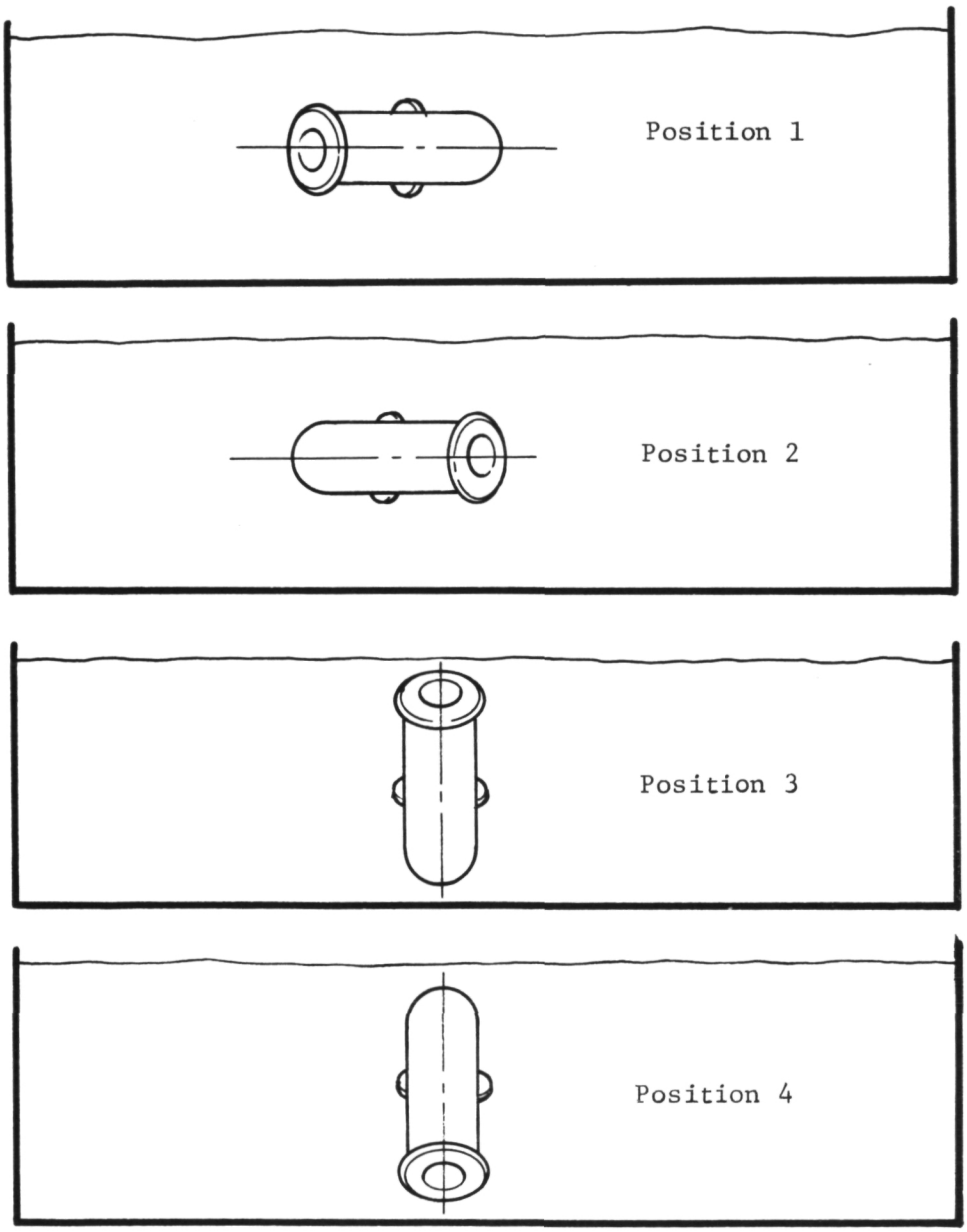

Figure V-5. - Time Controlled Tube Positioning in Chem-Milling Solution

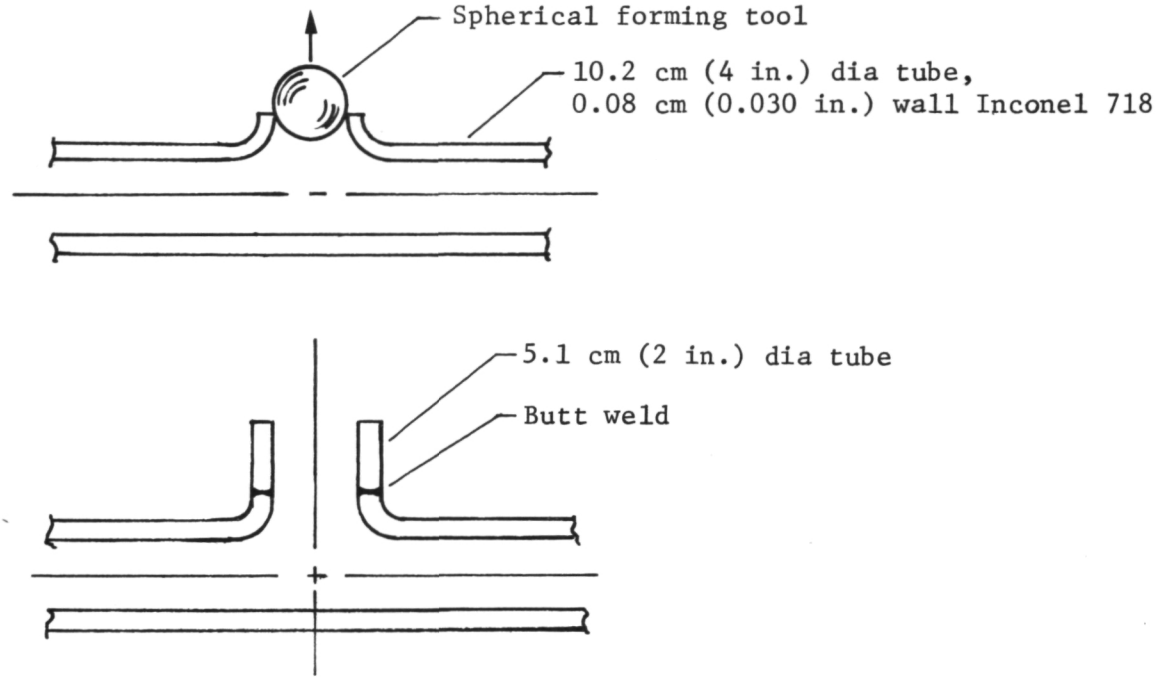

Figure V-6. - Fabrication of Tee Junction in Metal Liner

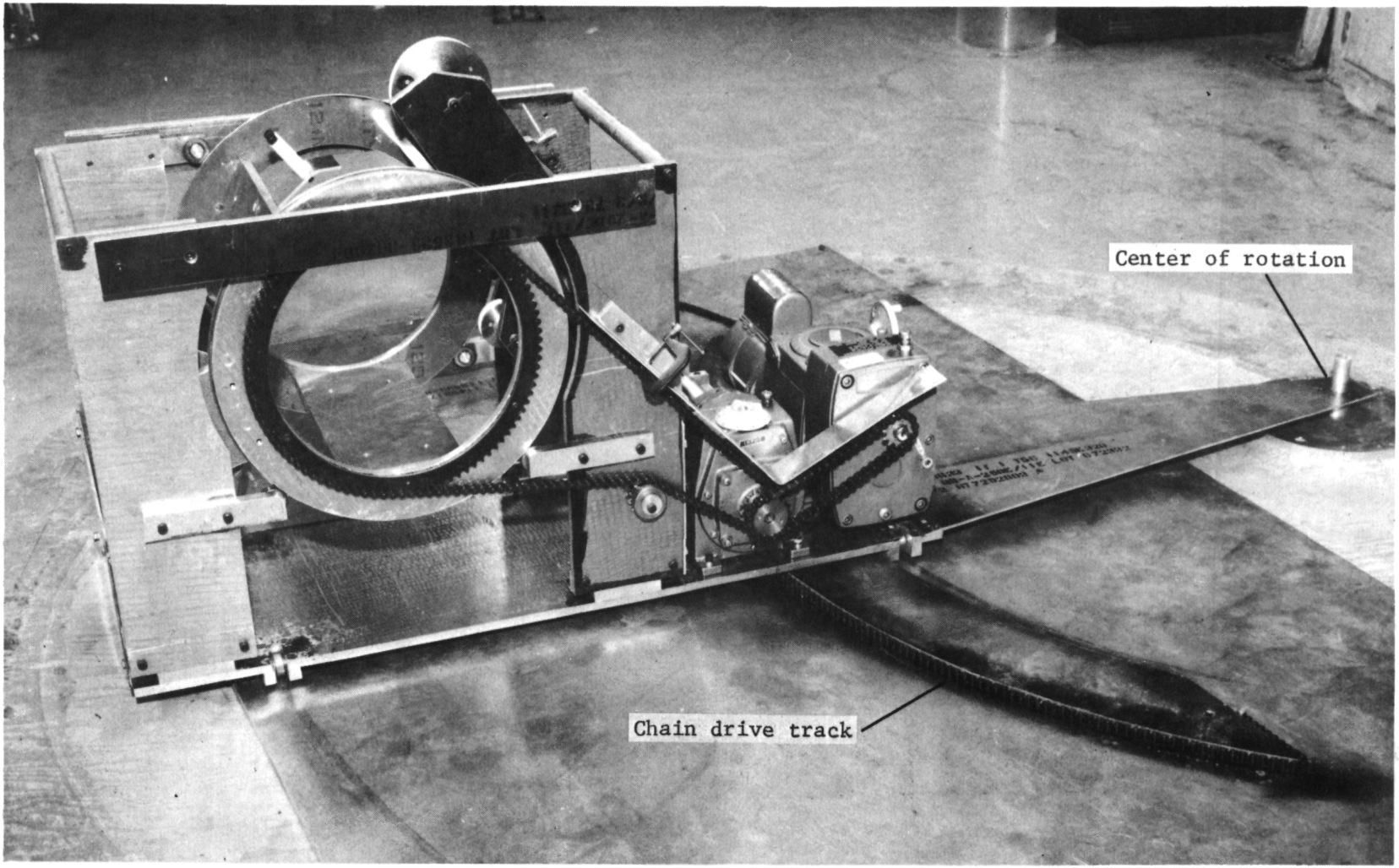

Figure V-7. - Polar Winding Tool for Applying Composite Overwrap on Curved Tubes

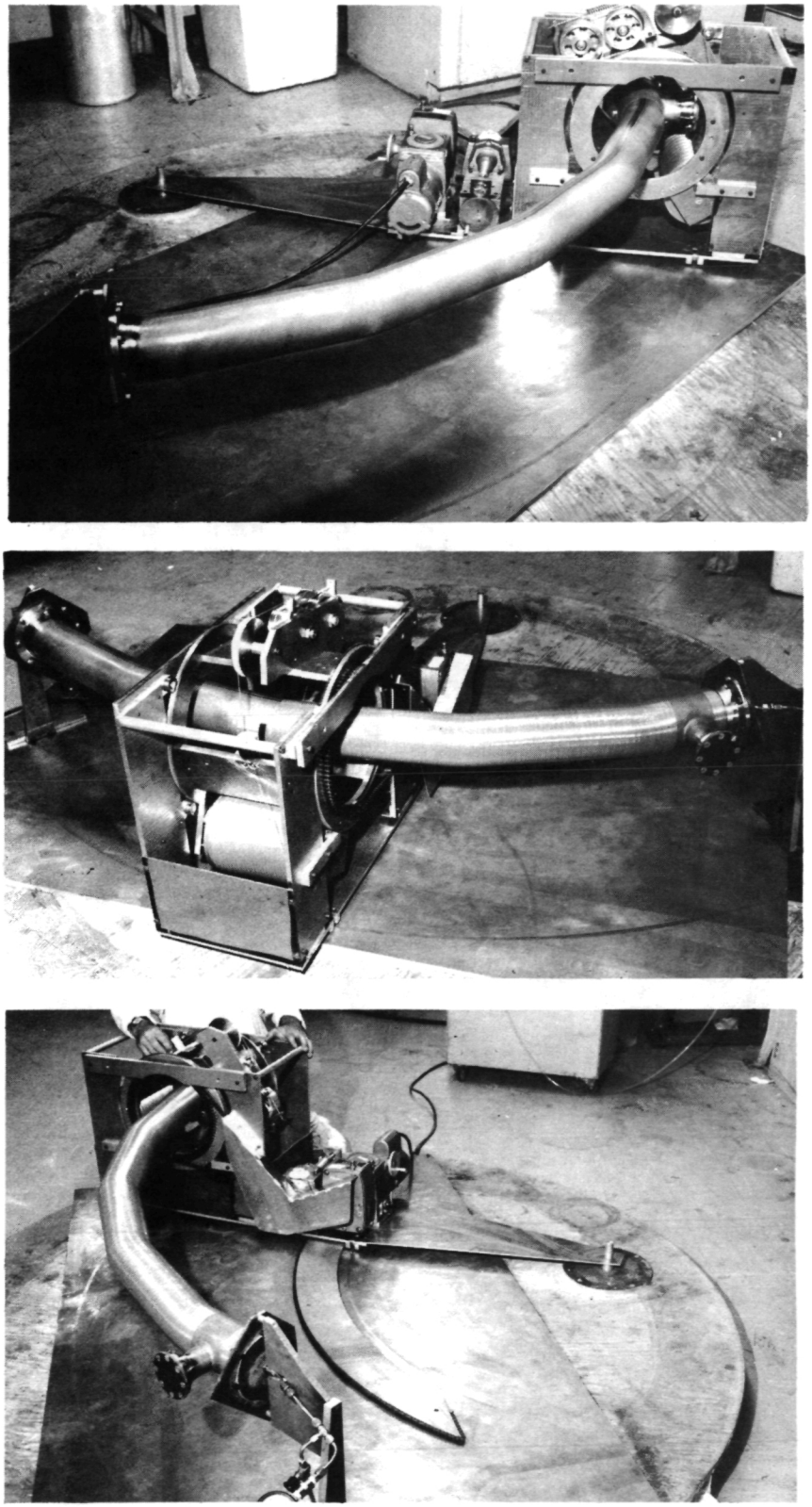

Figure V-8. - In-Process Photos of Filament Winding Operation

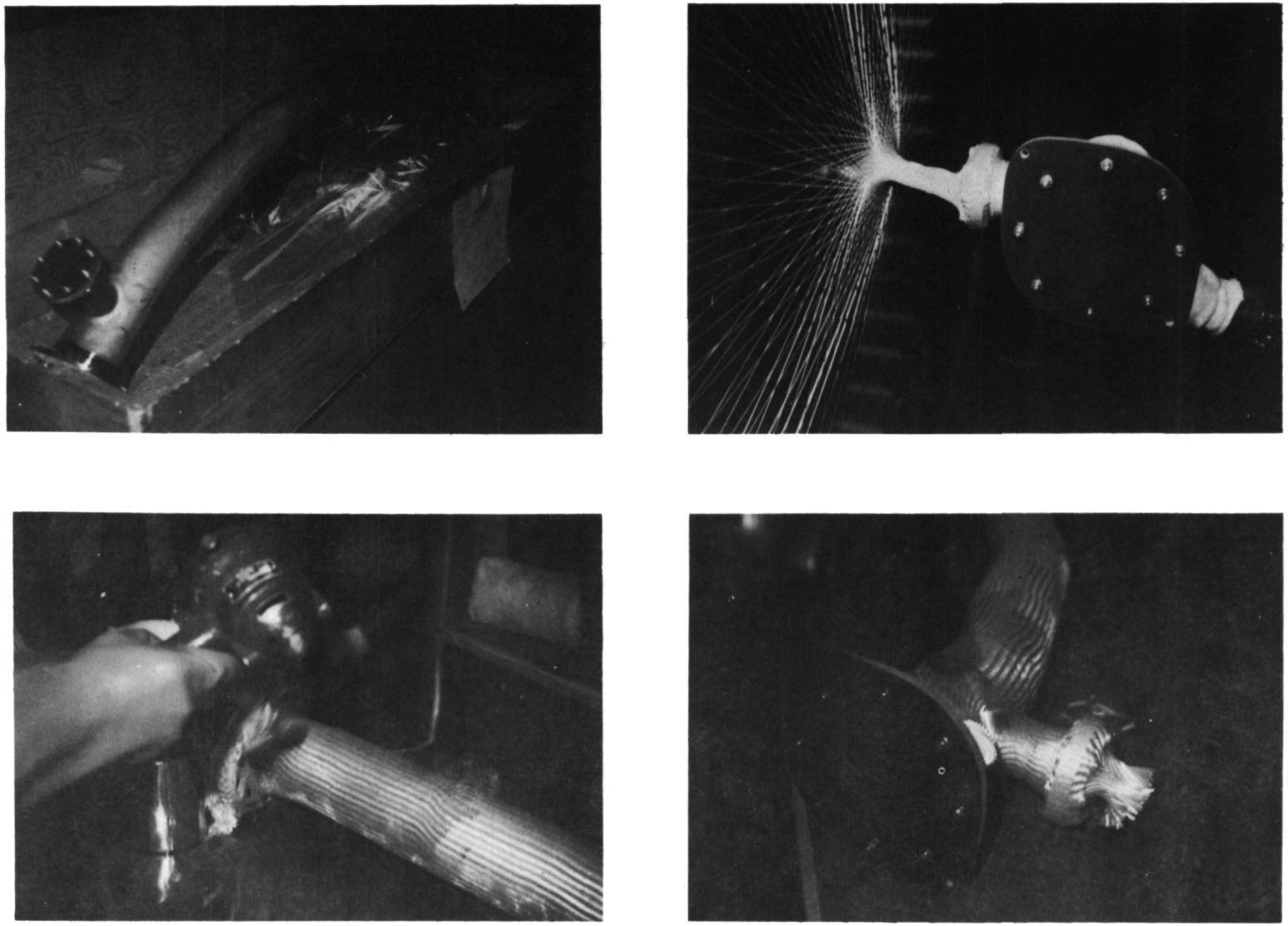

Figure V-9 - In-Process Photos of Braiding Operation

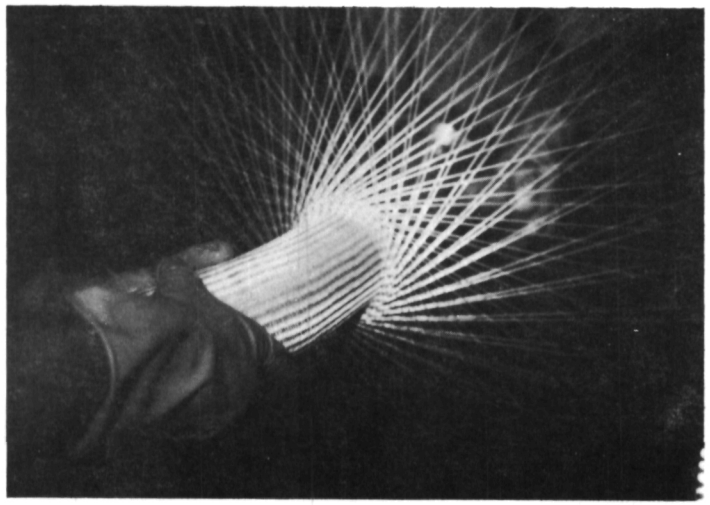

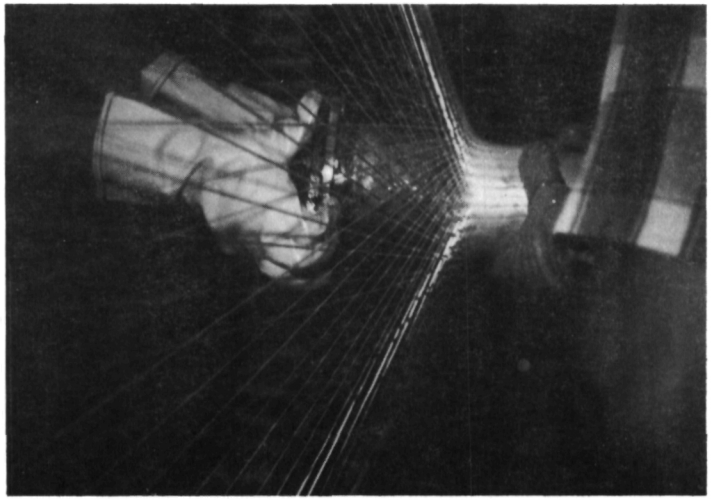

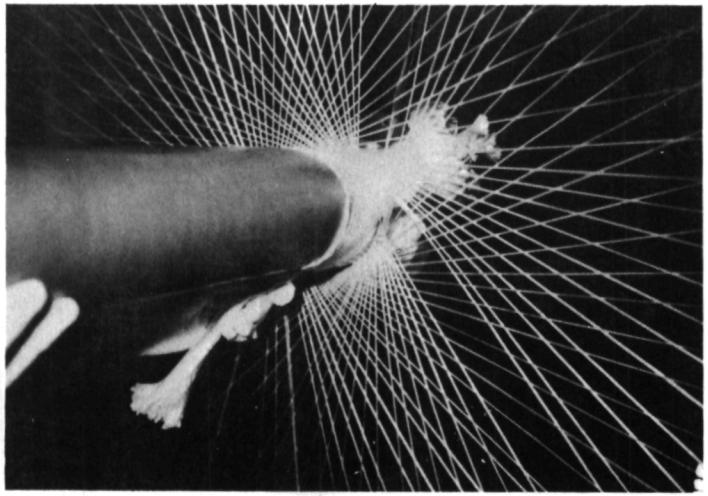

Figure V-9 . - Continued

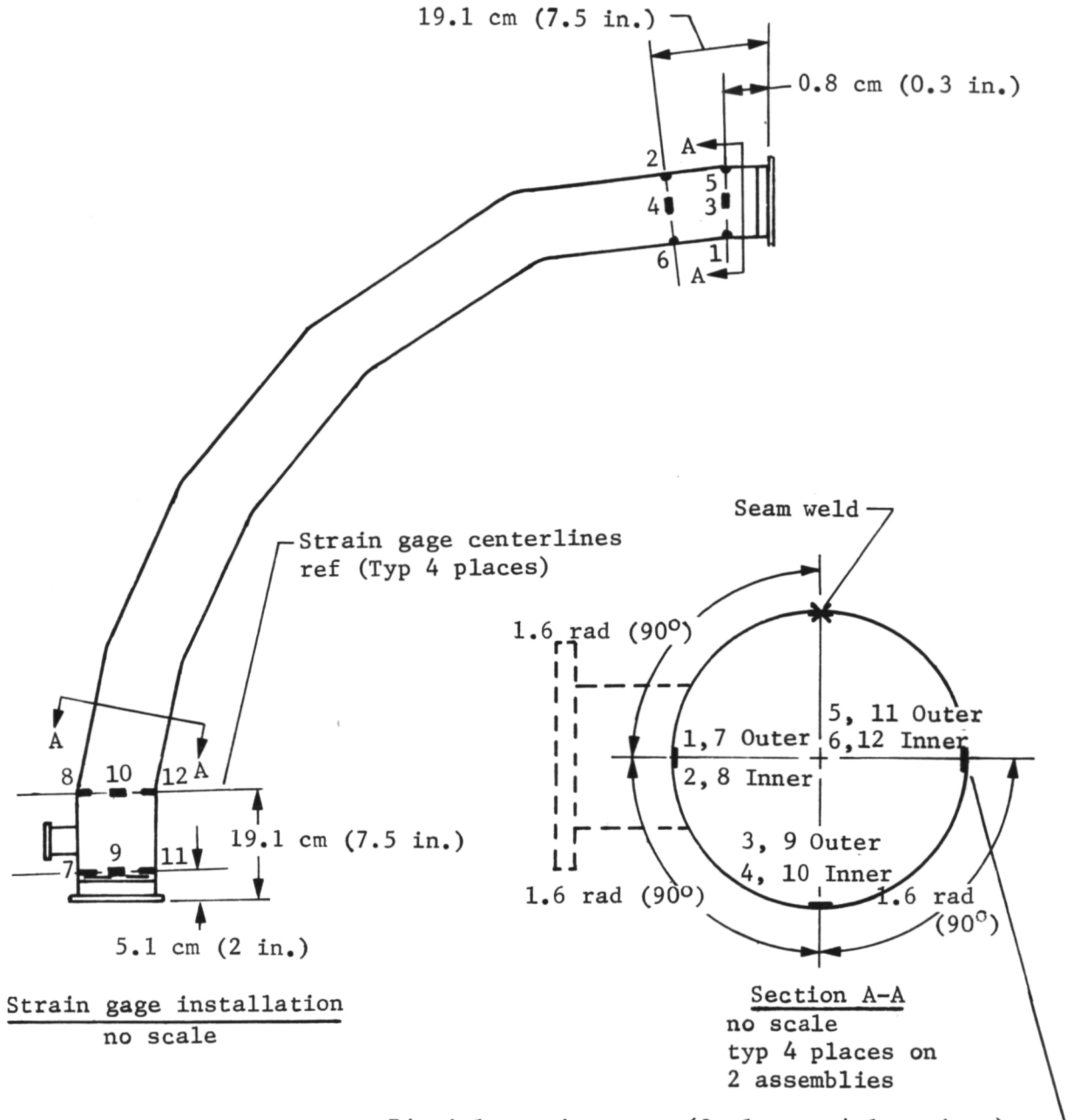

Figure VI-1. - Strain Gage Location

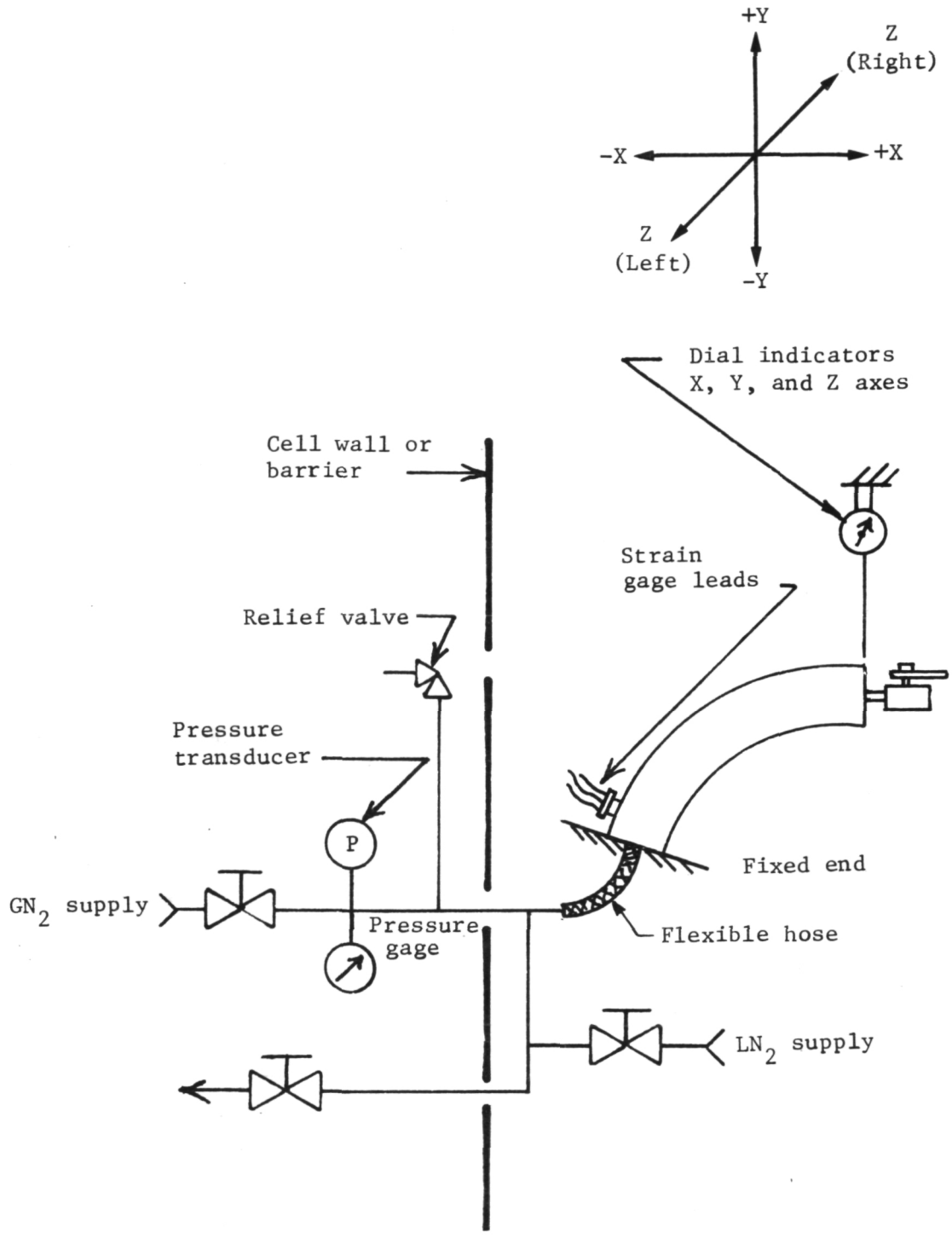

Figure VI-2. - Pressure Versus Strain and Deflection Test Schematic

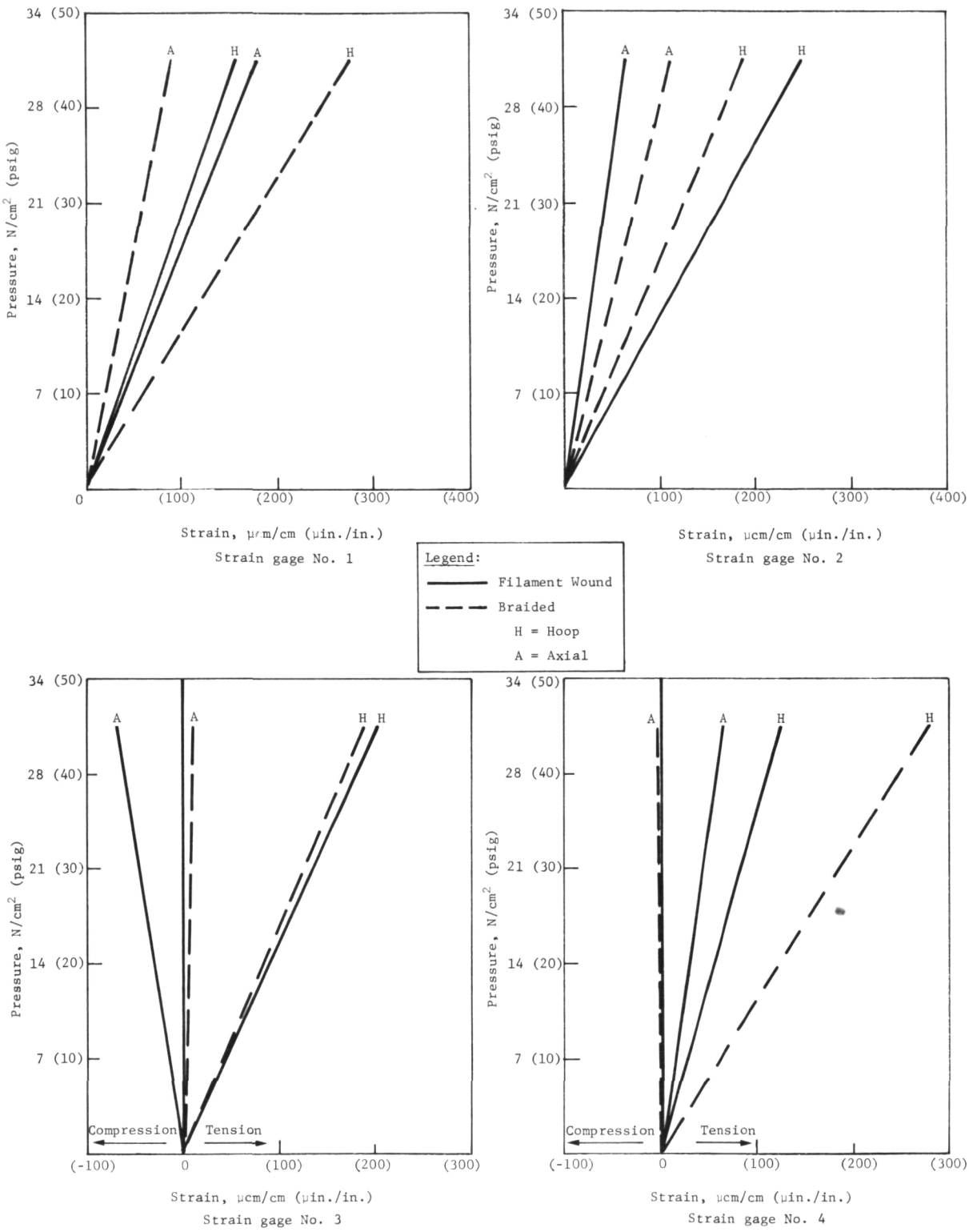

Figure VI-3. - Strain Versus Pressure Data for Filament Wound and Braided Curved Composite Tubing (Ambient Temperature)

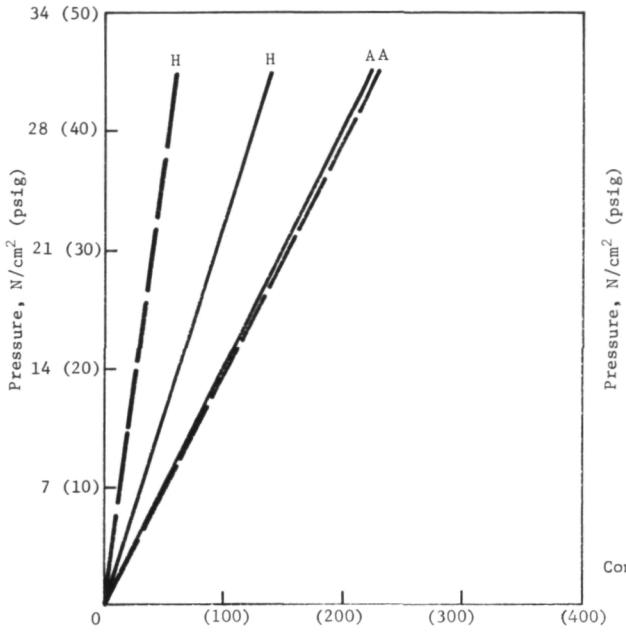

Strain, μcm/cm (μin./in.)
Strain gage No. 5

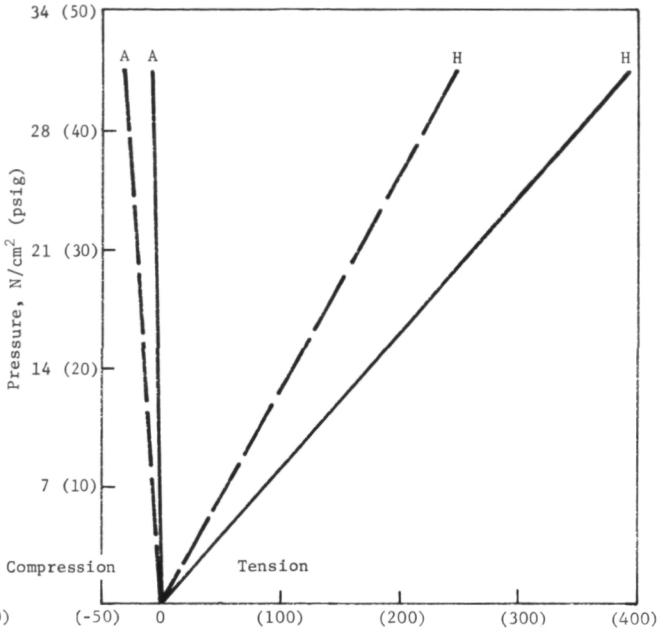

Strain, μcm/cm (μin./in.)
Strain gage No. 6

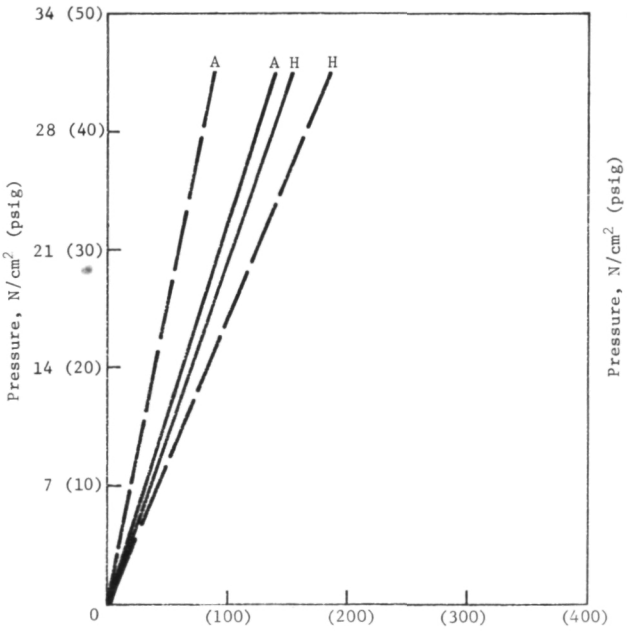

Strain, μcm/cm (μin./in.)
Strain gage No. 7

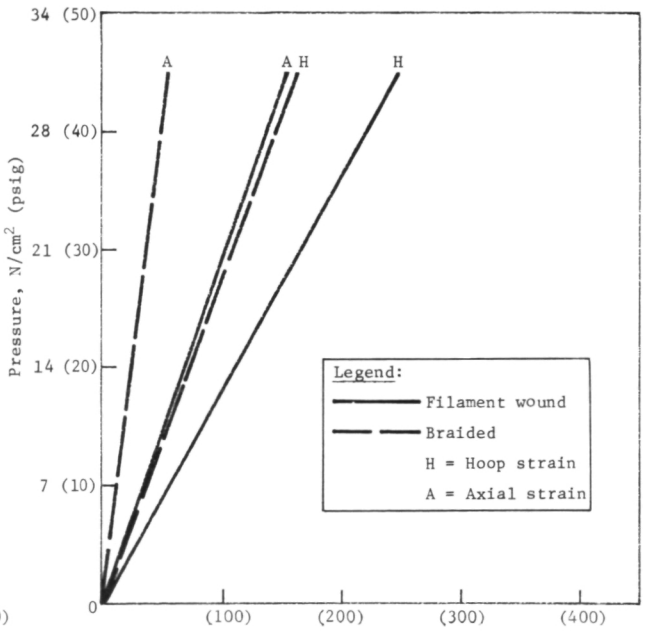

Strain, μcm/cm (μin./in.)
Strain gage No. 8

Figure VI-3. - Continued

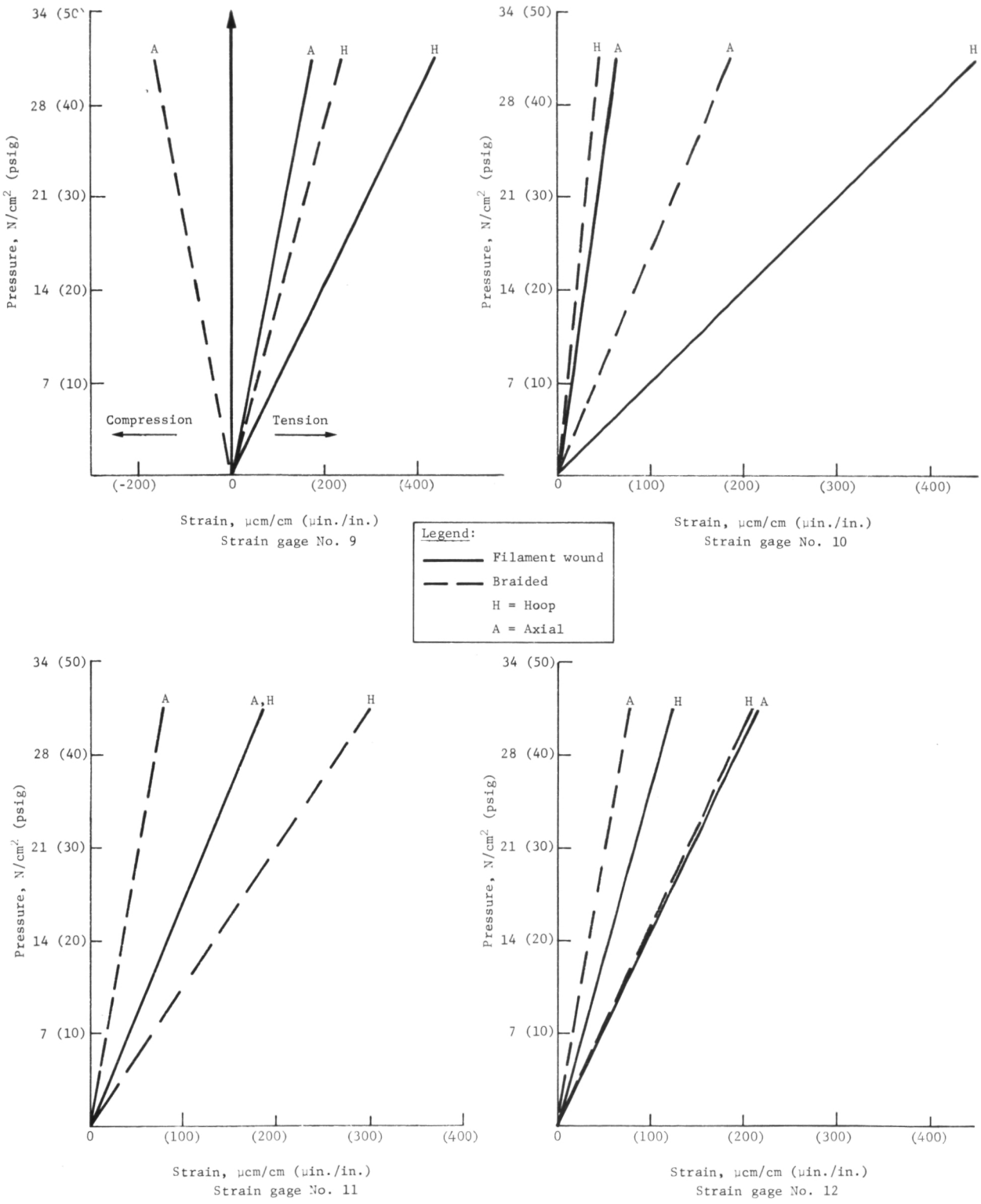

Figure VI-3. - Concluded

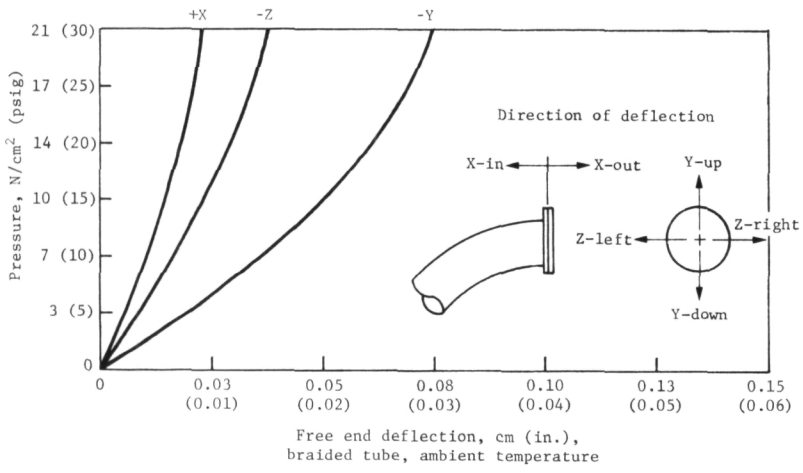

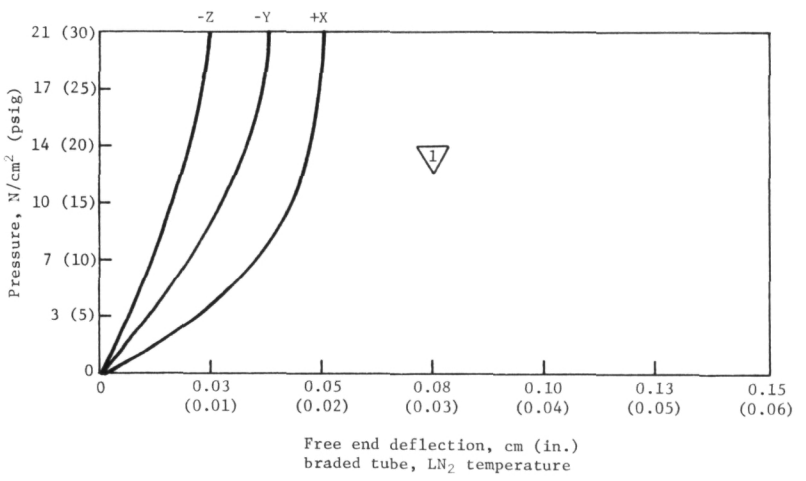

1 Deflection due to Pressure.
Dial Indicators zeroed after tube was filled with LN_2

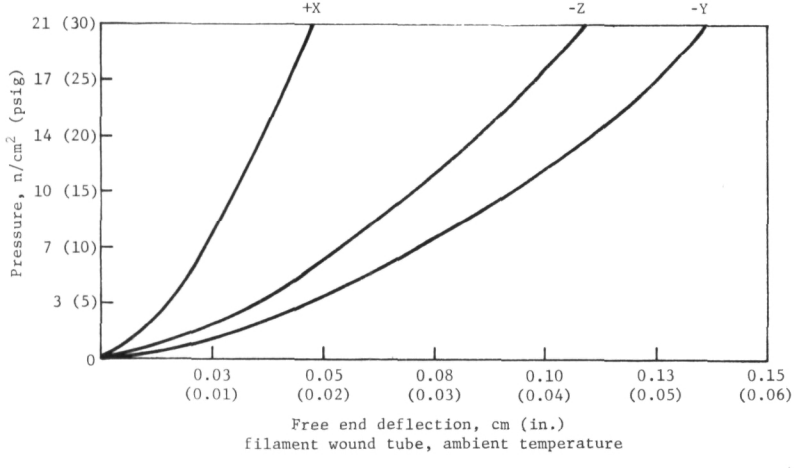

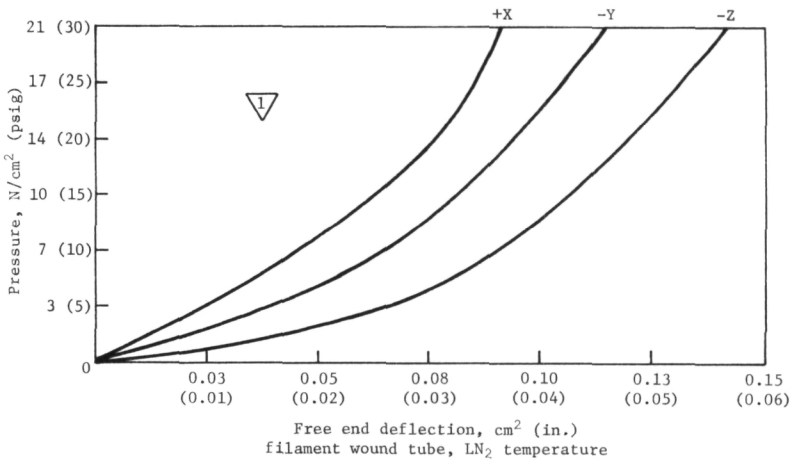

Figure VI-4. - Pressure Versus Deflection Data for Filament Wound and Braided Curved Composite Tubing

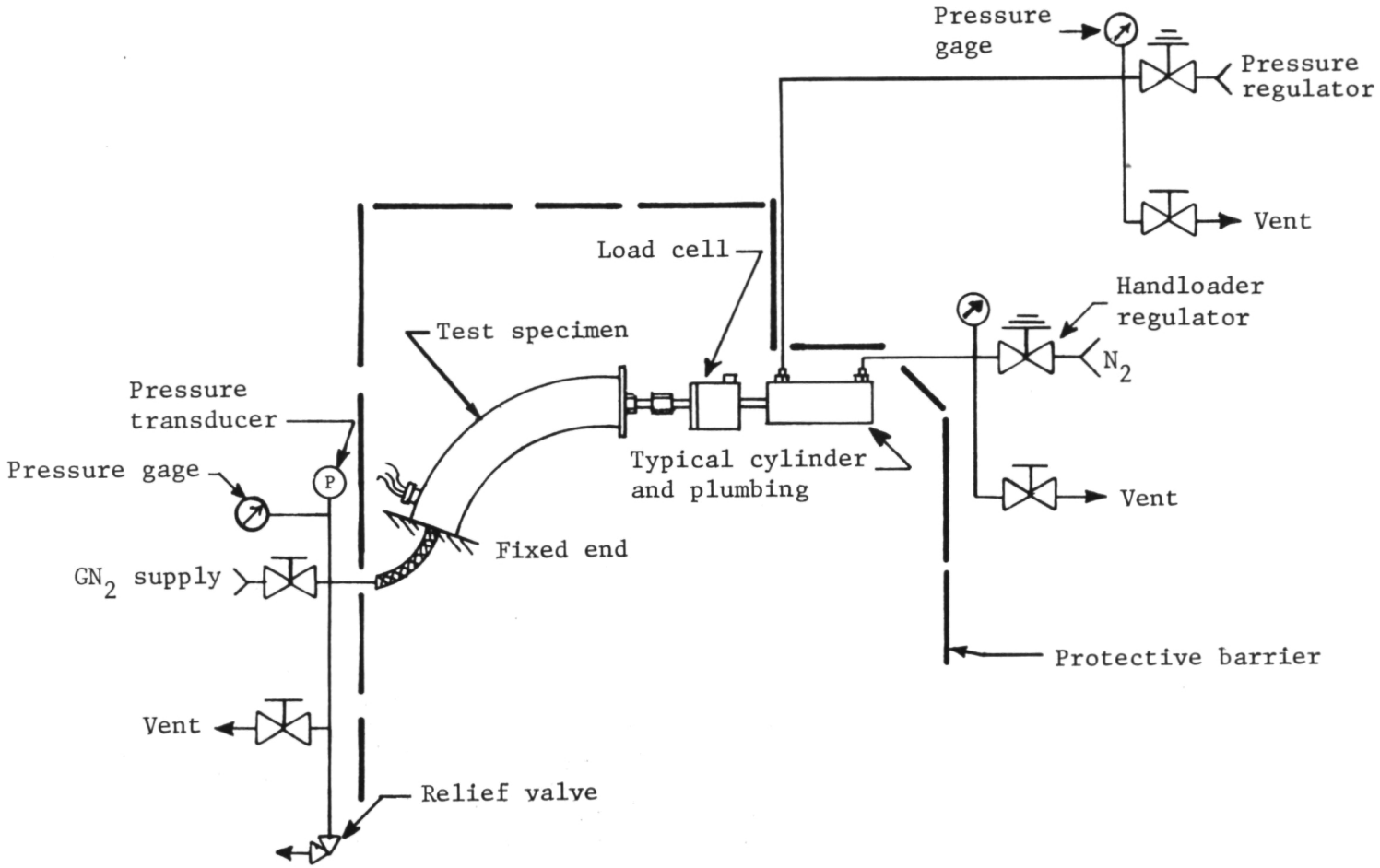

Figure VI-5. - External Load Versus Deflection Test Setup Schematic

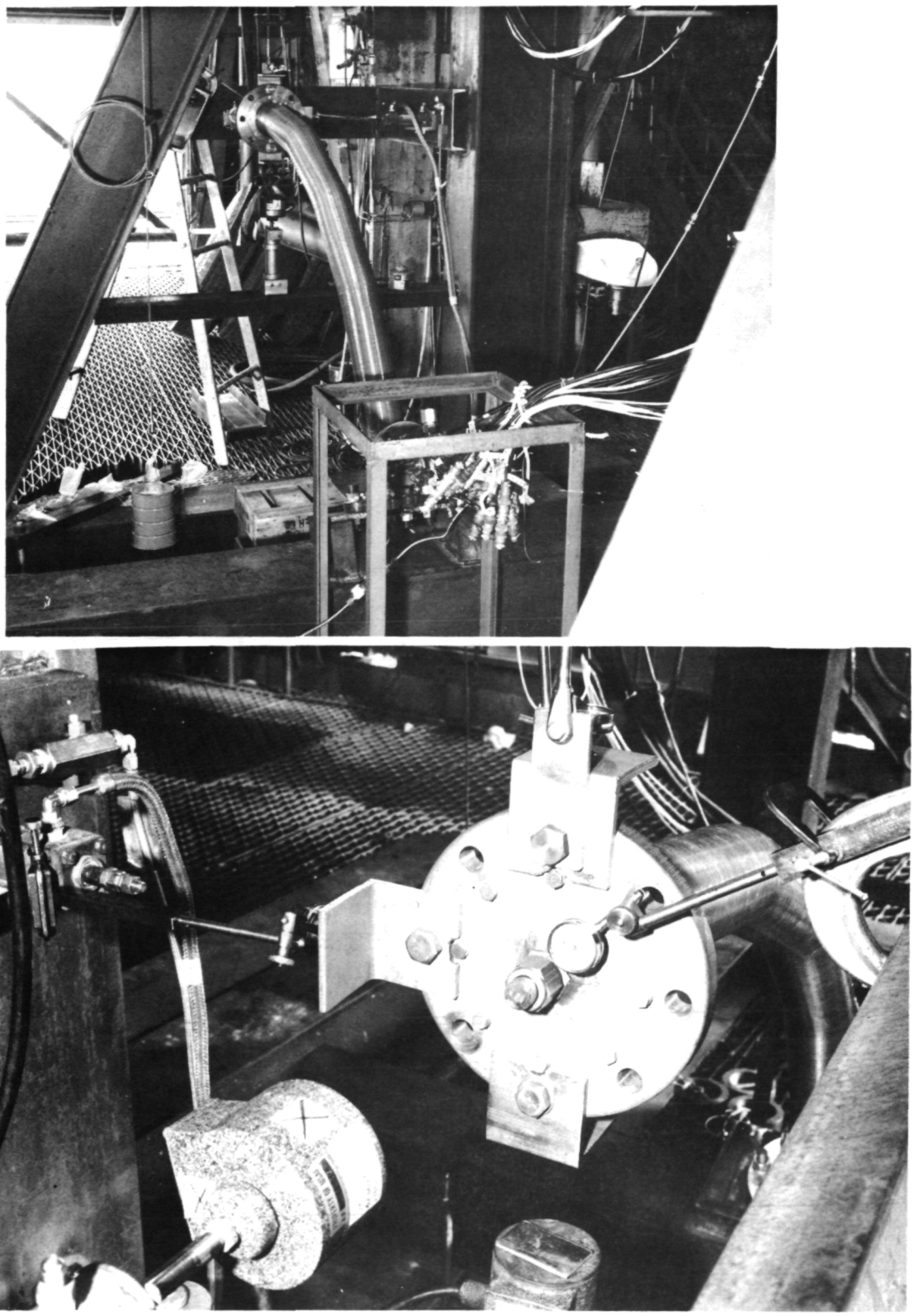

Figure VI-6. - Photos of Test Setup - External Load Versus Deflection

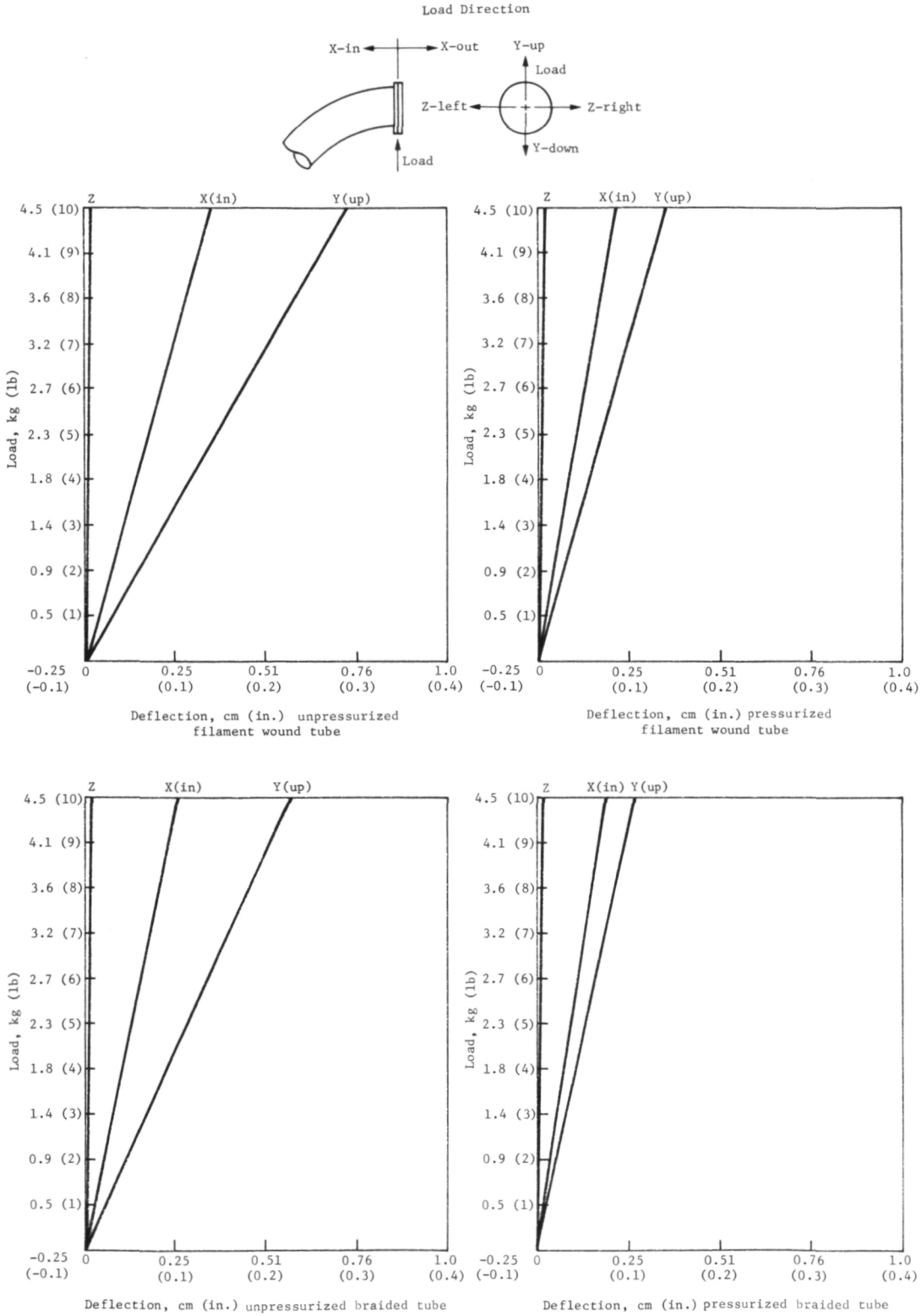

Figure VI-7. - Load Versus Deflection Data for Pressurized and Unpressurized Curved Composite Tubing

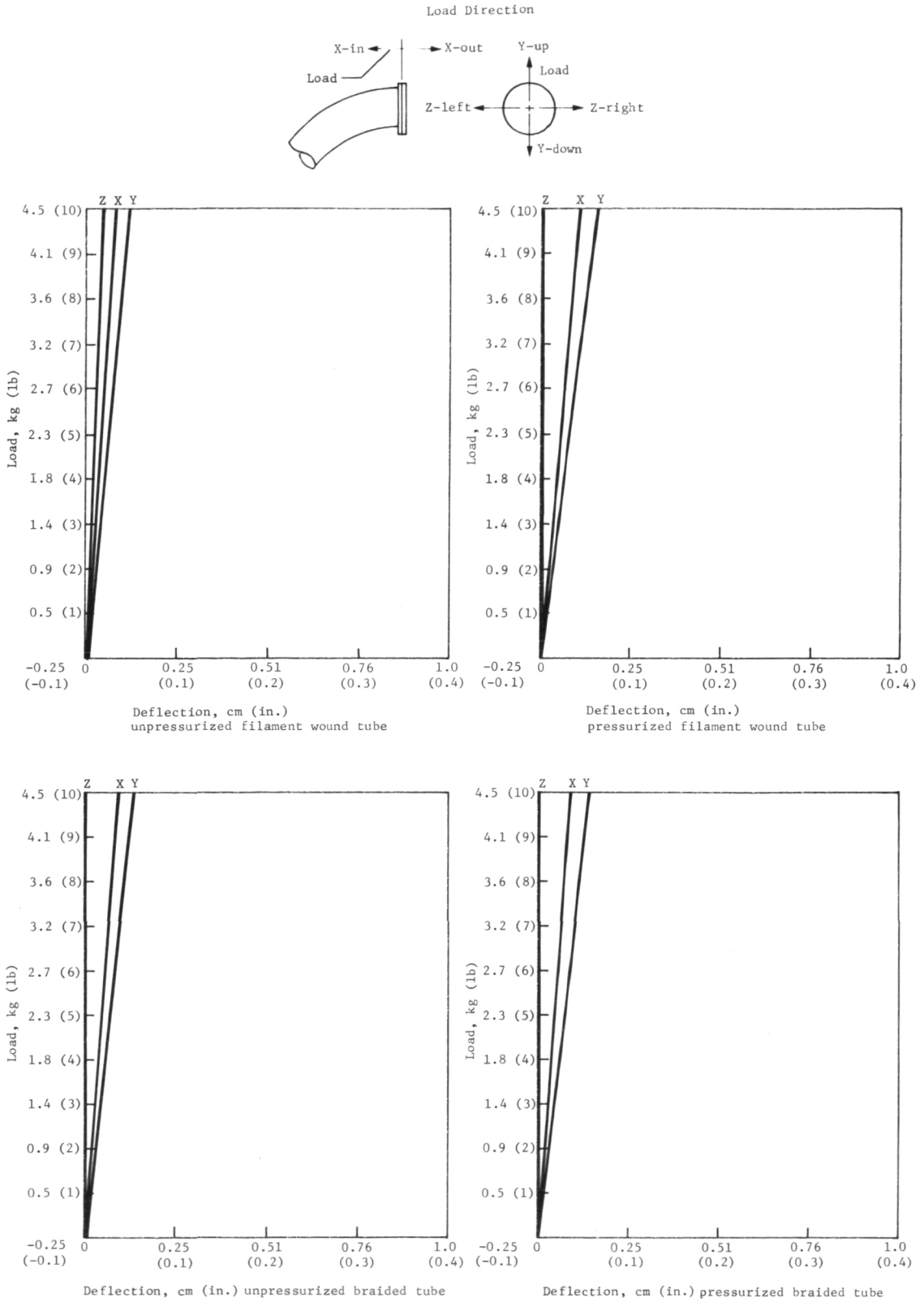

Figure VI-7. - Concluded

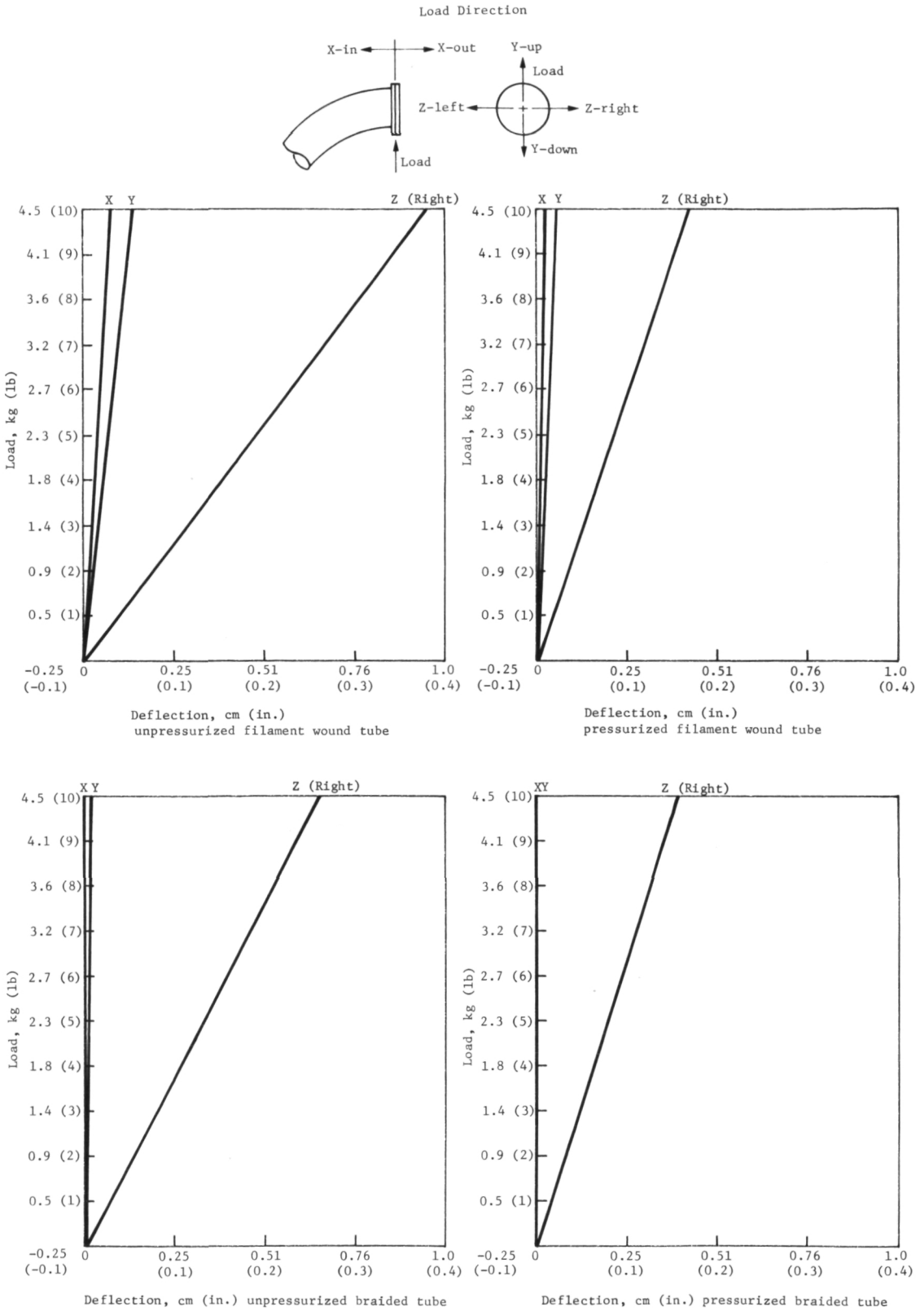

Figure VI-7. - Concluded

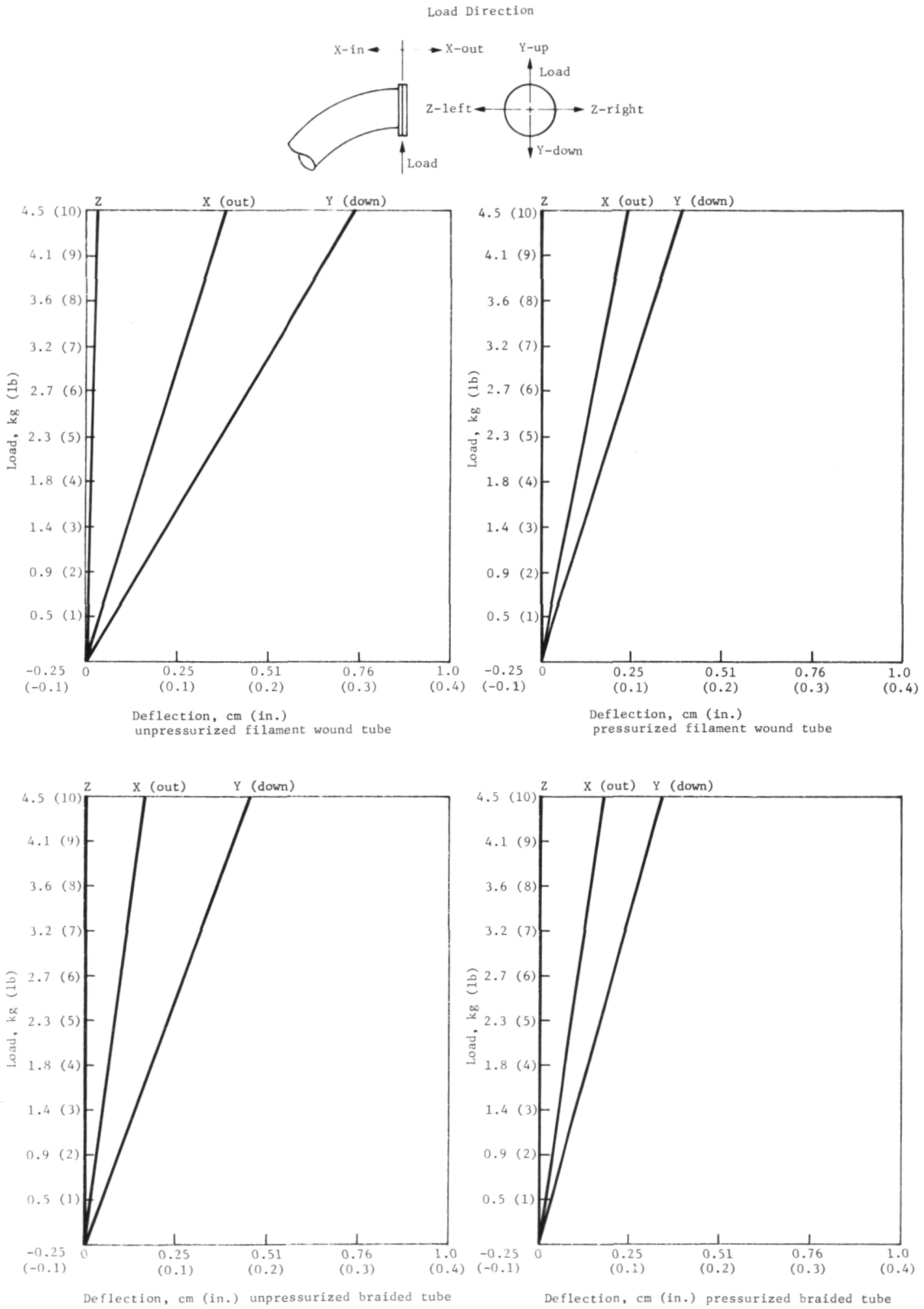

Figure VI-7. - Concluded

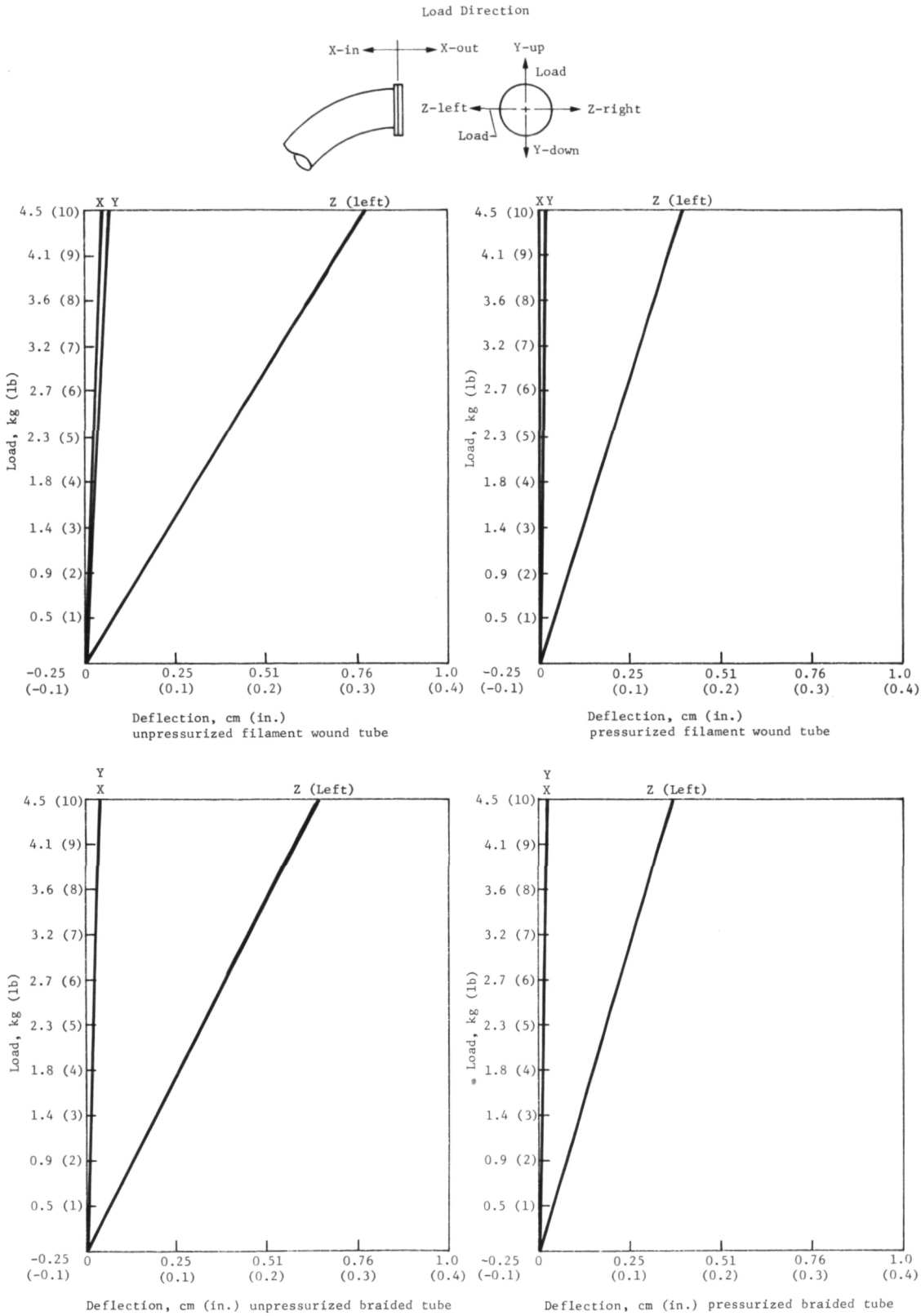

Figure VI-7. - Concluded

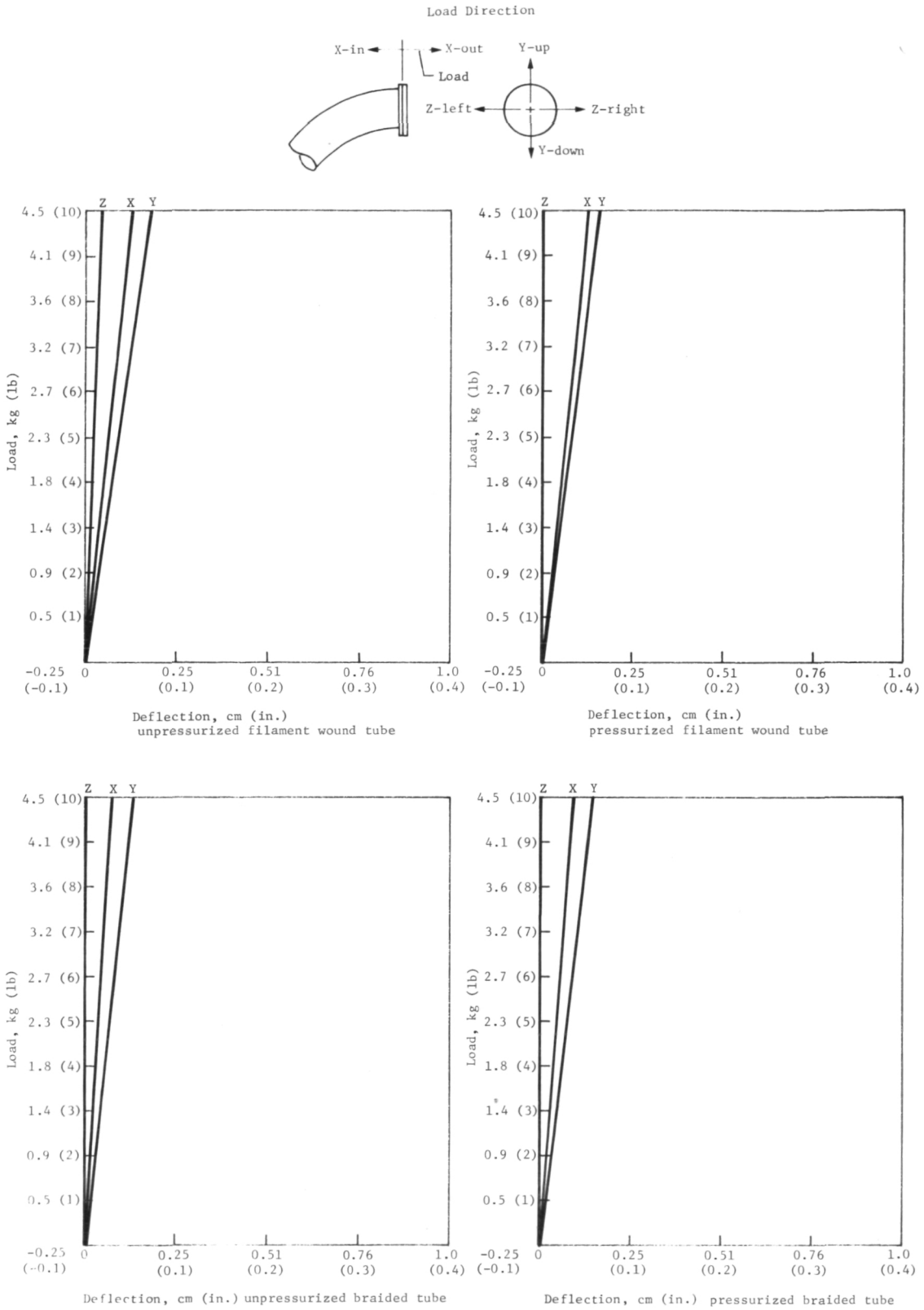

Figure VI-7. - Concluded

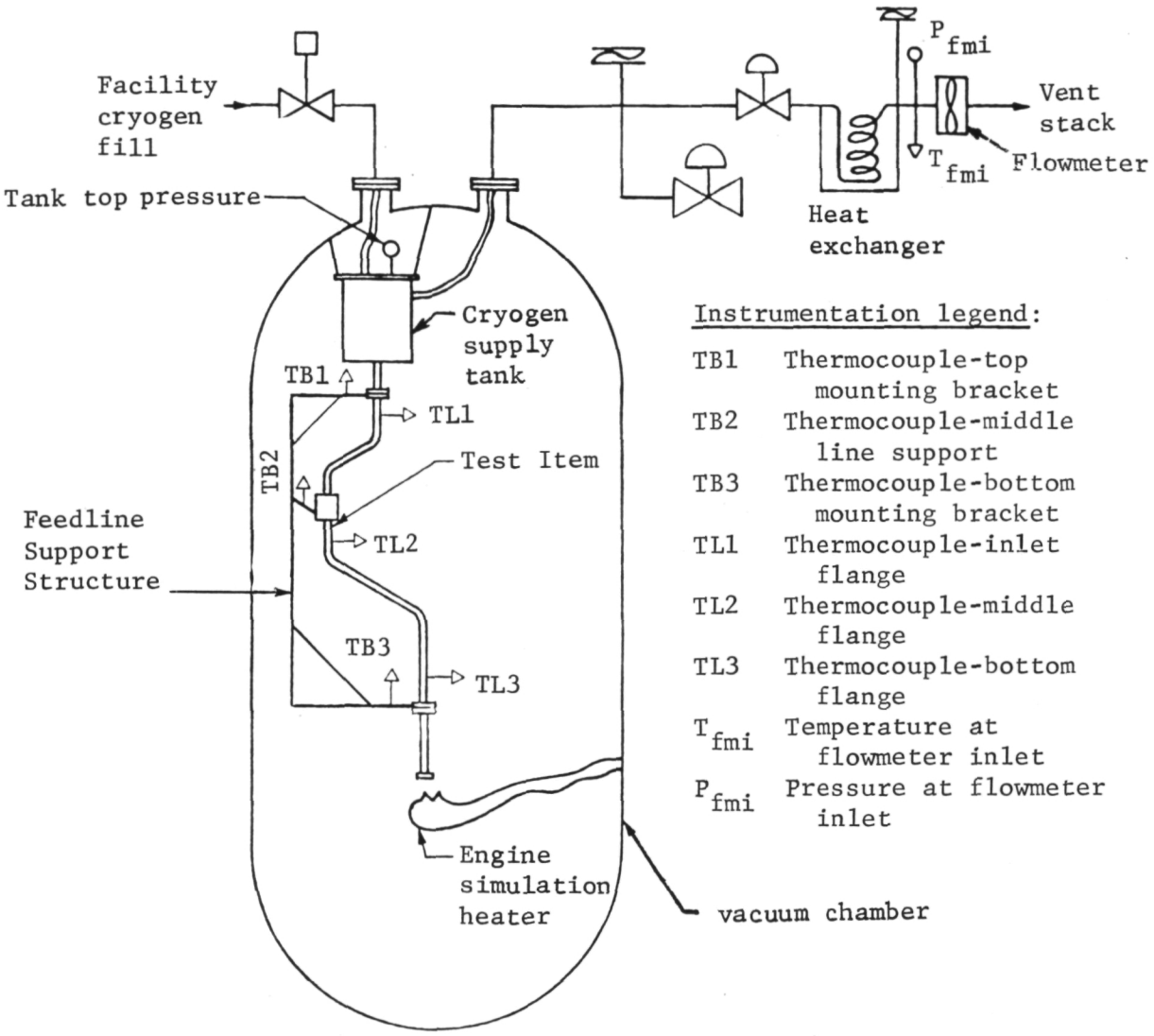

Figure VI-8. - Steady-State Heat Input Test Schematic

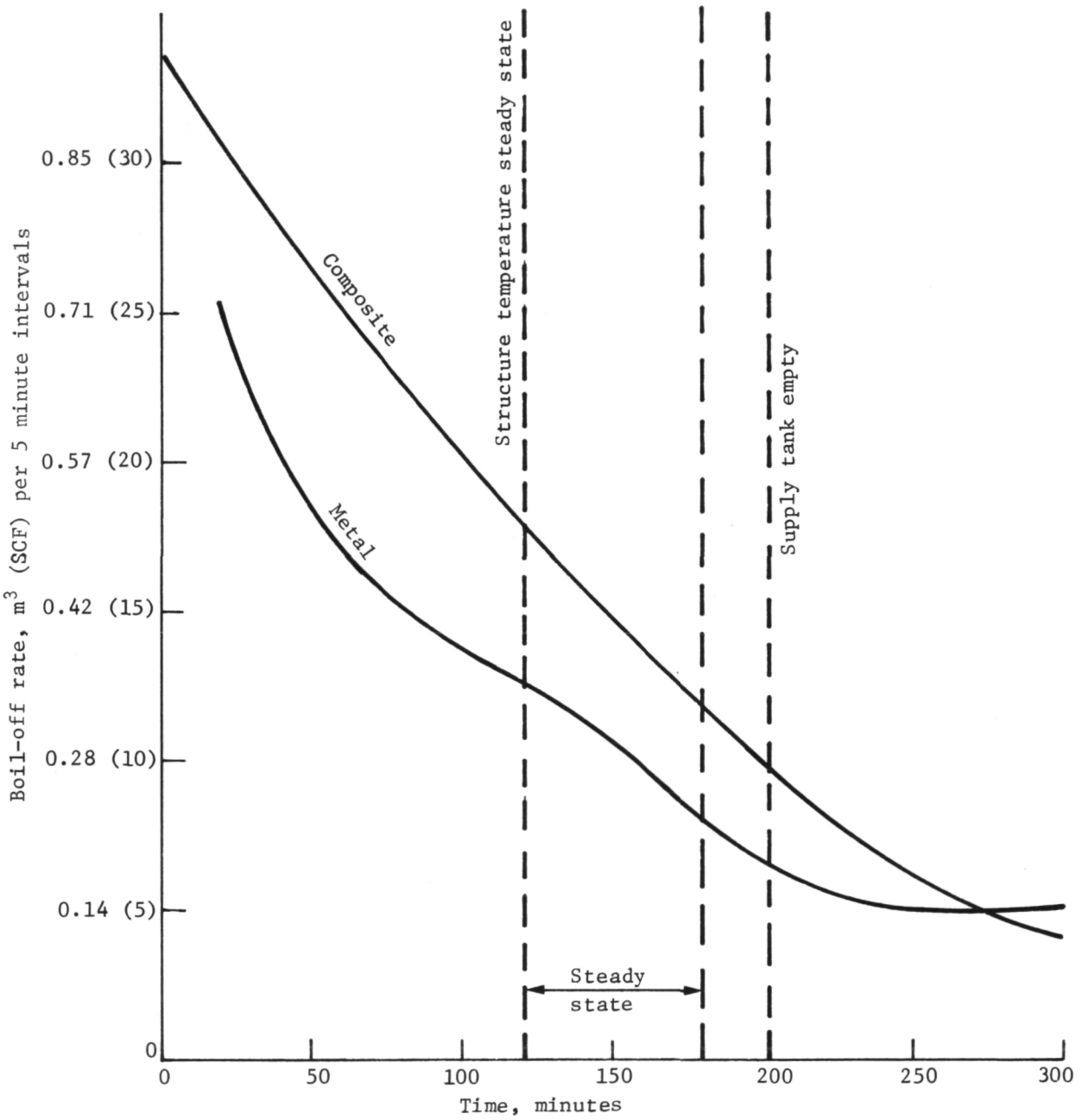

Figure VI-9a. - Boil-off Data - Steady State Heat Input Test

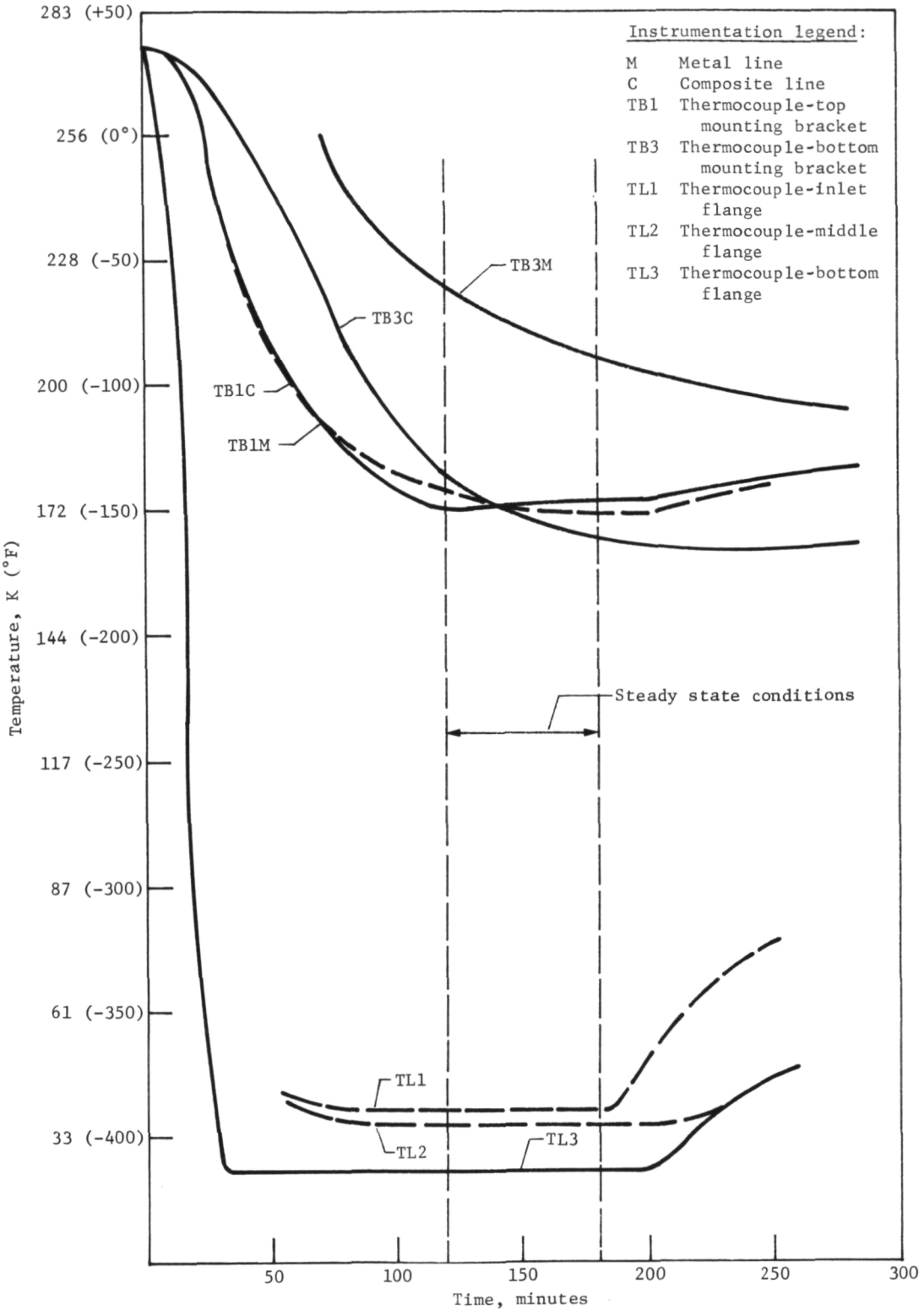

Figure VI-9b. - Temperature Profiles of Feedlines and Support Structure - Steady State Heat Input

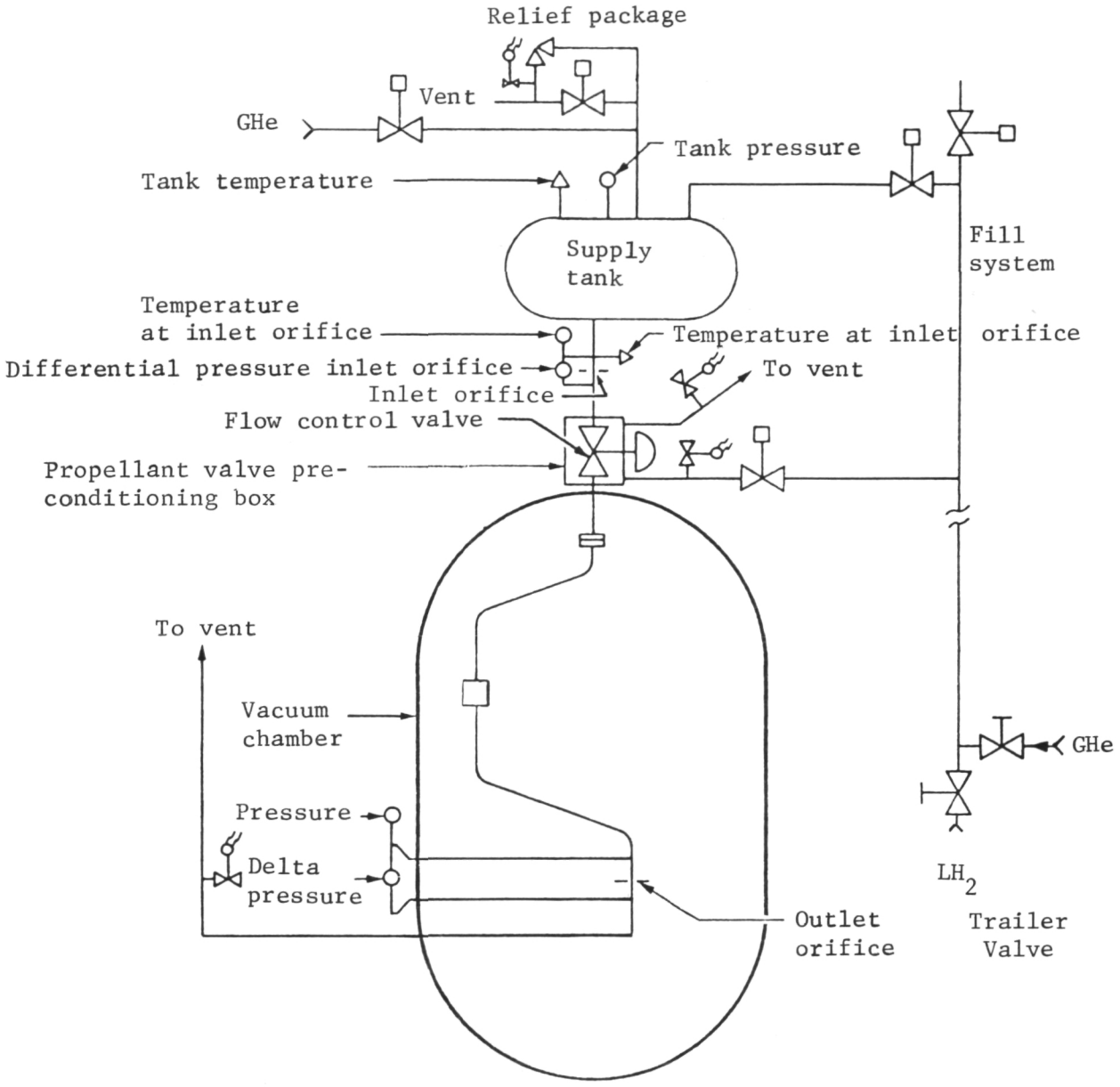

Figure VI-10. - Chilldown and Flow Quality Test Schematic

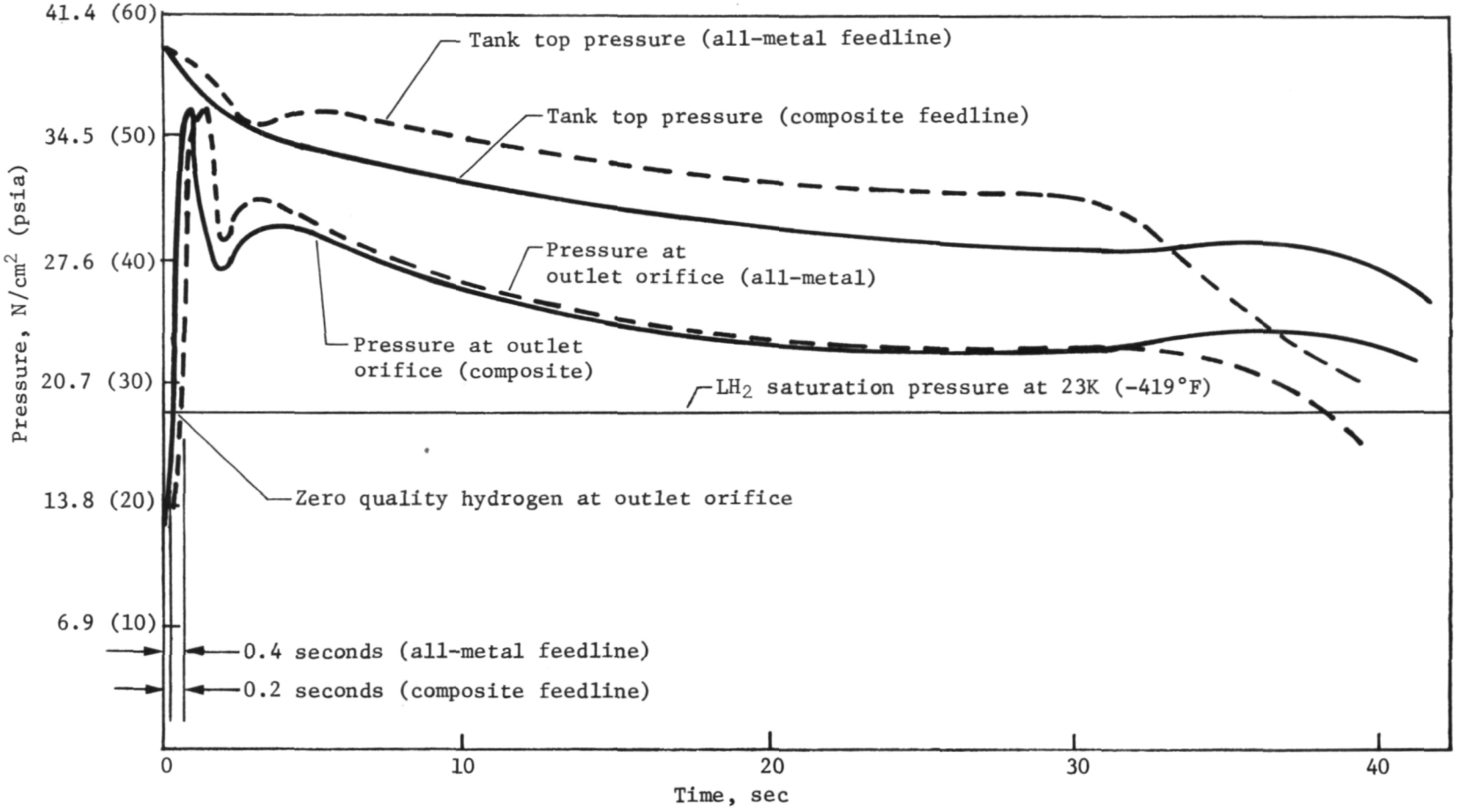

Figure VI-11. - Feedline Chilldown Test Data

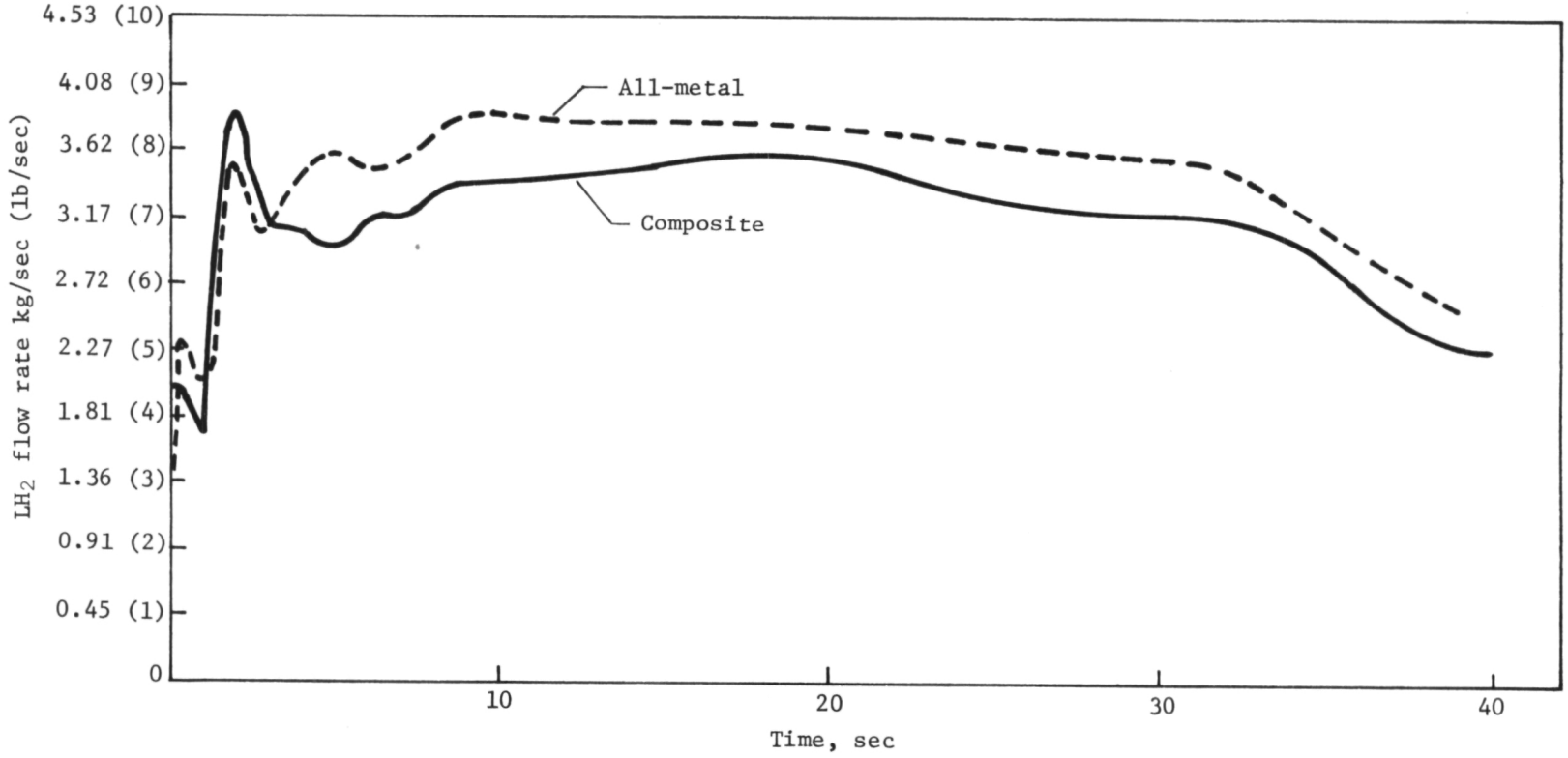

Figure VI-12. - Mass Flow Rate, Feedline Chilldown Test

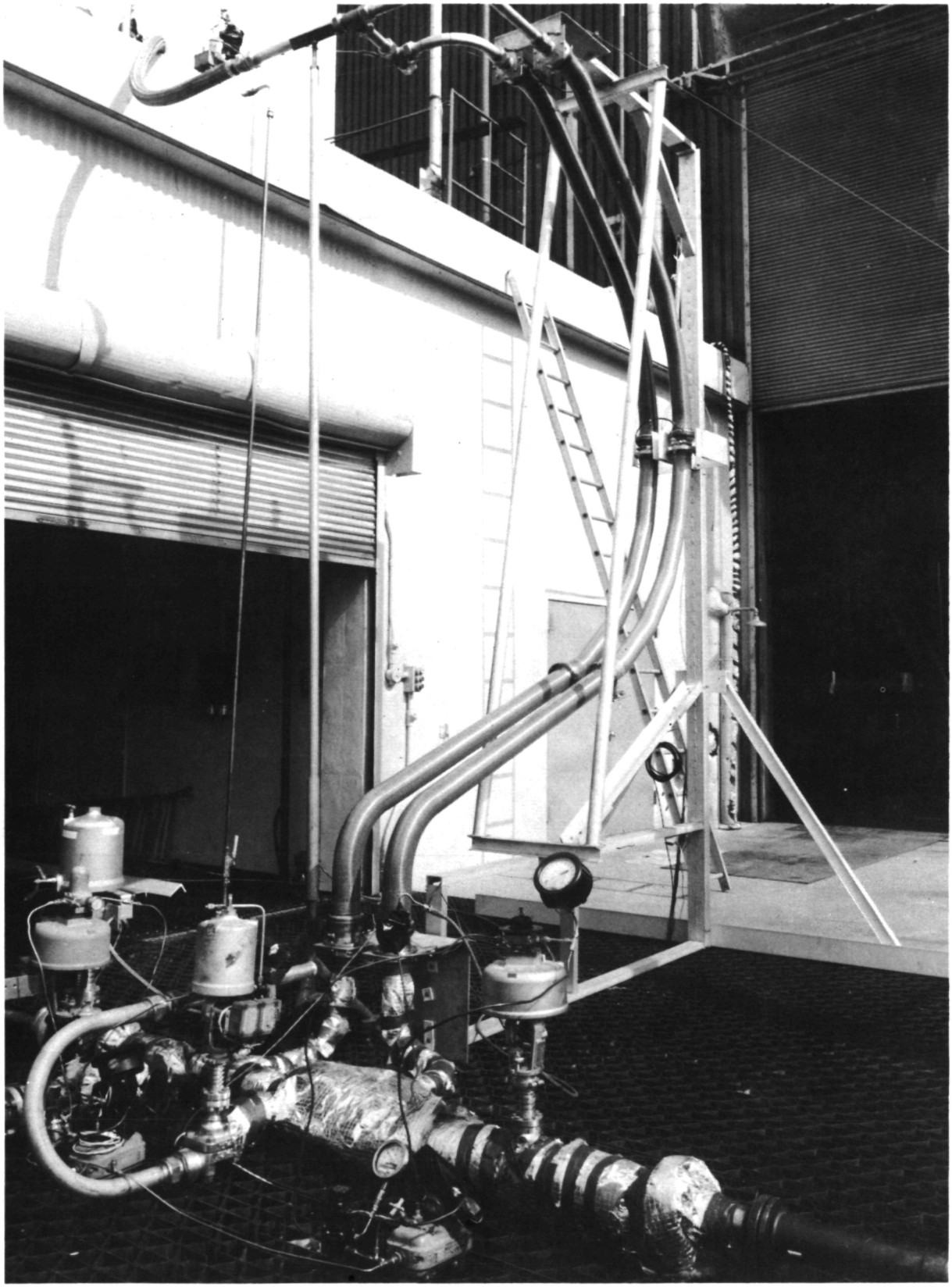

Figure VI-13. - Strain Cycling Test Setup

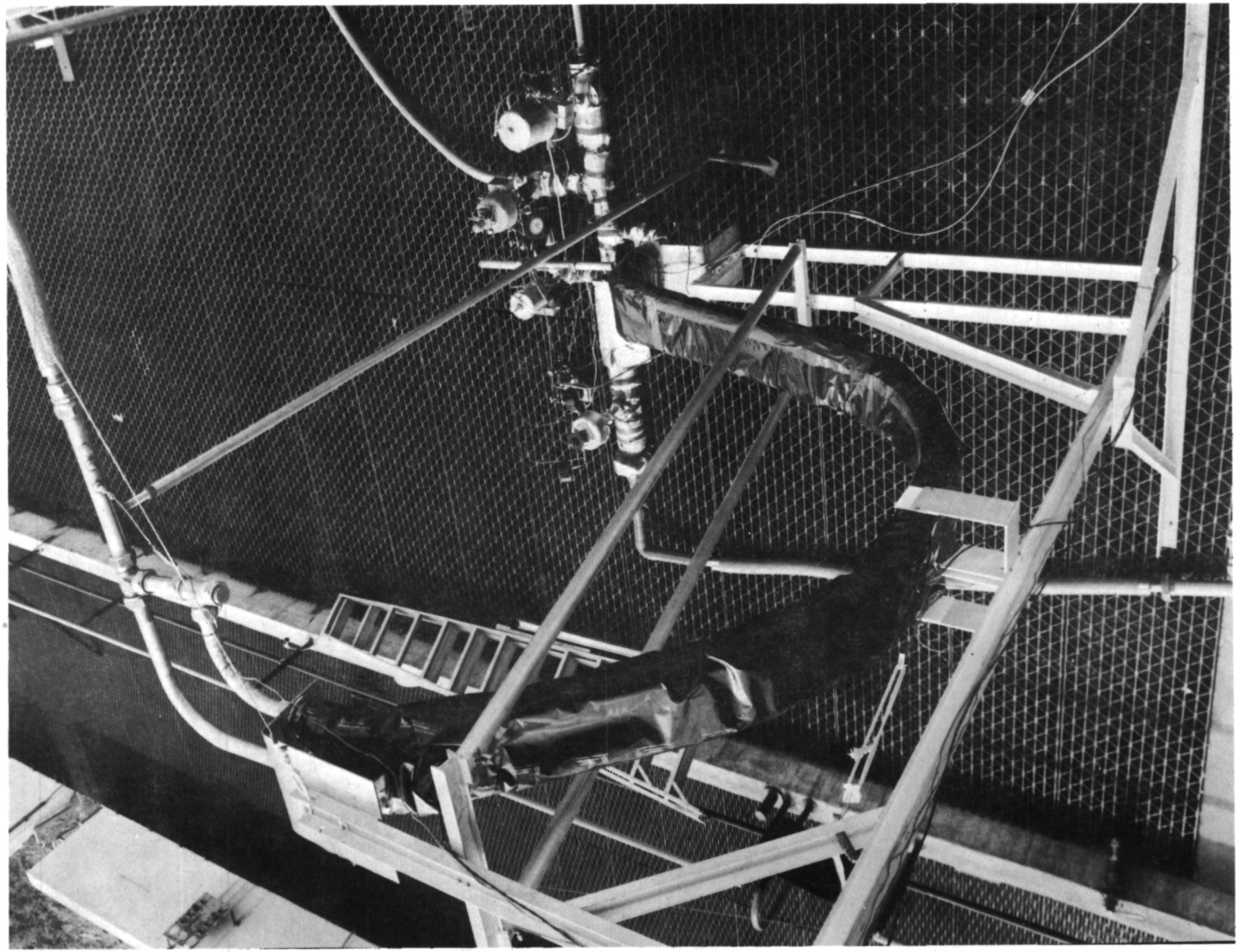

Figure VI-14. - Composite Lines in Purged Polyethylene Bag During Strain Cycle Test

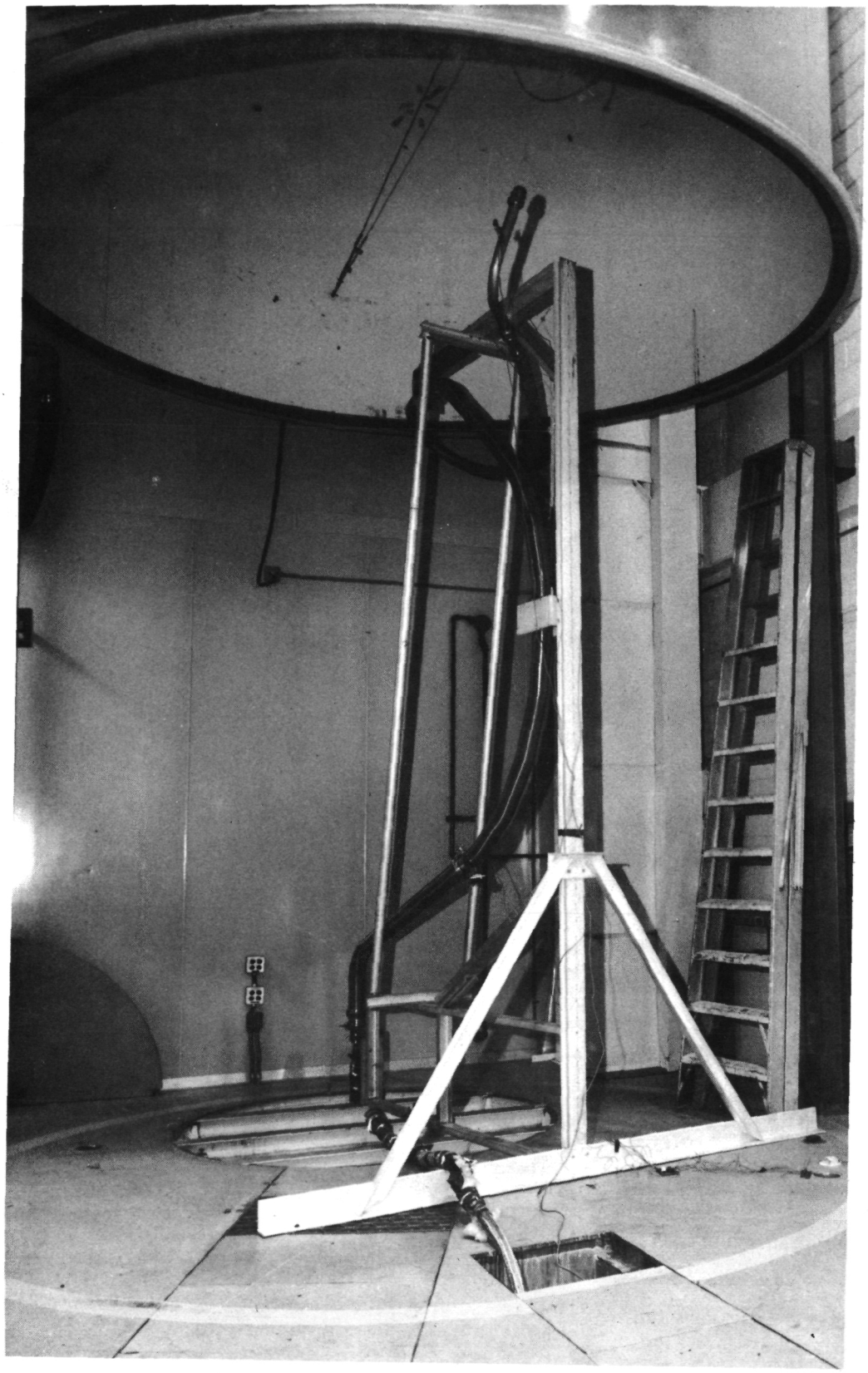

Figure VI-15. - Acoustic Test Setup, Composite Feedline Assembly, S/N 3, Overall View

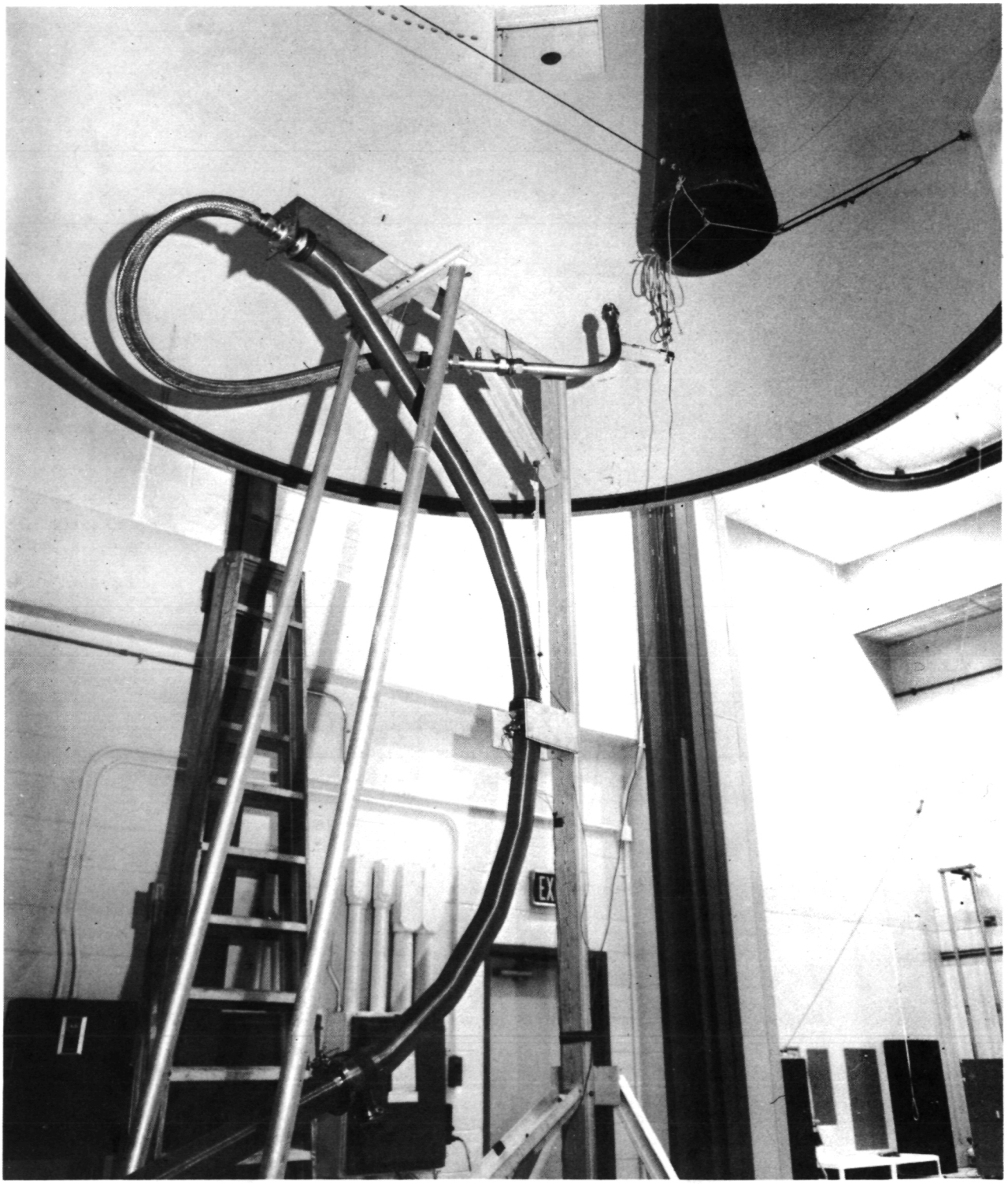

Figure VI-16. - Acoustic Test Setup, Composite Feedline Assembly, S/N 3, Closeup View of Feedline

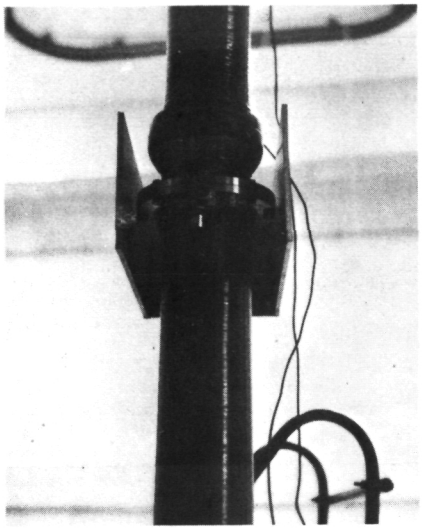

Upper flange

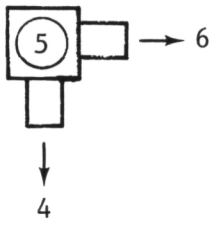

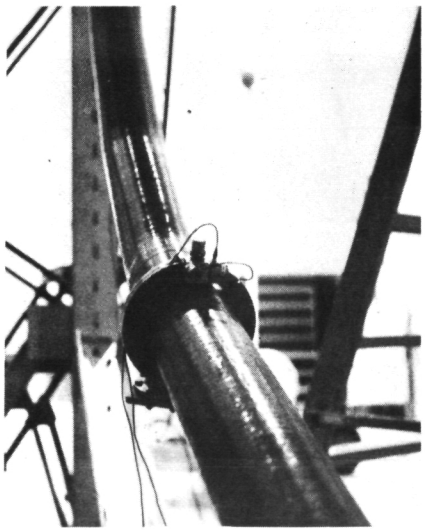

Lower flange

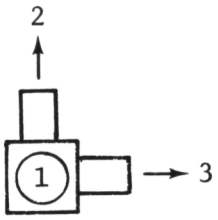

Figure VI-17. - Accelerometer Locations, Acoustic Test

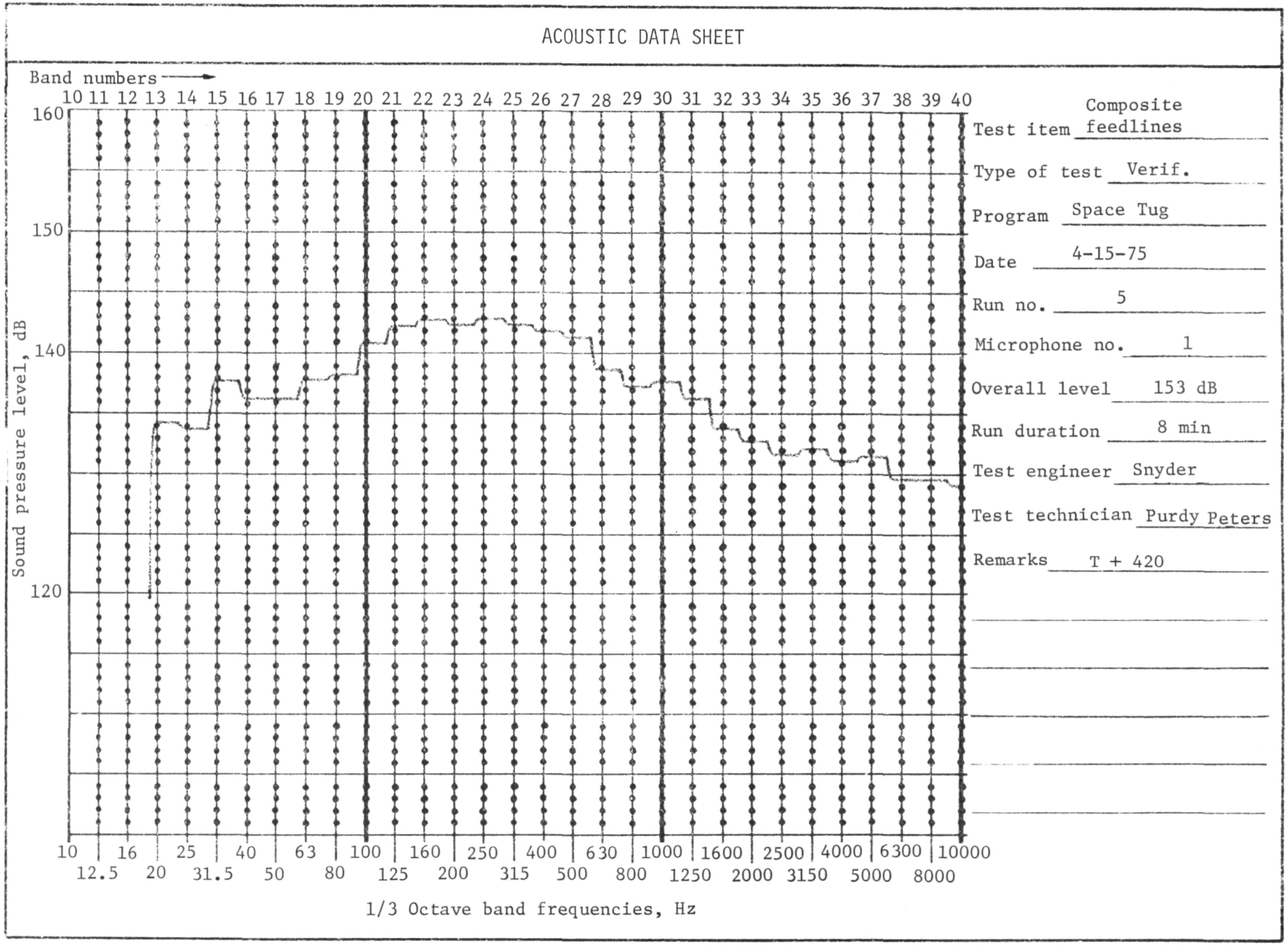

Figure VI-18. - Acoustic Test, Liftoff Environment

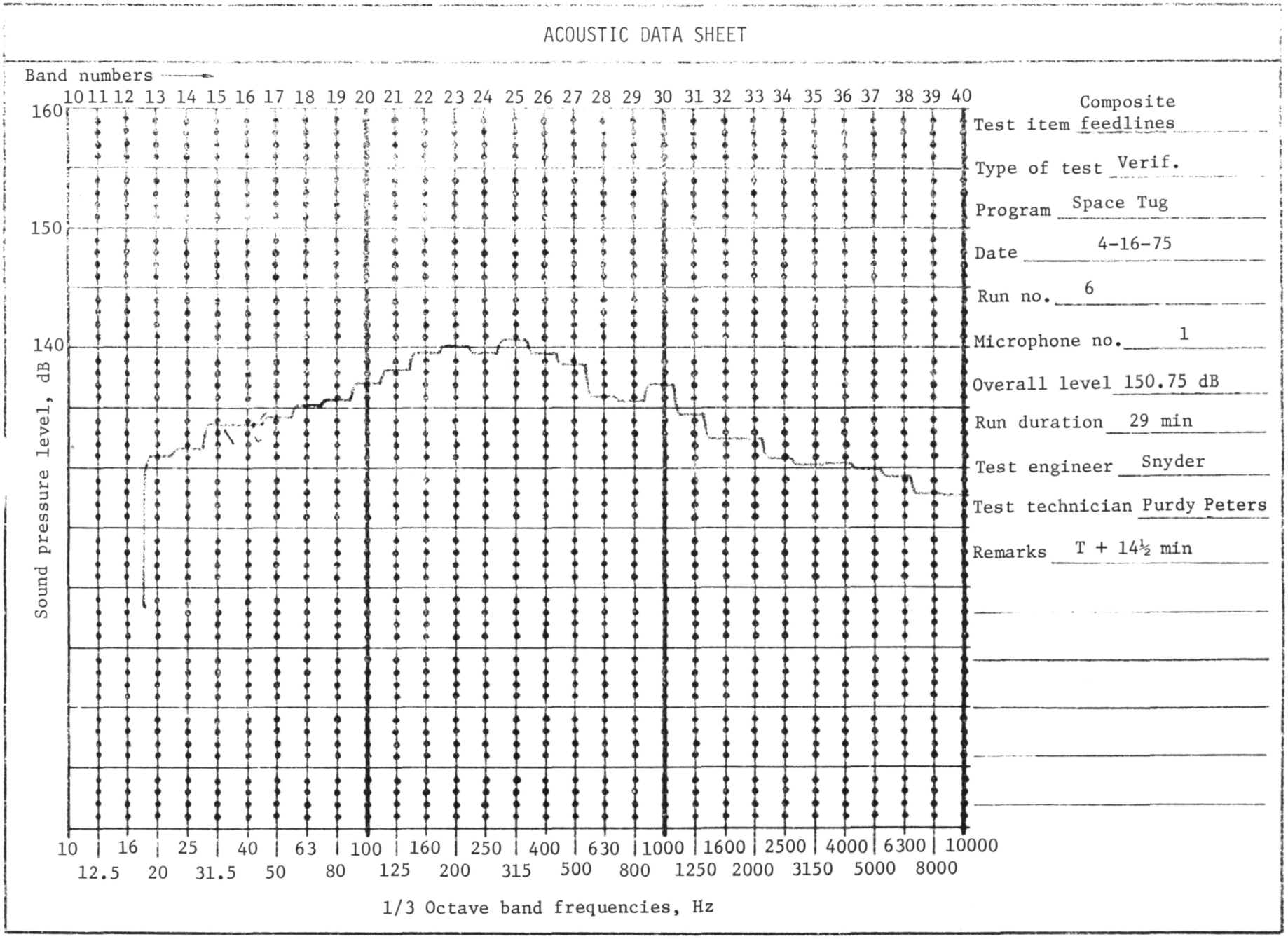

Figure VI-19. - Acoustic Test Boundary Layer

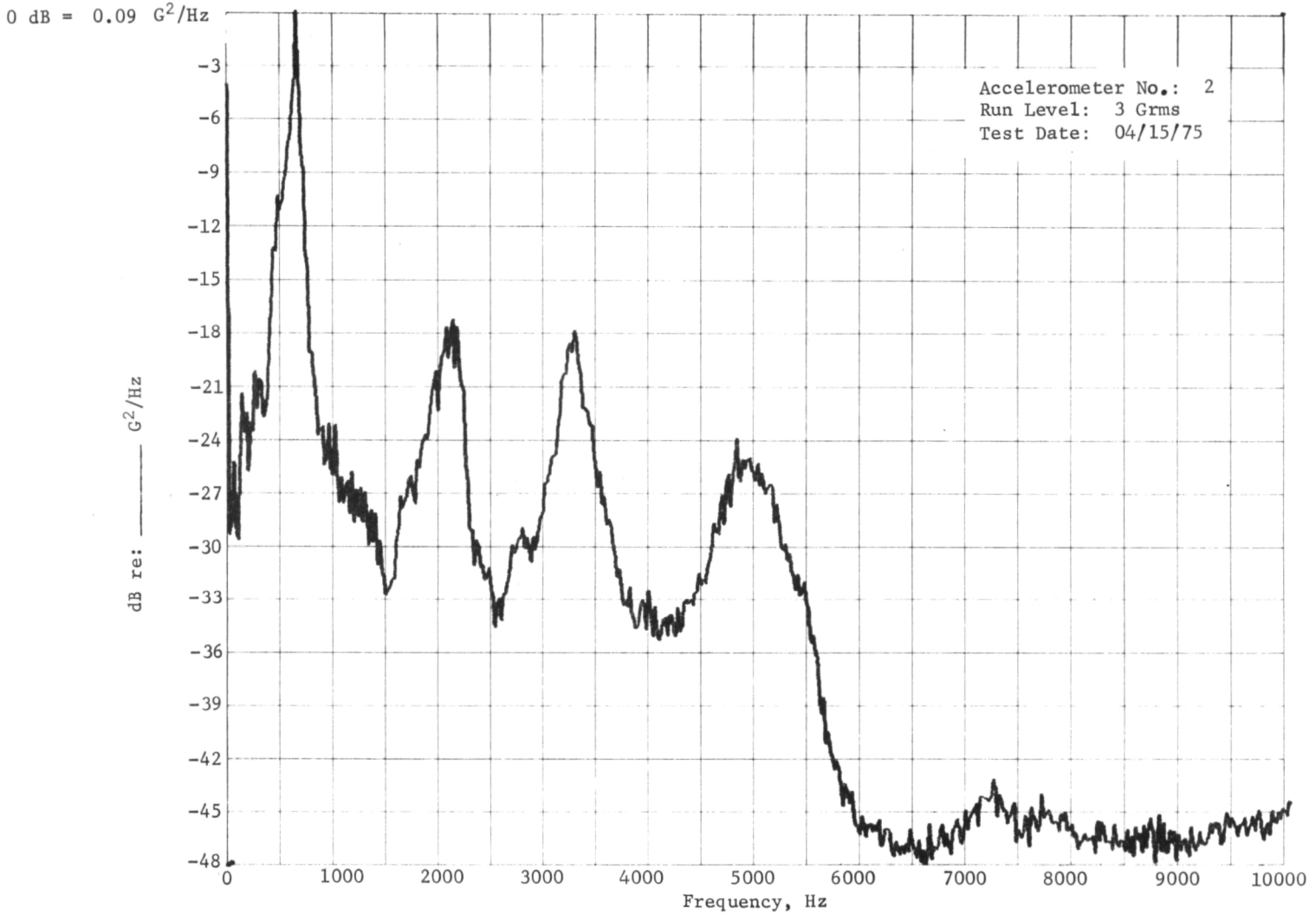

Figure VI-20. - Random Vibration Analysis, Liftoff Environment

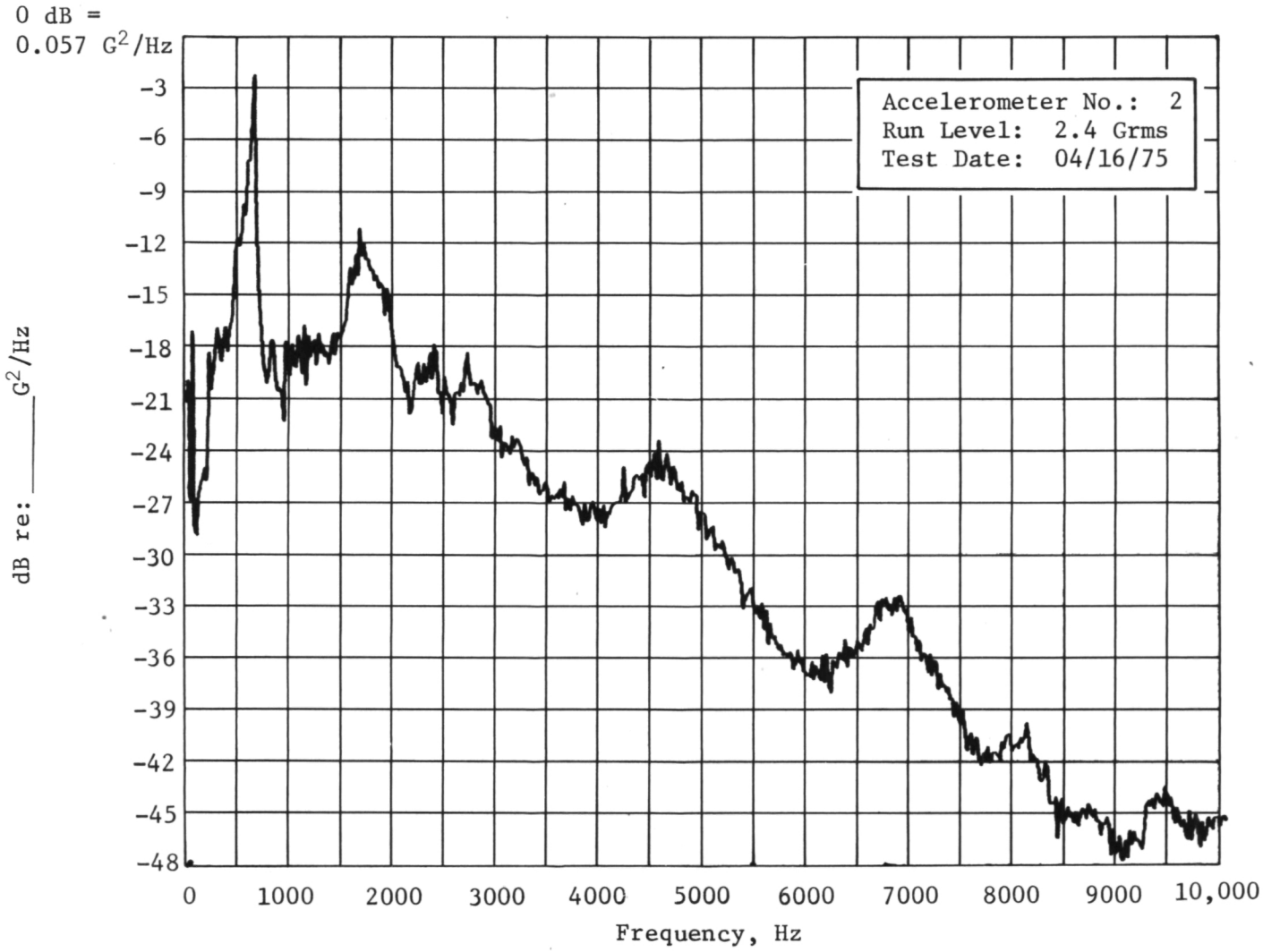

Figure VI-21.- Random Vibration Analysis, Boundary Layer Environment

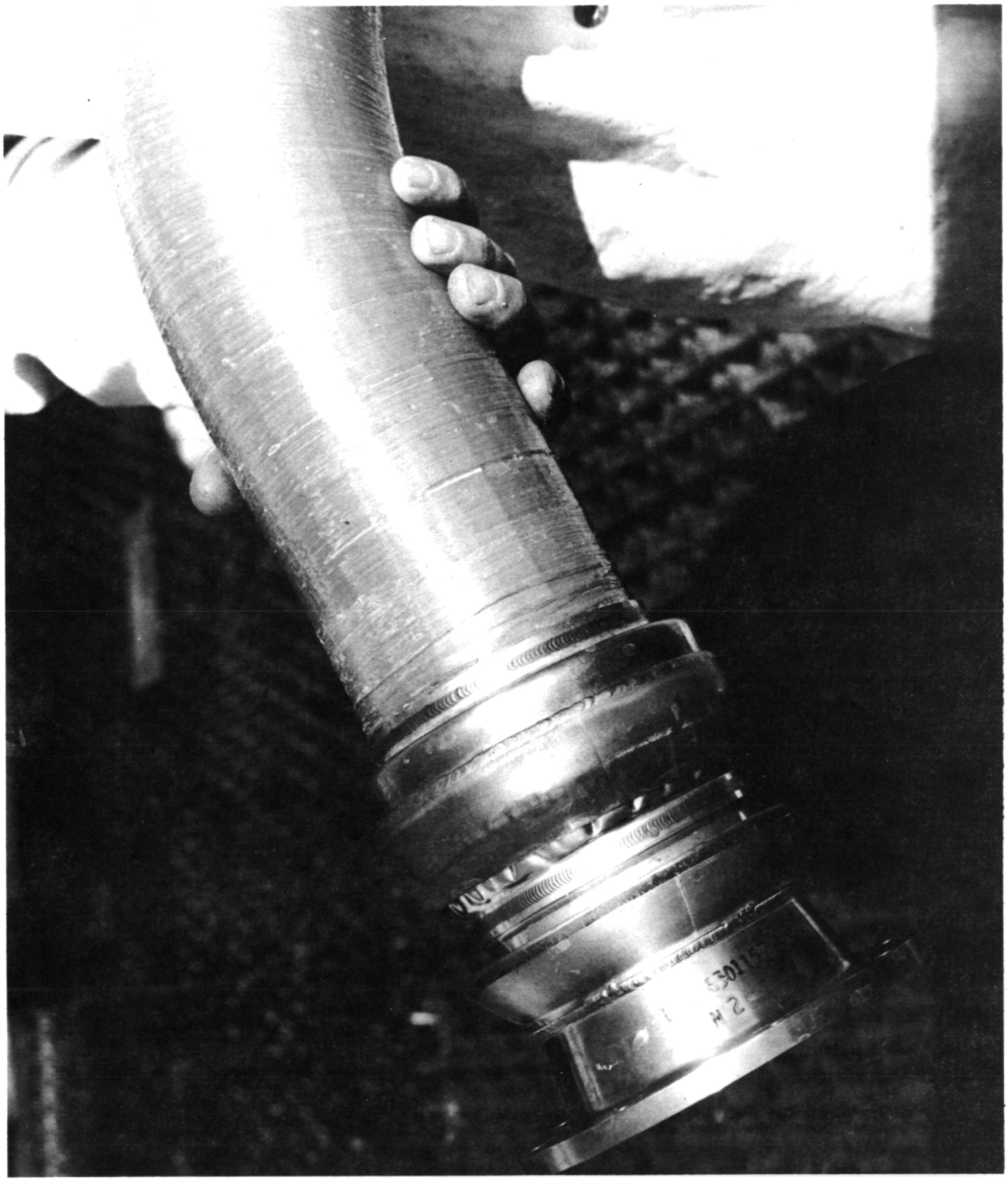

Figure VI-22. - Gimbal Joint Failure, Composite Line Burst Test

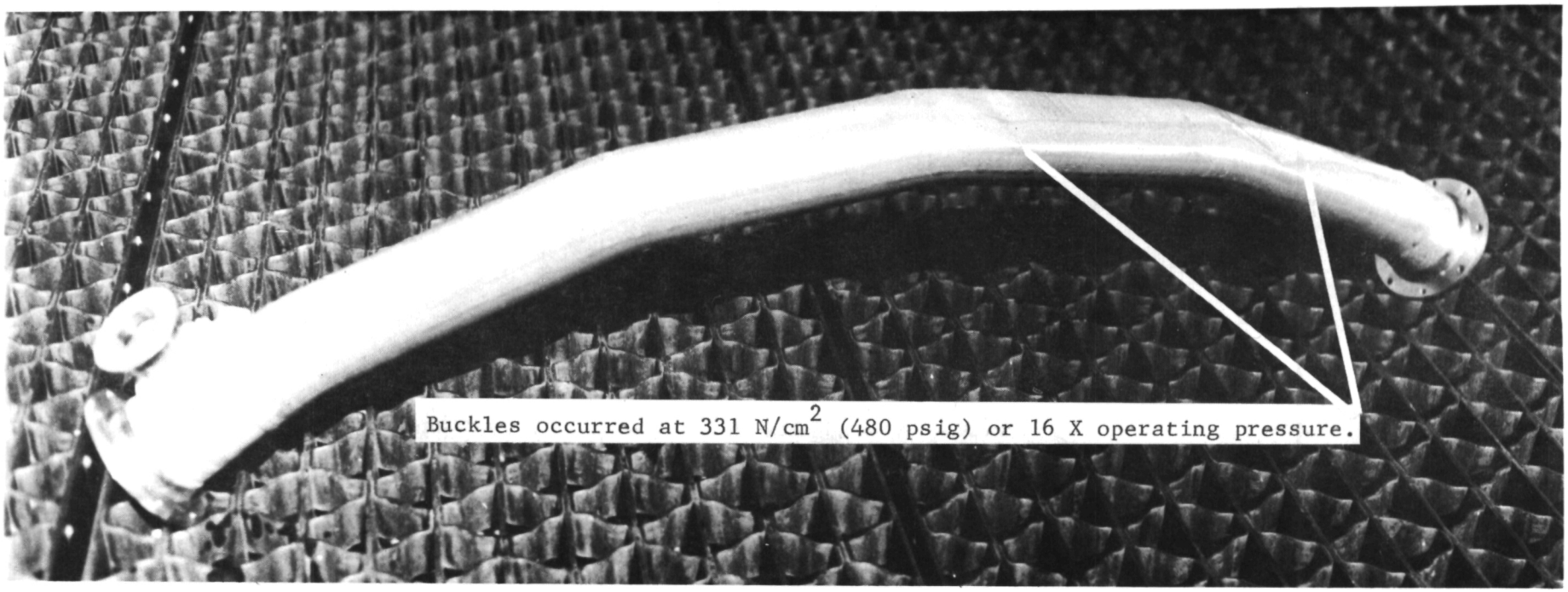

Figure VI-23. - Curved Filament-Wound Composite Line Showing Buckling Failure During Burst Test

Figure VI-24. - Curved Filament Wound Line Rupture During Burst Test

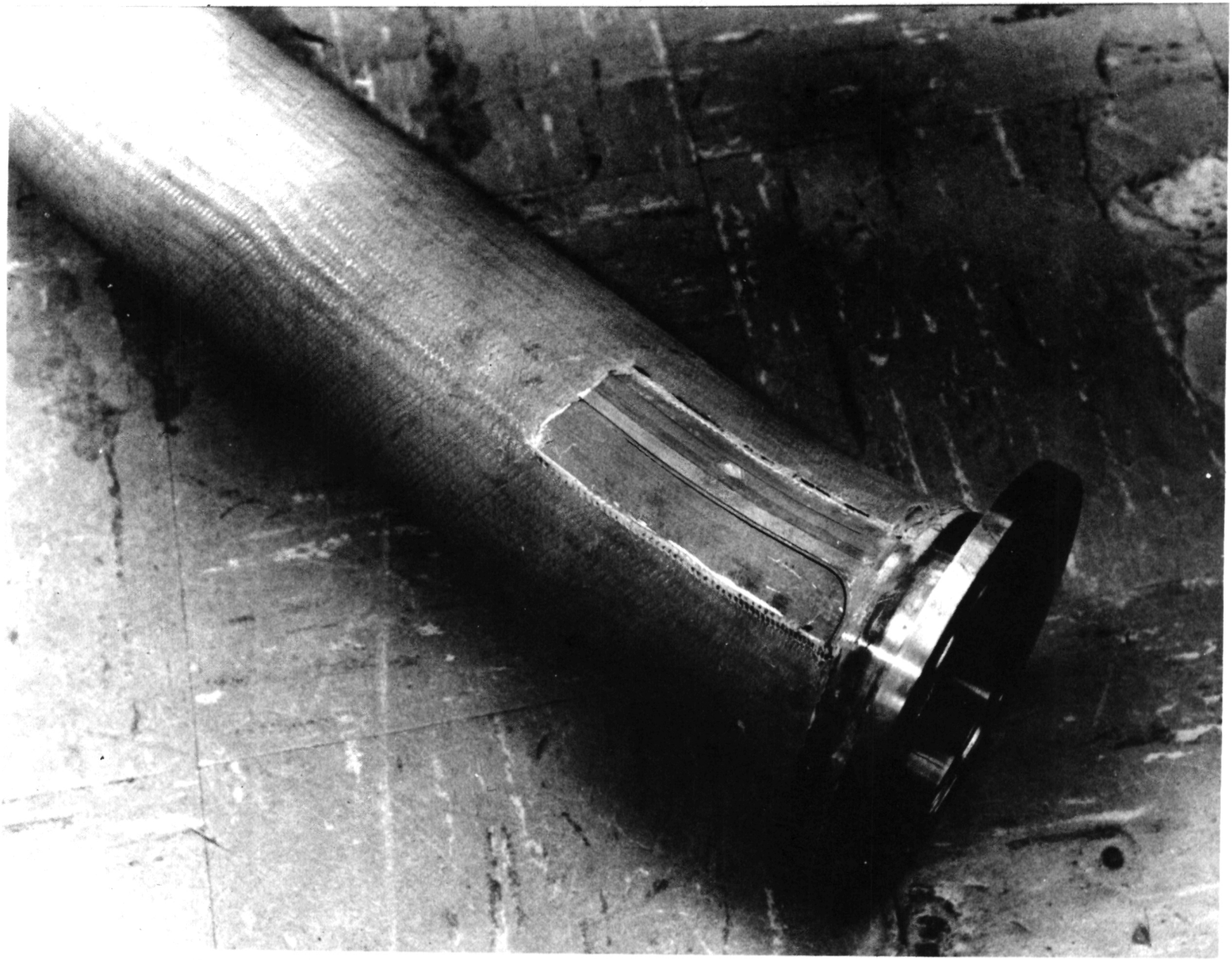

Figure VI-25. - Curved Braided Composite Line Rupture During Burst Test

APPENDIX A

FEEDLINE ASSEMBLY CONCEPT DRAWINGS

REVISIONS				
BTH	ZONE	DESCRIPTION	DATE	APPROVED

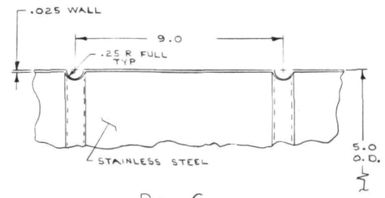

DETAIL G
NO SCALE
TYPICAL CONCEPT 1

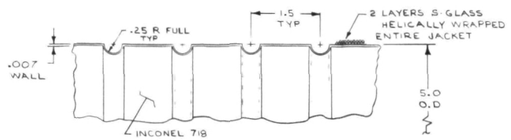

DETAIL F
NO SCALE
TYPICAL CONCEPT 2

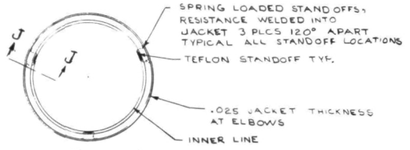

DETAIL H
NO SCALE
TYPICAL CONCEPTS 1 & 2

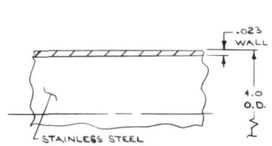

DETAIL D
NO SCALE
TYPICAL CONCEPT 1

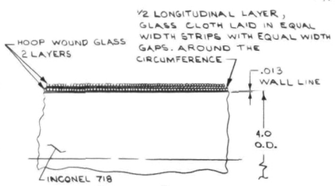

DETAIL E
NO SCALE
TYPICAL CONCEPT 2

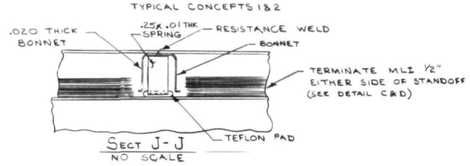

SECT J-J
NO SCALE

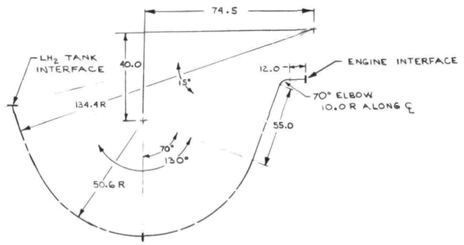

DIMENSIONAL LAYOUT
CONCEPT 1 & 2 LINE

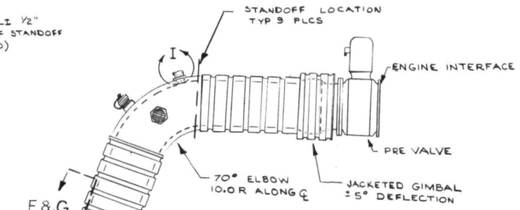

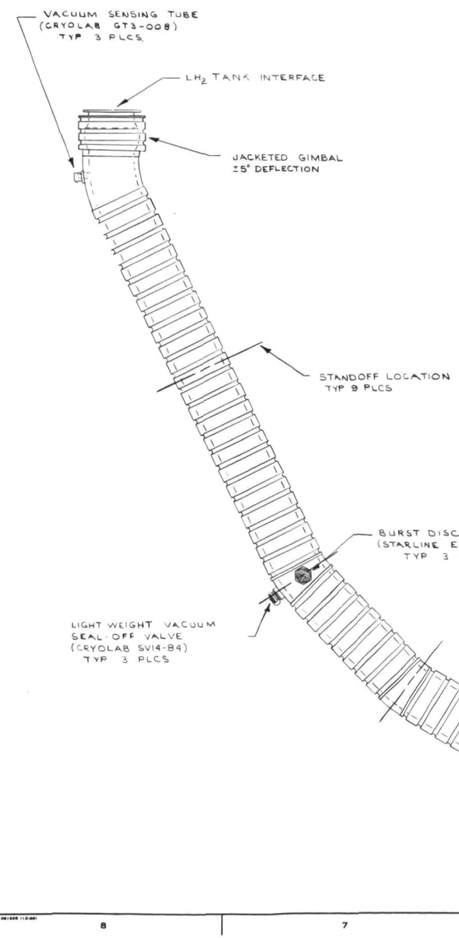

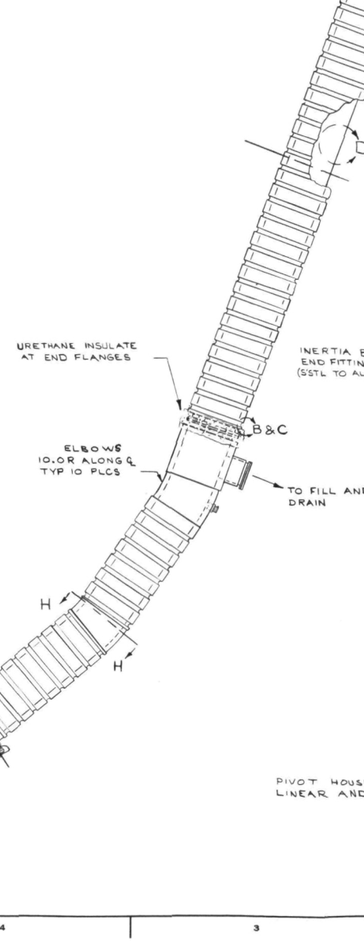

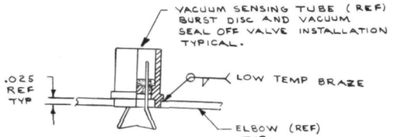

DETAIL I
NO SCALE
TYP SERVICE PORT CONCEPT 1 & 2

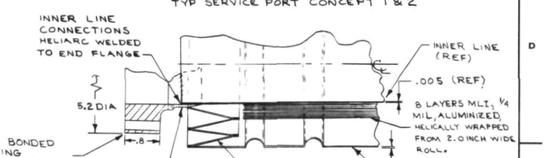

DETAIL C
NO SCALE
TYP JACKET END CLOSURE
CONCEPT 2

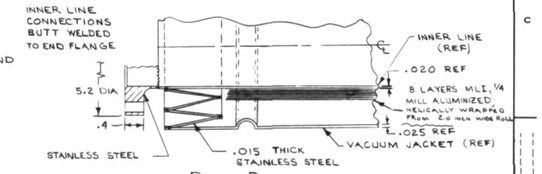

DETAIL B
NO SCALE
TYP JACKET END CLOSURE.
CONCEPT 1

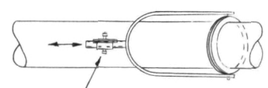

VIEW A-A
NO SCALE

DESIGN CONCEPTS 1 & 2 VACUUM JACKETED, UNINSULATED, WET, FEEDLINE			
CONCEPT 1		CONCEPT 2	
INNER LINE	VACUUM JACKET	INNER LINE	VACUUM JACKET
4.0 OUTSIDE DIAMETER	5.0 OUTSIDE DIAMETER	4.0 OUTSIDE DIAMETER	5.0 OUTSIDE DIAMETER
.023 WALL	.025 WALL	.013 WALL	.007 WALL
STAINLESS STEEL (SEE DETAIL 'D')	STAINLESS STEEL (SEE DETAIL 'G')	INCONEL 718 OVERWRAPPED 2 ½ LAYERS S-GLASS HOOP, ½ LONGITUDINAL & HOOP. (SEE DETAIL 'E')	INCONEL 718 OVERWRAPPED 2 LAYERS, S-GLASS HELICALLY WRAPPED (SEE DETAIL 'F')
EMISSIVITY IMPROVEMENT INSULATION TYP CONCEPTS 1 & 2			
¼ MIL (.00025 INCH) THICK DOUBLE ALUMINIZED MYLAR, "SUPERFLOC", 8 LAYERS HELICALLY WRAPPED FROM A 2.0 INCH WIDE SPOOL WITH 1.0 INCH OVERLAP. FASTEN START AND STOP WITH VACUUM COMPATIBLE TAPE.			

Design Concepts 1 and 2

115 & 116

A3

REVISIONS				
BTH	ZONE	DESCRIPTION	DATE	APPROVED

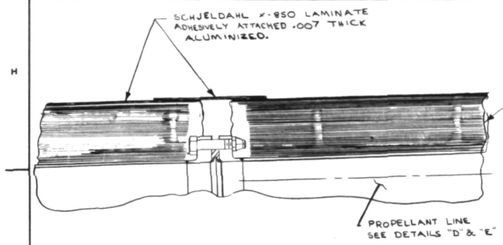

DETAIL F
TYP CONCEPTS 3&6
NO SCALE

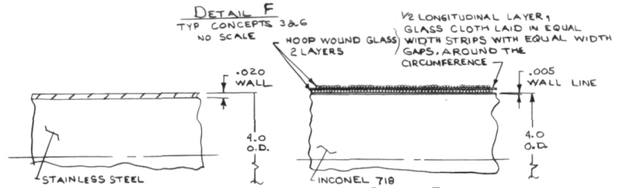

DETAIL D
NO SCALE
TYPICAL CONCEPT 3

DETAIL E
NO SCALE
TYPICAL CONCEPT 6

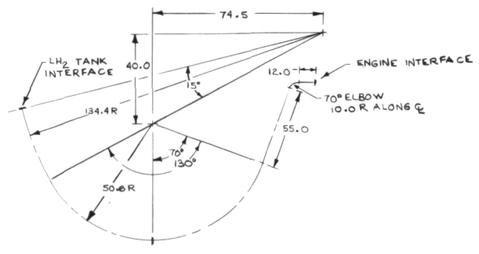

DIMENSIONAL LAYOUT
CONCEPT 3 & 6 LINE

DESIGN CONCEPTS 3 & 6		
PURGED MLI INSULATED, WET, FEEDLINE		
CONCEPT 3		CONCEPT 6
FEED LINE	INSULATION (TYP BOTH CONCEPTS)	FEEDLINE
4.0 OUTSIDE DIAMETER .020 WALL STAINLESS STEEL (SEE DETAIL "D")	MLI INSULATION SYSTEM; 1/4 MIL (.00025) THICK, DOUBLE ALUMINIZED MYLAR, 30 LAYERS SPIRALLY WRAPPED OVER LINE FROM A 2.0 WIDE SPOOL WITH 1.0 WIDE OVER LAP. (MLI IS SUPER FLOC), FASTEN START AND STOP WITH ALUMINIZED MYLAR TAPE. WRAP OUTSIDE WITH SCHJELDAHL X-850 LAMINATE, CLOSE ENDS AND ATTACH PURGE. (SEE DETAIL F)	4.0 OUTSIDE DIAMETER .005 WALL INCONEL 718 OVERWRAPPED 2½ LAYERS, S-GLASS HOOP, ½ LONGITUDINAL & HOOP. (SEE DETAIL "E")

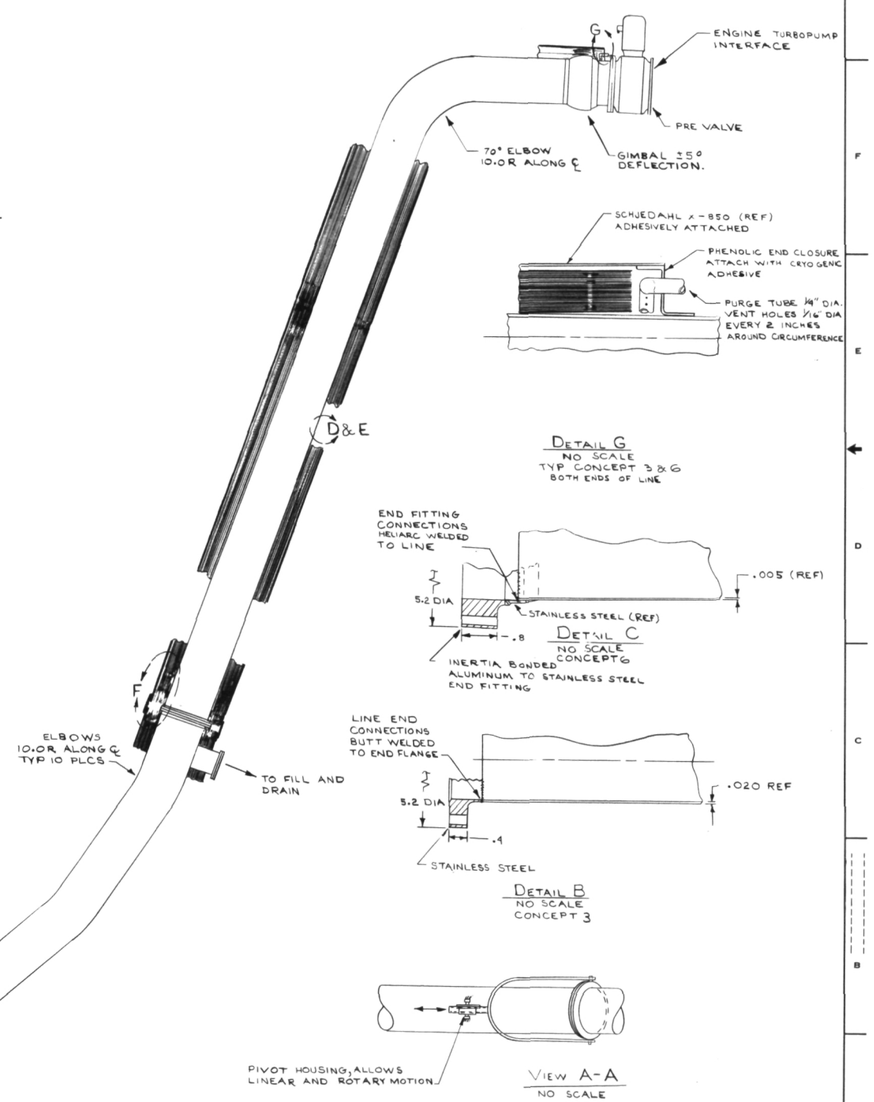

DETAIL G
NO SCALE
TYP CONCEPT 3 & 6
BOTH ENDS OF LINE

DETAIL C
NO SCALE
CONCEPT 6

DETAIL B
NO SCALE
CONCEPT 3

VIEW A-A
NO SCALE

REVISIONS

SYM	ZONE	DESCRIPTION	DATE	APPROVED

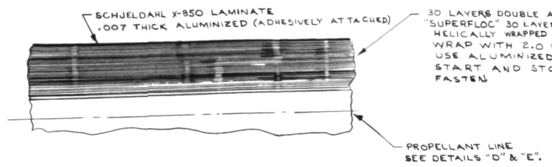

DETAIL F
NO SCALE
TYP CONCEPT 4 & 5

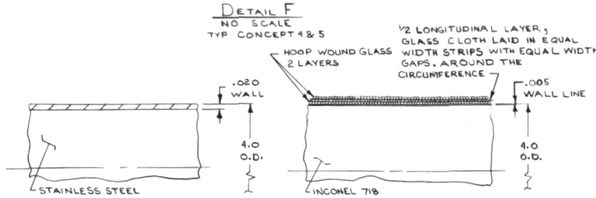

DETAIL D
NO SCALE
TYPICAL CONCEPT 4

DETAIL E
NO SCALE
TYPICAL CONCEPT 5

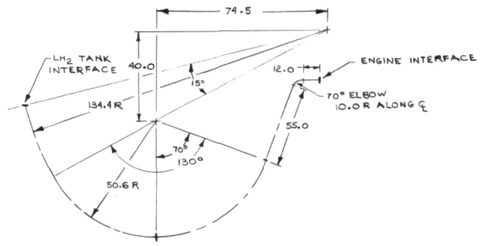

DIMENSIONAL LAYOUT
CONCEPT 4 & 5 LINE

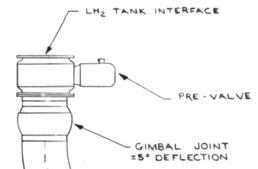

DESIGN CONCEPTS 4 & 5 MLI INSULATED, DRY, FEEDLINE		
CONCEPT 4		CONCEPT 5
FEEDLINE	INSULATION-(TYP BOTH CONCEPTS)	FEEDLINE
4.0 OUTSIDE DIAMETER .020 WALL STAINLESS STEEL (SEE DETAIL "D")	MLI INSULATION SYSTEM; 4 MIL (.00025) THICK, DOUBLE ALUMINIZED MYLAR, 30 LAYERS HELICALLY WRAPPED OVER LINE FROM A 2.0 WIDE SPOOL WITH 1.0 OVERLAP. FASTEN START AND STOP WITH ALUMINIZED MYLAR TAPE. WRAP OUTSIDE WITH SCHJELDAHL X-850 LAMINATE (SEE DETAIL F)	4.0 OUTSIDE DIAMETER .005 WALL INCONEL 718 OVERWRAPPED 2½ LAYERS, 3-GLASS HOOP, ½ LONGITUDINAL & HOOP. (SEE DETAIL "E")

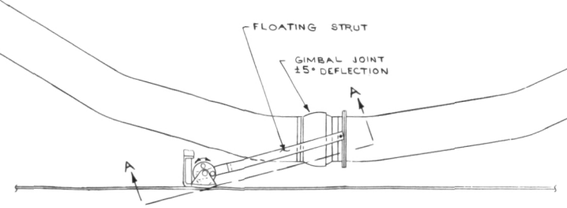

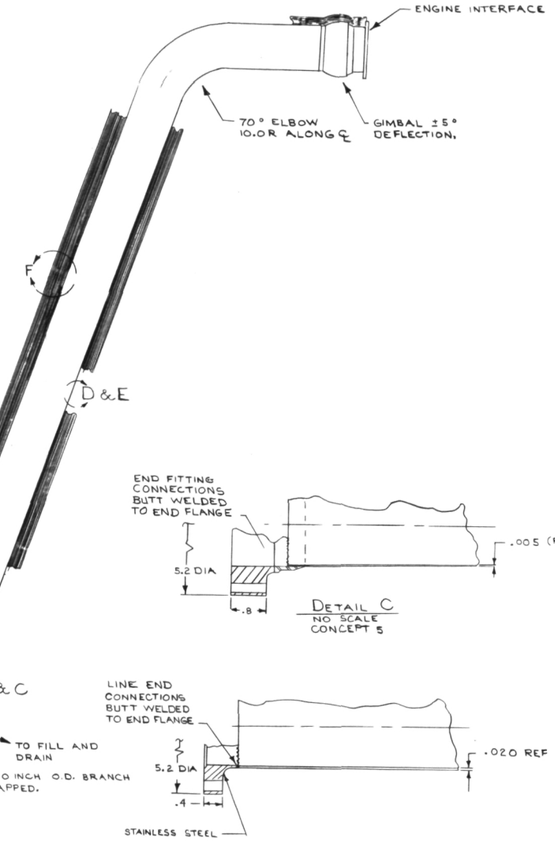

DETAIL C
NO SCALE
CONCEPT 5

DETAIL B
NO SCALE
CONCEPT 4

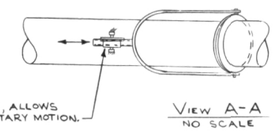

VIEW A-A
NO SCALE

REFERENCES

1. C. A. Hall, T. J. Pharo, J. M. Phillips, and J. P. Gille: Low Thermal Flux Glass-Fiber Tubing for Cryogenic Service, Martin Marietta Corporation, Denver, Colorado, NASA CR-72797, March 1971.

2. C. A. Hall, D. J. Laintz, and J. M. Phillips: Composite Propulsion Feedlines for Cryogenic Space Vehicles. Martin Marietta Corporation, Denver, Colorado, NASA CR-121137, August 1973.

3. D. E. Spond, D. J. Laintz, C. A. Hall, and D. E. Dulaigh: Vacuum Jacketed Composite Propulsion Feedlines for Cryogenic Launch and Space Vehicles, Martin Marietta Corporation, Denver, Colorado, NASA CR-134550, March 1974.

4. D. E. Spond, R. E. Holzworth and C. A. Hall: Lightweight Thermally Efficient Composite Feedlines, Preliminary Design and Evaluation, Topical Report - Martin Marietta Corporation, Denver, Colorado, NASA CR-134631, June 1974.

5. Space Tug Point Design Studies, McDonnell-Douglas Astronautics, February 1972.

6. Space Tug Point Design Studies, North American Rockwell, February, 1972.

7. Baseline Tug Definition Document, Rev. A, George C. Marshall Space Flight Center, June 26, 1972.

8. Space Tug Systems Study, 18 September 1973, GD/Convair, Contract No. NAS8-29676, Volume V - Systems Data Dump.

9. Space Tug Systems Study (Storable), performed by the Martin Marietta Corporation under Contract NAS8-29675.

DISTRIBUTION LIST

No. of Report Copies	Recipient
	National Aeronautics & Space Administration Lewis Research Center 21000 Brookpark Road Cleveland, Ohio 44135
1	Attn: Contracting Officer, MS 500-313
5	E. A. Bourke, MS 500-205
1	Technical Utilization Office, MS 3-16
1	Technical Report Control Office, MS 5-5
2	AFSC Liaison Office, MS 501-3
2	Library MS 60-3
1	Office of Reliability & Quality Assurance, MS 500-211
12	J. J. Notardonato, Project Manager, MS 500-203
1	Director, Manned Space Technology, RS Office of Aeronautics & Space Technology NASA Headquarters Washington, DC 20546
2	Director Space Prop. and Power, RP Office of Aeronautics & Space Technology NASA Headquarters Washington, DC 20546
1	Director, Launch Vehicles & Propulsion, SV Office of Space Science NASA Headquarters Washington, DC 20546
1	Director, Materials & Structures Div., RW Office of Aeronautics & Space Technology NASA Headquarters Washington, DC 20546
1	Director, Advanced Missions, MT Office of Manned Space Flight NASA Headquarters Washington, DC 20546
2	Director Space Prop. and Power, RP Office of Aeronautics & Space Technology NASA Headquarters Washington, DC 20546

1 Director, Launch Vehicles & Propulsion, SV
Office of Space Science
NASA Headquarters
Washington, DC 20546

1 Director, Materials & Structures Division, RW
Office of Aeronautics & Space Technology
NASA Headquarters
Washington, DC 20546

1 Director, Advanced Manned Mission, MT
Office of Manned Space Flight
NASA Headquarters
Washington, DC 20546

1 National Aeronautics & Space Administration
Ames Research Center
Moffett Field, California 94035
Attn: Library

1 National Aeronautics & Space Administration
Flight Research Center
P.O. Box 273
Edwards, California 93523
Attn: Library

1 Director, Technology Utilization Division
Office of Technology Utilization
NASA Headquarters
Washington, DC 20546

1 Office of the Director of Defense
Research & Engineering
Washington, DC 20301
Attn: Office of Asst Dir (Chem Technology)

1 Office of Aeronautics & Space Technology, R
NASA Headquarters
Washington, DC 20546

10 NASA Scientific and Technical Information Facility
P.O. Box 33
College Park, Maryland 20740
Attn: NASA Representative

1 National Aeronautics & Space Administration
Goddard Space Flight Center
Greenbelt, Maryland 20771
Attn: Library

1 National Aeronautics & Space Administration
John F. Kennedy Space Center
Cocoa Beach, Florida 32931
Attn: Library
1 I. Moore

1 National Aeronautics & Space Administration
Langley Research Center
Langley Station
Hampton, Virginia 23365
Attn: Library

1 National Aeronautics & Space Administration
Manned Spacecraft Center
Houston, Texas 77001
Attn: Library
1 W. Chandler
1 W. Dusenberry
1 C. Yodzis
1 R. High
1 D. Medlock
1 R. Allgeier

1 National Aeronautics & Space Administration
George C. Marshall Space Flight Center
Huntsville, Alabama 35912
Attn: Library
1 J. M. Stuckey
1 I. G. Yates
1 E. H. Hyde
1 P. L. Muller

1 Jet Propulsion Laboratory
4800 Oak Grove Drive
Pasadena, California 91103
Attn: Library
1 L. Stimson
1 J. Kelly
1 R. Breshears

1 Defense Documentation Center
Cameron Station
Building 5
5010 Duke Street
Alexandria, Virginia 22314
Attn: TISIA

1 RDT (RTNP)
Bolling Air Force Base
Washington, DC 20332

1 Arnold Engineering Development Center
Air Force Systems Command
Tullahoma, Tennessee 37389
Attn: Library

1 Advanced Research Projects Agency
Washington, DC 20525
Attn: Library

1 Aeronautical Systems Division
Air Force Systems Command
Wright-Patterson Air Force Base,
Dayton, Ohio
Attn: Library
1 AFML (MAAE)
1 AFML (MAAM)

1 Air Force Rocket Propulsion Laboratory (RPM)
Edwards, California 93523
Attn: Library

1 Air Force FTC (FTAT-2)
Edwards Air Force Base, California 93523
Attn: Library

1 Air Force Office of Scientific Research
Washington, DC 20333
Attn: Library

1 Space & Missile Systems Organization
Air Force Unit Post Office
Los Angeles, California 90045
Attn: Technical Data Center

1 Office of Research Analyses (OAR)
Holloman Air Force Base, New Mexico 88330
Attn: Library
RRRD

1 U. S. Air Force
Washington, DC
Attn: Library

1 Commanding Officer
U. S. Army Research Office (Durham)
Box CM, Duke Station
Durham, North Carolina 27706
Attn: Library

1 Bureau of Naval Weapons
Department of the Navy
Washington, DC
Attn: Library

1 Director (Code 6180)
U. S. Naval Research Laboratory
Washington, DC 20390
Attn: Library

1 Picatinny Arsenal
Dover, New Jersey 07801
Attn: Library

1 Air Force Aero Propulsion Laboratory
Research & Technology Division
Air Force Systems Command
United States Air Force
Wright-Patterson AFB, Ohio 45433
Attn: APRP (Library)

1 Electronics Division
Aerojet-General Corporation
P.O. Box 296
Azusa, California 91703
Attn: Library

1 Space Division
Aerojet-General Corporation
9200 East Flair Drive
El Monte, California 91734
Attn: Library

1 Aerojet Ordnance and Manufacturing
Aerojet-General Corporation
11711 South Woodruff Avenue
Fullerton, California 90241
Attn: Library

1 Aerojet Liquid Rocket Company
P.O. Box 15847
Sacramento, California 95813
Attn: Technical Library 2484-2015A

1 Aeronutronic Division of Philco Ford Corp.
Ford Road
Newport Beach, California 92663
Attn: Technical Information Department

1 Aerospace Corporation
2400 E. El Segundo Blvd.
Los Angeles, California 90045
Attn: Library-Documents

1 Arthur D. Little, Inc.
20 Acorn Park
Cambridge, Massachusetts 02140
Attn: Library
1 R. B. Hinckley

1 Astropower Laboratory
McDonnell-Douglas Aircraft Company
2121 Paularino
Newport Beach, California 92163
Attn: Library

1 ARO, Incorporated
Arnold Engineering Development Center
Arnold AF Station, Tennessee 37389
Attn: Library

1 Susquehanna Corporation
Atlantic Research Division
Shirley Highway & Edsall Road
Alexandria, Virginia 22314
Attn: Library

1 Beech Aircraft Corporation
Boulder Facility
Box 631
Boulder, Colorado
Attn: Library

1 Bell Aerosystems, Inc.
Box 1
Buffalo, New York 14240
Attn: Library

1 Instruments & Life Support Division
Bendix Corporation
P.O. Box 4508
Davenport, Iowa 52808
Attn: Library

1 Boeing Company
Space Division
P.O. Box 868
Seattle, Washington 98124
Attn: Library
1 D. H. Zimmerman

1 Boeing Company
1625 K Street, N.W.
Washington, DC 20006

1 Chemical Propulsion Information Agency
Applied Physics Laboratory
8621 Georgia Avenue
Silver Spring, Maryland 20910

1 Chrysler Corporation
Missile Division
P.O. Box 2628
Detroit, Michigan
Attn: Library

1 Chrysler Corporation
Space Division
P.O. Box 29200
New Orleans, Louisiana 70129
Attn: Librarian

1 Curtiss-Wright Corporation
Wright Aeronautical Division
Woodridge, New Jersey
Attn: Library

1 University of Denver
Denver Research Institute
P.O. Box 10127
Denver, Colorado 80210
Attn: Security Office

1 Fairchild Stratos Corporation
Aircraft Missiles Division
Hagerstown, Maryland
Attn: Library

1 Research Center
Fairchild Hiller Corporation
Germantown, Maryland
Attn; Library

1 Republic Aviation
Fairchild Hiller Corporation
Farmington, Long Island
New York

1 General Dynamics/Convair
P.O. Box 1128
San Diego, California 92112
Attn: Library
1 R. Tatro

1 Missiles and Space Systems Center
General Electric Company
Valley Forge Space Technology Center
P.O. Box 8555
Philadelphia, Pa. 19101
Attn: Library

1 General Electric Company
Flight Propulsion Lab. Department
Cincinnati, Ohio
Attn: Library

1 Grumman Aircraft Engineering Corporation
Bethpage, Long Island, New York
Attn: Library
1 B. Aleck
1 M. Martin

1 Honeywell Inc.
Aerospace Division
2600 Ridgeway Road
Minneapolis, Minnesota
Attn: Library

1 IIT Research Institute
Technology Center
Chicago, Illinois 60616
Attn: Library

1 Ling-Temco-Vought Corporation
P.O. Box 5907
Dallas, Texas 75222
Attn: Library

1 Lockheed Missiles and Space Company
P.O. Box 504
Sunnyvale, California 94087
Attn: Library

1 Linde--Division of Union Carbide
P.O. Box 44
Tonawanda, N.Y. 11450
Attn: G. Nies

1 Marquardt Corporation
16555 Saticoy Street
Box 2013 - South Annex
Van Nuys, California 91409

1 Denver Division
Martin Marietta Corporation
P. O. Box 179
Denver, Colorado 80201
Attn: Library
1 R. W. Vandekoppel

1 Western Division
McDonnell Douglas Astronautics
5301 Bolsa Avenue
Huntington Beach, California 92647
Attn: Library
1 P. Klevatt

1 McDonnell Douglas Aircraft Corporation
P. O. Box 516
Lambert Field, Missouri 63166
Attn: Library
1 L. F. Kohrs

1 Rocketdyne Division
Rockwell International
6633 Canoga Avenue
Canoga Park, California 91304
Attn: Library, Department 596-306

1 Space & Information Systems Division
Rockwell International
12214 Lakewood Blvd.
Downey, California
Attn: Library
1 E. Hawkinson
1 R. Boudreaux

1 Northrop Space Laboratories
3401 West Broadway
Hawthorne, California
Attn: Library

1 Purdue University
Lafayette, Indiana 47907
Attn: Library (Technical)

1 Goodyear Aerospace Corporation
1210 Massilon Road
Akron, Ohio 44306
Attn: C. Shriver

1 Hamilton Standard Corporation
Windsor Locks, Connecticut 06096
Attn: Library

1 Stanford Research Institute
333 Ravenswood Avenue
Menlo Park, California 94025
Attn: Library

1 TRW Systems Inc.
1 Space Park
Redondo Beach, California 90278
Attn: Tech. Lib. Doc. Acquisitions

1 United Aircraft Corporation
Pratt & Whitney Division
Florida Research & Development Center
P.O. Box 2691
West Palm Beach, Florida 33402
Attn: Library

1 United Aircraft Corporation
United Technology Center
P.O. Box 358
Sunnyvale, California 94038
Attn: Library

1 Vickers Incorporated
Box 302
Troy, Michigan

1 Airesearch Mfg. Div.
Garrett Corporation
9851 Sepulveda Blvd
Los Angeles, California 90009

1 Airesearch Mfg. Div.
Garrett Corporation
402 South 36th Street
Phoenix, Arizona 85034
Attn: Library

1 Commanding Officer
U.S. Naval Underwater Ordnance Station
Newport, Rhode Island 02844
Attn: Library

1 National Science Foundation, Engineering Division
1800 G. Street N.W.
Washington, DC 20540
Attn: Library

1 G. T. Schjeldahl Company
Northfield, Minn. 55057
Attn: Library

1 General Dynamics
P.O. Box 748
Fort Worth, Texas 76101

1 Cryonetics Corporation
Northwest Industrial Park
Burlington, Massachusetts

1 Institute of Aerospace Studies
University of Toronto
Toronto 5, Ontario
Attn: Library

1 FMC Corporation
Chemical Research & Development Center
P.O. Box 8
Princeton, New Jersey 08540

1 Westinghouse Research Laboratories
Beulah Road, Churchill Boro
Pittsburgh, Pennsylvania 15235

1 Cornell University
Department of Materials Science & Eng.
Ithaca, New York 14850
Attn: Library

1 Marco Research & Development Co.
Whittaker Corporation
131 N. Ludlow Street
Dayton, Ohio 45402

1 General Electric Company
Apollo Support Dept. P.O. Box 2500
Daytona Beach, Florida 32015
Attn: C. Ray

1 E. I. DuPont, DeNemours and Company
Eastern Laboratory
Gibbstown, New Jersey 08027
Attn: Library

1 Esso Research and Engineering Company
Special Projects Unit
P.O.Box 8
Linden, New Jersey 07036
Attn: Library

1 Minnesota Mining and Manufacturing Company
900 Bush Avenue
St. Paul, Minnesota 55106
Attn: Library

R. Motta E452/106/2-6751 16 MAY 77

D. D. Anglin E243/101A/3/48769 DEC - 1991